Diffusion and Adsorption of Aromatics in Zeolites by Zero Length Column Technique

By

Sharif Fakhruz Zaman

A thesis presented to the

DEANSHIP OF GRADUATE STUDIES

KING FAHD UNIVERSITY OF PETROLEUM & MINERALS

DHAHRAN, SAUDI ARABIA

In partial fulfillment of the

Requirements for the degree of

MASTER OF SCIENCE

In

CHEMICAL ENGINEERING

April, 2004

KING FAHD UNIVERSITY OF PETROLEUM AND MINERALS
DHAHRAN 31261, SAUDI ARABIA

DEANSHIP OF GRADUATE STUDIES

This thesis, written by

SHARIF FAKHRUZ ZAMAN

Under the direction of his Thesis Advisor and approved by his Thesis Committee, has been presented to and accepted by the Dean of Graduate Studies, in partial fulfillment of the requirements for the degree of

MASTERS OF SCIENCE IN CHEMICAL ENGINEERING

Thesis Committee

_____
Dr. Kevin F. Loughlin
(Thesis Advisor)

_____
Dr. Sulaiman Al-Khattaf
(Thesis Co-advisor)

_____
Dr. Nadhir A. H. Al-Baghli
(Member)

_____
Prof. Mohamed B. Amin
(Department Chairman)

_____
Dr. Ashrafhusein I.Fatehi
(Member)

_____
Dr. Mohammed A. Al-Ohali
(Dean of Graduate Studies)

_____
Dr. Ibnelwaleed Ali Hussein
(Member)

_____
Date

Dedication

This work is dedicated to my loving parents.

Acknowledgement

In the name of Allah, Most Gracious, Most Merciful

All praise to Allah, *subhanahu-wa-ta'ala*, the almighty, for his blessings on me to accomplish this work. I feel privilege to glorify His name in the sincerest way through this small accomplishment. I seek his mercy, favor and forgiveness. And I ask Him to accept my little effort as an act of worship. May the peace and blessings of Allah be upon His prophet, Muhammad (Salla Allahu Alaehi' wa-sallam). May He guide us to the path of glory and success. (*amen*)

The support provided by King Fahd University of Petroleum & Minerals to attain my MS degree, complete this research and overall to enrich my knowledge in the field of Chemical Engineering is gratefully acknowledge.

With deep sense of gratitude and appreciation, I would like to express my sincere thanks to my thesis advisor, Dr. K.F. Loughlin for his invaluable support, guidance, continuous encouragement and every possible cooperation through out the period of my research and preparation of my thesis documentation. Working with him was indeed a wonderful and learning experience, which I thoroughly enjoyed. I am also indebted to my thesis co-advisor, Dr. Sulaiman A. Khattaf, for his suggestions, and inspiration to complete the thesis. I owe special thanks to my thesis committee members, Dr. Nadhir A. Baghli, Dr. Ashrafhusein I. Fatehi, and Dr. Ibnelwaleed A. Hussain for their critical review and suggestions.

I would like to thank Dr. A. B. Amin, chairman, Chemical Engineering Department, King Fahd University of Petroleum & Minerals for providing me all the available facilities. I am also grateful to all the faculty members and staffs of the Chemical Engineering Department who have in one way or other enriched my academic and research experience at KFUPM.

I would like to thank the laboratory stuff and technicians specially Mr. Romeo, Mr. Mahdi, Mr. Ebrahim, Mr. Bashir, Mr. Kamal and Mr. Mofizul Islam for their help during the experimental work.

Special thanks to all of my friends and colleagues for their continuous encouragement and providing me a wonderful time during my stay at KFUPM.

Last but not least, I would like to appreciate my family members for their prayers, encouragement and support that permitted me to indulge my passion for the long task to completing this work.

[Sharif F. Zaman]

Table of contents

List of Table

List of Figures

ABSTRACT

NAME OF STUDENT	Sharif Fakhruz Zaman
TITLE OF STUDY	Diffusion and Adsorption of Aromatics in Zeolites by Zero Length Column Technique.
MAJOR FIELD	Chemical Engineering
DATE OF DEGREE	April, 2004

Zero length column (ZLC) method is used to determine the intracrystalline diffusivity of aromatics in NaY and HZSM5 zeolite crystals and in NaY FCC catalyst pellets. The equilibrium region of investigation is nonlinear and the slope of the long time asymptotic solution of the nonlinear ZLC model is used to analyze the diffusivity data.

Diffusivity of 1,3,5 tri-isopropyl benzene is greater than 1,3 di-isopropyl benzene. The desorption curve of 1,3,5 tri-isopropyl benzene contains a discontinuty indicating that this molecule is possibly cracking into isomers of di-isopropyl benzene and propylene. The measured desorption diffusivity of 1,3,5 tri-isopropyl benzene reactant mixture is hypothesized to be the nonlinear co-diffusion of isomers of di-isopropyl benzene and propylene. In pellets diffusion of 1,3 di-isopropyl benzene and 1,3,5 tri-isopropyl benzene is micropore controlled. Diffusivity of 1,3 di-isopropyl benzene and 1,3,5 tri-isopropyl benzene in alumina particles is also examined. The alumina particle system has

a log-normal distribution, equilibrium is nonlinear, and diffusion appears to be macropore controlled.

Diffusivity of xylene isomers in HZSM-5 is also accomplished. The measured and reported literature diffusivity values are analyzed assuming a positive concentration dependence of diffusion. This results in a satisfactory explanation of much of the literature data when extrapolated to a zero loading basis.

Master of Science

King Fahd University of Petroleum & Minerals

Dhahran, Saudi Arabia

April 2004

Chapter 1

1.1 Introduction

Zeolites are crystalline microporous minerals, built up of silicon, aluminum and oxygen atoms. The name zeolite comes form Greek word *'zeo'* meaning to boil and *'lithos'* meaning stone. Nowadays, zeolites are available on a large scale and in a variety of applications. They are used as adsorbents in the purification of gas streams, removal of water and volatile organic species, and in the separation of different isomers and gas mixtures, and also in catalysis for the conversion of hydrocarbons.

1.2 Zeolite structure

Zeolite structures consist of silicon cations (Si^{+4}) and aluminum cations (Al^{+3}) that are surrounded by oxygen anions (O^{-2}). Each oxygen anion connects two cations and this yields a three dimensional framework with net neutral SiO_2 and negatively charged AlO_2^- tetrahedral building blocks. The negative charge arises from the difference in formal valency between the silicon and aluminum cations and is located on one of the oxygen ions connected to an aluminum cation. Commonly the negative charge is compensated by additional non-framework cations like sodium (Na^+) which are generally present after the synthesis of zeolite. However for catalytic application the sodium ion is replaced by protons (H^+) that form a bond with negatively charged oxygen anions of the zeolite. This results in Bronsted OH acid sites, and has been proven to be highly active in catalyzing

cracking and isomerization reactions. The zeolite structure consists of pore system with channels in one or two or three dimensions and additionally inner cavities may be present. The diameter of the pores and cavities ranges from 3Å to 12 Å, which coincides with the dimensions of many hydrocarbon molecules for which they are applied for adsorption and catalysis [Breck, 1974].

1.3 Zeolite Catalysis

As a catalyst zeolites exhibit exceptional properties with respect to both activity and selectivity because of their ability to adsorb and transform molecules in their inner pore volume. An important class of reactions performed by zeolites is the acid catalyzed reactions such as crude oil cracking, isomerization and fuel synthesis. After the introduction or deposition of metal into framework, zeolites can also act as a matrix accommodating oxidation reduction reactions. For all these types of reactions the major benefit lies in the unique microporous structure of zeolite. Because of their shape selective nature caused by the steric hindrance of intermediate and product species in the pore structure, zeolites have become important catalysts. The restrictive size of zeolite cages reduces the formation of intermediates that cannot fit into them without significant strain on their structure. Some of the products of a reaction may be bulkier than others; the less bulky one is then able to diffuse out faster. This creates a surplus of undesired product inside the catalyst structure, thus reaction is driven towards the formation of desired products [Rebo, 1976].

1.4 Diffusion in zeolite

As mentioned before, the micropore diameters of zeolite have similar dimensions to the molecules for which they are largely applied as catalysts. The migration of molecules through the zeolite occurs therefore in close contact with the micropore walls. The order of diffusion coefficients lies beyond molecular and Knudsen diffusion regimes and is known as "configurational diffusion" or intracrystalline diffusion. The typical values of diffusion coefficients lies between 10^{-8} to 10^{-20} m^2/sec [Ruthven, 1984]. Actual number is mainly determined by the size and nature of the sorbate molecule, the zeolite pore structure and temperature. In many cases low effective diffusivity in zeolite limits the rate of reaction [Van Bekkum et al. 1991].

1.5 Measurement of diffusion in zeolite

In the literature various experimental procedures are described to establish diffusion coefficients in zeolites. In general the available experimental methods can be divided into macroscopic and microscopic techniques. Gravimetric, volumetric and piezometric uptake measurements are the most simple and straightforward macroscopic techniques in which sorption rate of molecules are detected by a microbalance or a pressure recording device. An alternative approach has been developed by Niessen and Karger (1991), who studied the uptake rate of hydrocarbons using *in situ* infrared (IR) spectroscopy to monitor the appearance of a characteristic IR-band with time. The best known microscopic method to determine diffusion in zeolite is Pulsed Field Gradient – Nuclear Magnetic Resonance (PFG-NMR) spectroscopy, developed by Karger and Pfeifer (1987).

The disadvantage of various uptake methods as described is that a large part of sorbent molecules may bypass the zeolite bed. This may introduce problems with respect to the accuracy of the data due the presence of film diffusion, or intra particle gradients or heat effects. To overcome these problems Eic and Ruthven (1988) developed the zero length column (ZLC) method. In this the zeolite sample is equilibrated with the sorbate molecules. Subsequent purging of the sorbent of the sample with an inert gas desorbs the molecules and their concentration is followed chromatographically. By using high purge rates, mass and heat transfer effects can be eliminated.

1.6 Properties of catalysts and hydrocarbons

In our study we used NaY zeolite, HZSM-5 zeolite, alumina crystals and FCC catalyst pellets. We investigated the diffusivity of benzene, cumene, 1,3 di isopropyl benzene, 1,3,5 tri isopropyl benzene and xylene isomers in these catalysts. The properties of these catalysts and hydrocarbons are tabulated next. The data has been collected from references [1,4,12] and texts [3,5,6,9,13,14]. Some measurements of particle properties have been performed by Shakeel [15] in the Research Institute at KFUPM. Particle size has been determined by a Scanning Electron Microscope (SEM) at the research Institute in KFUPM.

Table 1.1: Properties of HNaY catalyst

Zeolite Type [14]	Faujasite
Channel geometry [14]	Three dimensional
Cavity size(Å) [14]	12
Number of O atoms in the larger aperture ring [14]	12
Pore size(Å) [14]	7.4
BET surface area (m^2/gm) [1]	583
Hydrated Density (gm/cc) [3]	1.92
Na_2O (wt. %) [1]	0.25
SiO_2/Al_2O_3 (mole/mole) [1]	5.7
Unit cell size (Å) [1]	24.51
Crystal size (μm) [1]	0.9

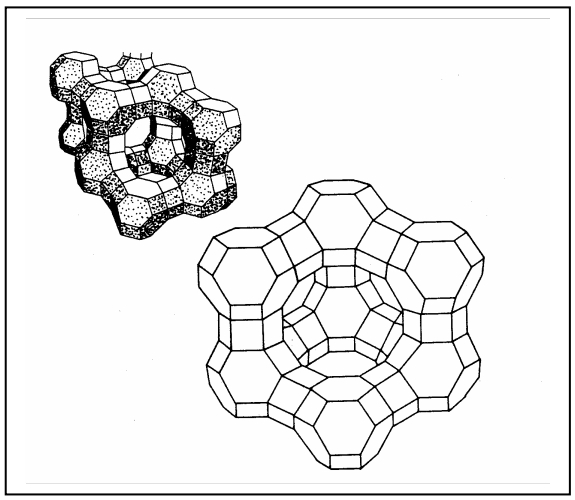

Figure 1.1: Y-Zeolite crystal.

Table 1.2: Properties of HZSM-5 catalyst

Zeolite Type [14]	MFI
Channel geometry [14]	Two dimensional
Number of O atoms in the larger aperture ring [14]	10
Pore size (Å) [14]	5.1x5.5 tube interconnecting with zig-zag 5.3x5.6 tube
BET surface area (m^2/gm) [15]	361
Hydrated Density (gm/cc) [15]	2.12
SiO_2/Al_2O_3 (mole/mole)[15]	31
Crystal size (μm) [15]	8.14

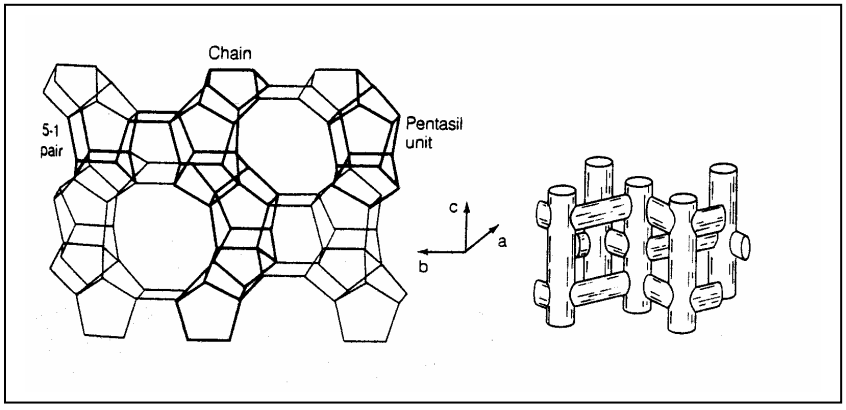

Figure 1.2: Zig-zag structure of ZSM5

Table 1.3: Properties of FCC catalyst

Pellet size (μm) *	50
Macropore size (Å) [1]	500
NaY Crystal size (μm) [1]	0.9
Hydrated pellet Density (gm/cc) [12]	1.5
Porosity [12]	0.5
Matrix [1]	SiO_2 (20 %) and Al_2O_3 (80 %)
Crystal vol (wt %) [1]	20

Ref : * SEM analysis, KFUPM-RI, 2003.

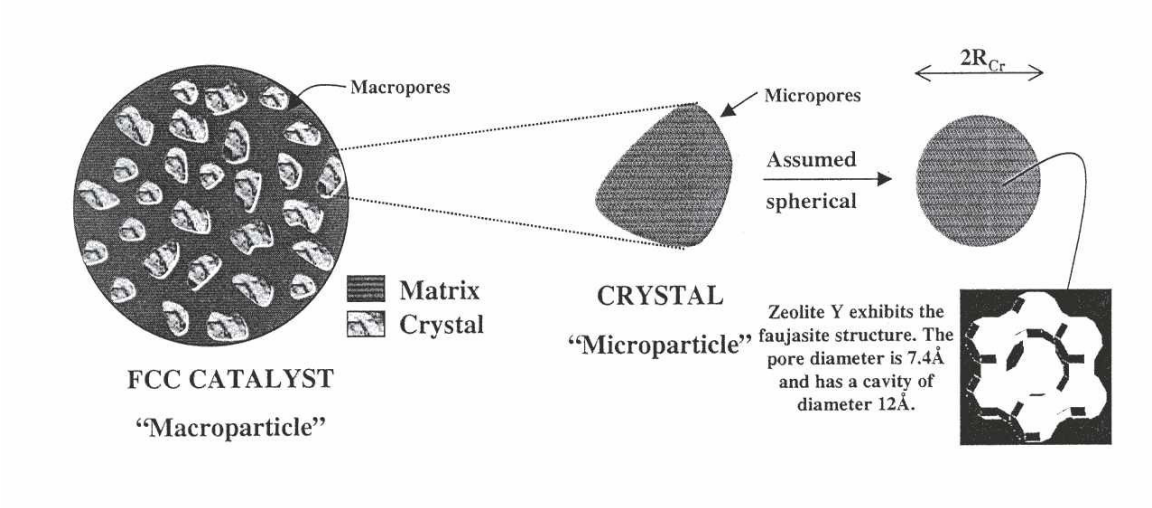

Figure 1.3: Pore network structure in a FCC pellet

Table 1.4: Properties of Alumina catalyst

Crystal size (μm)	50-300
Macropore size (Å)	>700
BET Surface area (m^2/gm)	370
Density (gm/cc)	2.8
Bulk density	0.7
Pore volume (cm^3/gm)	0.5

** Properties provided by Alcan Chemicals for AA-400 claus catalyst.*

Table 1.5: Properties of Hydrocarbon

Hydrocarbon Name	Chemical Formula	Molecular weight	Boiling point (^{o}C)	Molecular size (Å)
Benzene [9,13,14]	C_6H_6	78.12	80	5.85
Cumene [9,13,14] (Isopropyl benzene)	C_6H_5-CH-$(CH_3)_2$	120.2	159	6.8
1,3 di isopropyl benzene (3-Isopropyl Cumene) [9]	$C_{12}H_{18}$	162.28	210	8.4
1,3,5 tri isopropyl benzene [9]	$C_{15}H_{24}$	204.36	233	9.3
Para Xylene [4] (1,4 Dimethyl benzene)	C_8H_{10}	106.17	137	6.7
Meta Xylene [4] (1,3 Dimethyl benzene)	C_8H_{10}	106.17	137	7.4
Ortho Xylene [4] (1,2 Dimethyl benzene)	C_8H_{10}	106.17	145	7.3

N.B. : Boiling points are taken from HYSIS software database.

1.7 Objective of this work

The objectives of this thesis are

(1) To measure the diffusivity of benzene, cumene, 1,3 di isopropyl benzene and 1,3,5 tri isopropyl benzene in NaY zeolite crystals.

(2) To measure the diffusivity of benzene, cumene, 1,3 di isopropyl benzene and 1,3,5 tri isopropyl benzene in FCC catalyst pellets.

(3) To measure the diffusivity of xylene isomers in HZSM-5 zeolite crystals.

(4) To measure the diffusivity of 1,3 di isopropyl benzene and 1,3,5 tri isopropyl benzene in alumina crystals.

(5) To study the effect of temperature as a contributing factor controlling diffusion in zeolites and hence calculate the activation energies for diffusion.

(6) To investigate the adsorption equilibrium constants (Henry's law constants) and heat of adsorption for crystal system.

1.8 References

[1] Al-Khattaf, S., de Lasa, H., "The role of diffusion in alkyl-benzenes catalytic cracking", Applied catalysis, A: General, 5855 (2001) 1-15.

[2] Bekkum, H.V., Flanigen, E. M., Jansen J. C, "Introduction to zeolite science and practice studies in surface science and catalysis: vol 58, (1991).

[3] Breck, D. W., "Zeolite molecular sieves structure, chemistry, and use", John Wiley & Sons, Inc., New York, (1974).

[4] Choudhary, V. R., Nayak, V. S., Choudhary, T. V., "Single component sorption/diffusion of cyclic compounds from their bulk liquid phase in H-ZSM-5 zeolite", Ind. Eng. Chem. Res., (1997), 36, 1812-1818.

[5] Do, D. D., "Adsorption analysis: Equilibria and Kinetics", Imperial College Press, London, Vol 2, (1998).

[6] Eic, M., Ruthven, D.M., "A new experimental technique for measurement of intracrystalline diffusivity", Zeolites, (1988), 8, 40-45.

[7] Fogler, H. S., "Elements of chemical reaction engineering", Prentice Hall International Series, NJ, 2nd edition, (1999).

[8] Karger, J., Pfeifer, H., "NMR self diffusion studies in zeolite science and technology", Zeolite (1987), 7(2), 90-107.

[9] Karger, J.; Ruthven, D. M., "Diffusion in zeolites and other microporous solids", John Wiley & Sons, Inc., New York, (1992).

[10] Niessen, W., Karge, H. G., "Investigation of diffusion and counter diffusion of benzene and ethylebenzene in ZSM-5 type zeolite by novel IR technique", Studies in surface science and catalysis 60, 213-21 (1991).

[11] Rabo, Jule A. Ed., "Zeolite chemistry and catalysis", ACS monograph 171, ACS Washington, (1976).

[12] Ronald, G. McClung, "Effect of FCC catalyst physical properties on particulate emission", www.refiningonline.com/EngelhardKB/crep/TCR6_48.htm and TCR1_6.htm.

[13] Ruthven, D. M., "Principles of adsorption and adsorption process", John Wiley & Sons, New York, (1984).

[14] Satterfield, C. N., "Heterogeneous catalysis in industrial practice", McGraw Hill, New York 2nd edition, (1993).

[15] Shakeel ,A., personal communication, (2003).

Chapter 2

Theory and Literature review of the ZLC

2.1 Theory of Zero Length Column (ZLC) Chromatography

With strongly adsorbed species, determination of intracrystalline diffusivity from conventional uptake rate measurement becomes increasingly difficult. As the strength of adsorption increases, it becomes more and more difficult to eliminate the intrusion of heat transfer and bed diffusion resistance. Such effects may be minimized by the use of large crystals and very small adsorbent samples. But for most zeolites, crystals greater than about 100μm are not available and the minimum sample size is limited by the sensitivity of the equipment to a few mg. For accurate measurement of the rapid intracrystalline diffusion process with strongly adsorbed species; with the intrusion of extraneous heat and mass transfer resistance, an alternative experimental technique was invented, known as Zero Length Column method.

The original idea for ZLC system dates back to the late 1970s (Ruthven personal communication), but it was not until the late 1980s that the well known Eic and Ruthven (1988) paper appeared. It is a simple and relatively straight forward technique of measuring diffusion coefficients in zeolite particle. The zero length column technique retains the main feature of conventional chromatographic techniques and eliminates the

effect of axial dispersion. The ZLC is a differential bed of porous particle which is first equilibrated with the fluid mixture containing the adsorbed species, at time zero the adsorbing gas is stopped, and switched to carrier gas flow only through the ZLC at sufficiently high flow rate so as to eliminate rapid heat and mass transfer between gas and solid. The desorption curve is analyzed in terms of concentration of adsorbate versus time. This method is widely applied to gaseous systems (Brandani and Ruthven, 1996, Silva and Rodrigues, 1997) and liquid systems, (Ruthven and Stapleton, 1993; Brandani and Ruthven, 1995,1996).

2.2 Assumptions for Mathematical model

The mathematical model describing the ZLC system is based on the following assumptions:

(1) The adsorbent pellet has a porous structure containing micropores and macropores;

(2) Fick's law of diffusion is valid in both macropores and micropores;

(3) The adsorption equilibrium isotherm is linear;

(4) There is no film resistance at the adsorbent external surface;

(5) The ZLC cell is considered equivalent to a continuous stirred tank adsorber;

(6) Crystals have spherical geometry; and

(7) Isothermal operation is assumed.

2.3 Derivation of Mathematical model

Consider a very thin layer of zeolite crystals uniformly equilibrated with a gas phase at sorbate concentration C_0. At t=0, the carrier gas is switched to a purge (non adsorbing) carrier stream and the effluent concentration c(t) is monitored on a flame ionization detector.

The differential mass balance for the crystal is

$$\frac{\partial q}{\partial t} = D\left(\frac{\partial^2 q}{\partial r^2} + \frac{2}{r}\frac{\partial q}{\partial r}\right) \tag{2.1}$$

$$\left.\begin{aligned} &\frac{\partial q}{\partial r}(0,t) = 0 \\ &q(R,t) = Kc(t) \\ &q(r,0) = q_o = Kc_o \end{aligned}\right\} \tag{2.2}$$

From the mass balance over the cell a further boundary condition must be included.

$$D\frac{\partial q}{\partial r}(R,t) + \frac{1}{3}\frac{FR}{V_s K}q(R,t) = 0 \tag{2.3}$$

The solution of these equations, subject to these boundary conditions, is readily obtained by separation of variables or directly from known solutions (Crank, 1965).

The resulting expression for the desorption curve is:

$$\frac{\bar{q}}{q_o} = \frac{c}{c_o} = 2L\sum_{n=1}^{\infty}\frac{\exp\left(-\frac{\beta_n^2 Dt}{R^2}\right)}{\left[\beta_n^2 + L(L-1)\right]} \tag{2.4}$$

where, β_n is given by the roots of the following equation:

$$\beta_n \cot\beta_n + L - 1 = 0 \tag{2.5}$$

In this equation, L is given by,

$$L = \frac{1}{3}\frac{FR^2}{KV_s D} \tag{2.6}$$

L can be expressed as

$$L = \left(\frac{1}{3}\right)\left(\frac{Purge\ flow\ rate}{Crystal\ volume}\right)\left(\frac{R^2}{KD}\right) \tag{2.7}$$

Corresponding expression for a parallel sided adsorbent slab (half thickness) are:

$$\frac{c}{c_o} = 2L\sum_{n=1}^{\infty}\frac{\exp\left(-\frac{\beta_n{}^2 Dt}{l^2}\right)}{\left[\beta_n{}^2 + L(L-1)\right]} \tag{2.8}$$

where, β_n is given by

$$\beta_n \tan\beta_n = L = \frac{Fl^2}{KV_s D} \tag{2.9}$$

In the long time region Equation (2.4) reduces to a simple exponential decay curve since only the first term of the summation is significant:

$$\frac{c}{c_o} = \frac{2L}{\left[\beta_1{}^2 + L(L-1)\right]}\exp\left(-\frac{\beta_1{}^2 Dt}{R^2}\right) \tag{2.10}$$

Under these conditions we can thus determine D/R^2 and L directly from the slope and intercept of the semilogarithmic plot of c/c_o vs. t. This is known as long time (LT) analysis.

2.4 Short time analysis

The initial portion of the desorption curve is less sensitive to the errors that may arise from baseline drift or from a final rate of heat dissipation. A comparison between the long time and short time values may then be used as a check on the validity of the data. Brandani et al.(1996) derived an approximate solution for the short time solution

$$\frac{c}{c_o} \cong 1 - 2L\sqrt{\frac{Dt}{\pi R^2}} \tag{2.11}$$

This solution is of particular use for low values of the parameter L. From the slope of the plot of $(1 - c/c_o)$ vs $t^{1/2}$, we can get the value of $2L\left(\frac{D}{\pi R^2}\right)^{1/2}$. The choice of time zero has a large effect on the initial slope. More useful plot is therefore $(1-C/C_o)/t^{1/2}$ vs $t^{1/2}$. From the intercept we can get the value of $2L\left(\frac{D}{\pi R^2}\right)^{1/2}$.

Hufton and Ruthven (1994) proposed a method of analyzing the short time region of the desorption curve based on the approximate solution of equation (2.1) for a step change in surface concentration

$$1 - \frac{\bar{q}(t)}{q_o} = \frac{6}{R}\sqrt{\frac{Dt}{\pi}} - \frac{3Dt}{R^2} \tag{2.12}$$

where the average concentration is given by

$$\bar{q}(t) = \frac{3}{R^3}\int_0^R r^2 q(r,t)dr \tag{2.13}$$

The desorption curve has the expression

$$\frac{c}{c_o} = \frac{1}{L}\left[\sqrt{\frac{R^2}{\pi Dt}} - 1\right] \tag{2.14}$$

This equation cannot be correct in the time limit t → 0 or when L is small since under these conditions it predicts $C/C_o \rightarrow \infty$, due to the assumption based on the boundary condition.

The most severe limitation of the choice of operating conditions is generally that the rate of the process be slow enough to measure without intrusion of extraneous time delay resulting from the inevitable dead volume in the system. A reasonable criteria is $\frac{D}{r_c^2} << 0.05\,\sec^{-1}$ [Karger and Ruthven, 1992]. The use of the short time solution is probably more prone to this limitation than the long time solution.

2.5 Fluid phase holdup

The simple model of ZLC doesn't take account of the hold up of sorbate in the fluid phase. Brandani and Ruthven (1996) suggested the following model taking account of fluid phase hold up for more accurate results.

$$\frac{c}{c_o} = 2L\sum_{n=1}^{\infty} \frac{\exp\left(-\frac{\beta_n{}^2 Dt}{R^2}\right)}{\left[\beta_n{}^2 + (L-1-\gamma\beta_n^2)^2 + L-1+\gamma\beta_n^2\right]} \tag{2.15}$$

$$\beta_n \cot\beta_n + L - 1 - \gamma\beta_n^2 = 0 \tag{2.16}$$

where the parameter $\gamma = \frac{V_f}{3KV_s}$, characterizes the ratio of external to internal holdup. For gaseous system we can neglect the hold up but for liquid system proper allowance for extra particle hold up is essential.

2.6 External mass transfer effect

The original ZLC model assumes instantaneous equilibration at the external surface of the adsorbent particle, i.e. no external resistance to mass transfer. Eic and Ruthven (1989) extended the analysis to allow external mass transfer resistance. The final expression of the desorption curve remains same but the value of parameter L changes by the following equation

$$\frac{1}{L} = KD\left[\frac{3V_s}{FR^2} + \frac{2}{ShD_m}\right] \tag{2.17}$$

where the Sherwood number is given by

$$Sh = \frac{k_c 2R}{D_m} \tag{2.18}$$

2.7 Moment analysis

The method of moments is a commonly used technique for the extraction of kinetic parameters from chromatographic experiments (Ruthven 1984). The expressions for area under adsorption curve, first moment and second moment are as follows

$$I = \int_o^\infty \frac{c}{c_o} dt \quad ; \quad \mu = \frac{\int_o^\infty ct\, dt}{\int_o^\infty c\, dt} \quad ; \quad \sigma = \frac{\int_o^\infty ct^2\, dt}{\int_o^\infty c\, dt} - \mu^2 \tag{2.19}$$

Brandani and Ruthven (1996) derived the relevant equations for analyzing ZLC desorption curves using the moment approach. For gaseous systems ($\gamma = \frac{1}{3}\frac{V_f}{KV_s} \approx 0$), where diffusion controls process (1 < L < 20), the moment expressions are given by

$$\begin{aligned} I_0 &= \frac{1}{3L}\frac{R^2}{D} \\ \mu_0 &= \frac{1}{15}\frac{R^2}{D}\frac{5+L}{L} \\ \sigma_0^{\,2} &= \frac{1}{15}\left(\frac{R^2}{D}\right)^2\left(\frac{25}{L^2}+\frac{10}{L}+\frac{13}{7}\right) \end{aligned} \tag{2.20}$$

and the ratio is given by

$$\frac{\mu_o}{I_o} = 1+\frac{L}{5} \quad ; \quad \frac{\sigma_o^2}{\mu_o^2} = 15\left[1+\frac{6}{7}\left(\frac{L}{L+5}\right)^2\right] \tag{2.21}$$

These relationships can be used to obtain the parameter L and time constant D/R^2 from the experimental curves.

2.8 Equilibrium control

When the flow rate is sufficiently small contact time is large compared with the diffusion time (R^2/D) the system should approach equilibrium. Under these conditions the desorption curve reduces to simple exponential decay Brandani et al. (1996)

$$\frac{c(t)}{c_o} = \exp\left(-\frac{Ft}{KV_s}\right) \tag{2.22}$$

This expression can be derived directly from equation (2.4) by extracting the limit for L $\rightarrow$ 0. This equation is a good approximation for L < 0.5.

To avoid the region of equilibrium control it is desirable to make ZLC diffusion measurements under conditions such that L must be greater than 5. Higher value of L has the advantage that for L > 10, β_1 approaches π, so the diffusional time constant may be directly measured from the slope of the long time asymptote. Under these conditions the slope of the plot of ln(c/co) vs t becomes essentially independent of purge flow rate but the intercept decreases, approaching inverse proportionality with the flow rate at high L. Variation of purge flow rate thus provides a simple experimental test for kinetic or equilibrium control.

Sometimes it is useful to make measurements at very low flow rates within the equilibrium control regime, from which reliable values of the equilibrium parameter (KV_s) can be determined and checked with the high flow rate data (Brandani et al. 2003a).

2.9 Equilibration time

The initial steps in a ZLC experiment involve equilibrating the sample with a feed stream containing a known steady concentration of sorbate. The approach to equilibrium of the effluent fluid concentration is given by equation (2.4) providing there is no mass transfer

limitation while approach of the adsorbed phase concentration is given by the corresponding expression given by Crank (1965)

$$\frac{\bar{q}}{q_o} = \sum \frac{6L^2 \exp\left(-\frac{\beta_n^2 Dt}{R^2}\right)}{\beta_n^2\left[\beta_n^2 + L(L-1)\right]} \tag{2.23}$$

From these expressions one may calculate the time required for the effluent fluid concentration and the adsorbed phase concentration to approach within 1% of their final steady values ($C/C_o = q/q_o=0.99$). It is evident that the approach of the adsorbed phase equilibrium is much slower than that of the fluid phase concentration.

2.10 Effect of partial equilibrium

On the LT analysis

The largest error will be in the determination of intercept and therefore of L. Since the intercept will be lower than the value for a uniform initial condition, calculated value of L will be erroneously high and error in the equilibrium values may be large (K will be underestimated). The effect on D will be small (error less than 1%) since, at high L, β_1 is always approximately equal to π.

On ST analysis

The slope remains unchanged but the intercept is affected. The deviation is proportional to 1/L and the apparent L is lower. Since the derived diffusivity is proportional to $1/L^2$,

the apparent D can be overestimated. The error in K values will therefore be proportional to L, and the apparent K will be larger. This assumes no limitation due to dead volume in the operating conditions.

2.11 Heat effect in ZLC experiments

The intrusion of heat effects is a major drawback in the measurement of intracrystalline diffusivities in adsorbents from uptake experiments. Nonisothermal desorption in ZLC system has been studied by Brandani et al. (1998) and Silva et al. (2001) to yield a criterion for which heat effect can be neglected. The original isothermal model was extended to nonisothermal systems by adding the energy balance. It was assumed that the fluid phase is isothermal, and external mass transfer effects are negligible. The energy balance is given by

$$(-\Delta H)\frac{d\overline{q}}{dt} = C_p \frac{dT}{dt} + ha\left(T - T_o\right) \tag{2.24}$$

where h is the external heat transfer coefficient, T_o temperature of the carrier phase, T is the temperature of the sorbent, $(-\Delta H)$ is the heat of adsorption, and C_p is the heat capacity of the adsorbent.

Assuming that at low adsorbate loading the equilibrium relationship is linear and temperature changes are small, the equilibrium may be represented by the following equation

$$q = q_o + \left.\frac{\partial q}{\partial c}\right|_{c_o,T_o}(c - c_o) + \left.\frac{\partial q}{\partial T}\right|_{c_o,T_o}(T - T_o) \tag{2.25}$$

Initial conditions are

$t = 0;\ q = q_o = K(T_o)c_o;\ T = T_o;$ for all r (2.26)

These equations must be solved simultaneously with diffusion equations. From the solution it was found that the group parameter $3L\beta/\alpha$ can be used as a criterion for negligible heat effects, where $\alpha = \frac{ha}{C_p}\frac{r_c^2}{D_c}$ and $\beta = \frac{\Delta H}{C_p}\left.\frac{\partial q}{\partial T}\right|_{c_o,T_o}$. Thus the group parameter becomes, assuming van't Hoff relation of temperature dependence of K

$$\frac{3L\beta}{\alpha} = \frac{-F(-\Delta H)\left.\frac{\partial q}{\partial T}\right|_{c_o,T_o}}{KV_s ha} = c_o\frac{F}{V_s}\frac{(-\Delta H)^2}{RT_o^2 ha}. \tag{2.27}$$

The criterion for heat effects may be described as

$\frac{3L\beta}{\alpha} \pi\ 0.1$, the system is isothermal.

$\frac{3L\beta}{\alpha} \phi\ 100$, the system is completely dominated by heat transfer.

The long time straight line solution is practically parallel to the time axis meaning it takes a long time for the adsorbed species to leave the adsorbent.

The heat effects can be minimized by

(i) Decreasing the gas concentration c_o of the species used to saturate the adsorbent,

(ii) Decreasing the space velocity of (F/V_s) in the ZLC cell, or

(iii) Decreasing the particle size a (external surface area per unit volume of the adsorbent).

2.12 Isotherm nonlinearity

The assumption of linearity in the adsorption isotherm is not valid specially when considering strongly adsorbed species. It is therefore possible to have erroneous experimental results. Brandani (1998) developed the model for ZLC experiments to analyze the effect of nonlinear equilibrium on the resulting apparent diffusivities.

The nonlinear equilibrium is taken into account considering Langmuir adsorption isotherm. The cell mass balance for the desorption isotherm is given by:

$$V_s \frac{d\overline{q}}{dt} + Fc = 0 \tag{2.28}$$

where V_s is the volume of the solid, $\overline{q}$ is the average concentration inside the particle, F is the volumetric flow rate and c is the composition in the fluid phase mass balance. Assuming a spherical particle and the diffusivity to be concentration dependent, the mass balance is:

$$\frac{\partial q}{\partial t} = \frac{1}{r^2}\frac{\partial}{\partial r}\left(D(q) r^2 \frac{\partial q}{\partial r} \right) \tag{2.29}$$

From the overall mass balance in the solid the following relationship holds at the boundary:

$$\frac{\partial \overline{q}}{\partial t} = \frac{3}{R}\left(D(q)\frac{\partial q}{\partial r} \right)_{r=R} \tag{2.30}$$

For the boundary condition we assume Langmuir equilibrium at the surface and the symmetry condition:

$$\frac{q(R,t)}{q_s} = \frac{bc}{1+bc} \tag{2.31}$$

$$\left(\frac{\partial q}{\partial r} \right)_{r=0} = 0 \tag{2.32}$$

Final assumption is that the concentration dependence of the diffusivity may be described according to Darken's equation (Karger and Ruthven, 1992) for which the Langmuir isotherm yields:

$$D(q) = D_o \frac{d\ln p}{d\ln q} = \frac{D_0}{1-\frac{q}{q_s}} \tag{2.33}$$

where, D_o is the diffusivity at infinite dilution. The mathematical model is fully formulated once the initial conditions are defined. For desorption experiments they are $c(0) = c_o$ and $q(r,0) = q$, where c_o and q_o satisfy the equilibrium condition.

To derive the dimensionless form of the equations we have to define the following dimensionless variables:

$$Q = \frac{q}{q_s}, C = \frac{c}{c_o}, \ \tau = \frac{D_0 t}{R^2}, \ \xi = \frac{r}{R} \tag{2.34}$$

and dimensionless parameters

$$L = \frac{1}{3}\frac{FR^2}{KV_s D_o}, \quad \lambda = \frac{q_o}{q_s} \tag{2.35}$$

where the Henry's constant is given by K = bq_s. The resulting equations are:

$$\frac{1-\lambda+\lambda c}{1-\lambda}\left(\frac{\partial Q}{\partial \xi}\right)_{\xi=1} + \frac{LC}{1-\lambda} = 0 \tag{2.36}$$

$$\frac{\partial Q}{\partial \tau} = \frac{1}{1-\lambda}\left(\frac{\partial^2 Q}{\partial \xi^2} + \frac{2}{\xi}\frac{\partial Q}{\partial \xi}\right) + \frac{\lambda}{(1-\lambda Q)^2}\left(\frac{\partial Q}{\partial \xi}\right)^2 \tag{2.37}$$

$$Q(1,\tau) = \frac{C}{1-\lambda+\lambda C} \tag{2.38}$$

$$\left(\frac{\partial Q}{\partial \xi}\right)_{\xi=0} = 0 \tag{2.39}$$

The column mass balance can be written as

$$\frac{1}{3}\frac{d\overline{Q}}{dL\tau} + \frac{C}{1-\lambda} = 0 \tag{2.40}$$

The solution of these equations for LT asymptote is given by

$$\ln\frac{c}{c_o} = \ln(1-\lambda) - \lambda + \ln\left(\frac{2L}{\beta_1^2 + L(L-1)}\right) - \beta_1^2\frac{D_o t}{R^2} \tag{2.41}$$

If $\lambda \rightarrow 0$, the solution is the same as for the linear isotherm.

For tracer exchange (Hufton et al. 1994) the solution for LT asymptote is given by

$$\ln\frac{c}{c_o} = \ln\left(\frac{2L_{Tracer}}{\beta_{Tracer}^2 + L_{Tracer}(L_{Tracer}-1)}\right) - \beta_{Tracer}^2\frac{D_o t}{R^2} \tag{2.42}$$

where, $L_{Tracer} = \frac{L}{1-\lambda}$, and higher than L and in this case the actual diffusivity is always greater than D_o. The real LT asymptote is given by the average for the two solutions, which is

$$\ln\frac{c}{c_o} = \ln(1-\lambda) - \lambda + \ln\left(\frac{2L_{Tracer}}{\beta_{Tracer}^2 + L_{Tracer}(L_{Tracer}-1)}\right) + \ln\left(\frac{2L}{\beta_1^2 + L(L-1)}\right) - \beta_1^2\frac{D_o t}{R^2} \quad (2.43)$$

From the practical point of view we come to the conclusion that nonlinearity affects the intercept of the $\ln(c/c_o)$ vs t plot but has negligible effect on the slope at long time.

2.13 Model for liquid system

ZLC method was extended to the measurement of counter-diffusion in liquid phase adsorption systems (Ruthven and Stapleton, 1993). The application of this technique to liquid system is experimentally less convenient than for gas phase system because of much greater importance of the fluid phase holdup. In the liquid phase adsorption system the holdup in the external fluid is generally of the same order as in the adsorbed phase. So it is essential to take account of the time variation of the concentration at the surface of the adsorbent particle, which is assumed to be at equilibrium with the interstitial fluid. Brandani and Ruthven (1995) present an improved model to represent desorption curves and analytical solution for a more realistic model in which mass transfer is controlled by the intraparticle diffusion. Model was developed for linear adsorption isotherm.

Fluid phase mass balance:

$$V_s\frac{d\overline{q}}{dt} + V_f\frac{dc}{dt} + F.c = 0 \quad (2.44)$$

Solid phase mass balance

$$\frac{\partial q}{\partial t} = D\left(\frac{\partial^2 q}{\partial r^2} + \frac{2}{r}\frac{\partial q}{\partial r}\right) \quad (2.45)$$

Initial condition

$q(r,0) = q_0 K c_0; \quad c(0)=c_o$ (2.46)

Boundary condition:

$$\left(\frac{\partial q}{\partial r}\right)_{r=0} = 0. \tag{2.47}$$

Equation (2.44) can be considered as a boundary condition on the solid phase mass balance, [ie eq(2.45)]

$$\frac{4}{3}\pi R^3 \frac{d\overline{q}}{dt} = 4\pi R^2 D\left(\frac{\partial q}{\partial r}\right)_{r=R} \tag{2.48}$$

with equilibrium with the surface

$q(R,t)=Kc(t)$ (2.49)

Equation (2.44) can be rewritte as

$$\frac{3}{R} DV_s \frac{\partial q}{\partial r} + \frac{V_f}{K}\frac{\partial q}{\partial t} + \frac{F}{K} q = 0 \qquad at \quad r = R \tag{2.50}$$

The solution is therefore, for the adsorption phase assuming no mass transfer limitations

$$\frac{q(r,t)}{q_0} = \frac{R}{r}\sum \frac{2L}{\beta_n{}^2 + (1-L+\gamma\beta_n{}^2) + L - 1 + \gamma\beta_n{}^2} \times \frac{\sin[\beta_n (r/R)]}{\sin \beta_n} \exp\left(-\beta_n{}^2 \frac{D}{R^2} t\right) \tag{2.51}$$

and for the desorption curve

$$\frac{c(t)}{c_0} = \sum \frac{2L}{\beta_n{}^2 + (1-L+\gamma\beta_n{}^2) + L - 1 + \gamma\beta_n{}^2} \exp\left(-\beta_n{}^2 \frac{D}{R^2} t\right) \tag{2.52}$$

The eigenvalues are calculated using

$$\beta_n \cot \beta_n + L - 1 - \gamma\beta_n^2 = 0 \tag{2.53}$$

and the dimensionless parameter γ (ratio of the fluid capacity for the sorbate to that of sorbent) is given by,

$$\gamma = \frac{V_f}{3KV_s} \tag{2.54}$$

If we take γ = 0, for the special case, the equation reduces to original ZLC model in which the effect of fluid holdup is neglected.

Liquid phase systems tend to have adsorption coefficients (K) of approximately unity (Since the liquid and adsorbed phase densities are generally of the same order of magnitude). K values for vapor systems are of the order of hundreds or thousands. Thus the parameter γ may generally be neglected for gaseous systems.

2.14 Effect of crystal size distribution

Crystal size distribution introduces tailing into the normally linear long time region of the desorption curve. Analyzing such curve with standard ZLC model causes the diffusional time constant to be under predicted, where as the adsorption related parameter L is over predicted. Duncan and Moller (2002) developed a model to incorporate the effect of sorbate size distribution on the zero length column method for measuring intracrystalline diffusion. They showed that the curve may be well approximated by summing the desorption curves of the individual, discrete size fractions, weighted by their volume fraction. The solution of the desorption curve in Laplace domain is given

$$\frac{\hat{C}}{C_o} = \frac{1}{s} \frac{\int_{-\infty}^{\infty} \left[\left(e^{\sqrt{2}\sigma\varsigma}\sqrt{s}\right)\coth\left(e^{\sqrt{2}\sigma\varsigma}\sqrt{s}\right) - 1\right] e^{\sqrt{2}\sigma\varsigma - \varsigma^2} d\varsigma}{\sqrt{\pi} L_m e^{4.5\sigma^2} + \int_{-\infty}^{\infty} \left[\left(e^{\sqrt{2}\sigma\varsigma}\sqrt{s}\right)\coth\left(e^{\sqrt{2}\sigma\varsigma}\sqrt{s}\right) - 1\right] e^{\sqrt{2}\sigma\varsigma - \varsigma^2} d\varsigma} \tag{2.55}$$

where

$$\left.\begin{aligned} L_m &= \frac{FR_m^2}{3V_s KD} \\ R_m &= e^{\mu} \end{aligned}\right\} \tag{2.56}$$

This equation can be solved numerically using the Fast Fourier Transform technique, with the indicated integral being evaluated by Gauss-Hermite quadrature.

For σ = 0, the solution becomes the standard solution for ZLC in laplace domain (Brandani and Ruthven, 1996)

$$\frac{\hat{C}}{C_o} = \frac{1}{s}\frac{\sqrt{s}\coth\sqrt{s}-1}{L+\sqrt{s}\coth\sqrt{s}-1} \tag{2.57}$$

2.15 Measurement of adsorption equilibrium

If ZLC experiments are performed at a sufficiently low flowrate, the desorption curve will be determined by convection under equilibrium conditions. The effluent concentration history then directly yields the equilibrium isotherm. Brandani et al. (2003 a, b) developed the technique both for single component and multi-component systems and also accomplished the experimental validation of the model.

Differential mass balance for the ZLC system can be expressed as

$$V_s \frac{d\overline{q}}{dt} + V_g \frac{dc}{dt} + FC = 0 \tag{2.58}$$

For linear equilibrium

$$\overline{q} = q^* = Kc \tag{2.59}$$

with the initial condition

$$t = 0, \quad q = q_o = Kc_o \tag{2.60}$$

The concentration response curve is given by

$$\ln \frac{c}{c_o} = \frac{-Ft}{KV_s + V_g} \tag{2.61}$$

for Langmuir equilibrium

$$\frac{q^*}{q_s} = \frac{bc}{1+bc} \tag{2.62}$$

The concentration respond curve is given by

$$\ln \frac{c}{c_o} = \frac{-Ft}{KV_s + V_g} - \frac{KV_s}{KV_s + V_g}\left[\frac{1}{1+bc} - \frac{1}{1+bc_o} + \ln\left(\frac{1+bc_o}{1+bc}\right)\right] \tag{2.63}$$

Henry's constant can be found from the slope of the long time asymptote from the plot $\ln(c/c_o)$ vs Ft.

To calculate the complete isotherm we have to integrate equation (2.58). Equation (2.58) can be rewritten in the form

$$FC\frac{y}{1-y} = -V_s \frac{dq^*}{dt} - V_g C \frac{dy}{dt} \tag{2.64}$$

where y represents the mole fraction of the sorbate in the effluent gas stream. Integration from t = 0, y = y_o yields

$$q^* = \frac{FC}{V_s}\int_0^{\infty} \frac{y/y_o}{\frac{1}{y_o} - \frac{y}{y_o}} dt - \frac{FC}{V_s}\int_0^{t} \frac{y/y_o}{\frac{1}{y_o} - \frac{y}{y_o}} dt - \frac{V_g}{V_s} c_o \frac{y}{y_o} \tag{2.65}$$

Integration of the desorption curve thus yields the equilibrium isotherm q^* vs c.

For multicomponent systems, the differential mass balance for the ZLC cell becomes

$$V_s \frac{d\bar{q}_A^*}{dt} + V_g C \frac{dy_A}{dt} + \frac{FCy_A}{1 - y_A - y_B} = 0 \tag{2.66}$$

Integration of the response from the initial conditions $y_A = y_{Ao}$ at t = 0 yields

$$q_A^*(t) = \frac{FC}{V_s}\int_t^{\infty} \frac{y_A}{1 - y_A - y_B} dt - \frac{V_g C}{V_s} y_A \tag{2.67}$$

For component B we have a similar expression.

2.16 Extension of ZLC technique

Self diffusion measurement

A simple variant of the ZLC experiment (tracer ZLC or TZLC), can extend the technique to the measurement of self diffusion. The sample is pre-equilibrated with sorbate at a specific partial pressure and at time zero the flow is switched to a stream containing the same sorbate at the same concentration but in an isotopically different form. Desorption of the pre-equilibrated isotopic species is followed by an online mass spectrometer. Mathematical model is same as that for a normal ZLC experiment except that the

equilibrium constant (K) is replaced by equilibrium concentration ratio (q*/c). By varying the sorbate partial pressure such measurements can be made over a range of sorbate concentrations thus yielding the concentration dependence of the self diffusivity.

Counter diffusion measurement

Brandani et al. (2000) made further extension to ZLC technique to measure the counter diffusion. The sample is pre-equilibrated with a certain partial pressure of component A and then at time zero the flow is switched to a carrier stream containing component B. Depending on the equilibrium constants and partial pressure such an experiment can be made under conditions of net adsorption, desorption or equimolar counter diffusion. In this way it is possible to investigate hindrance effects by comparing counter exchange, normal ZLC or NZLC and TZLC response curve under comparable conditions.

2.17 Review of other studies accomplished by ZLC method

Benzene diffuses rapidly in NaX zeolite crystals. So it is difficult to obtain a reliable diffusivity data from the uptake or tracer exchange rate measurement. The new ZLC chromatographic method is well suited for the study of rapidly diffusing and strongly adsorbed species like benzene. Eic et al. (1988) measured the diffusion of benzene in large crystal of both natural faujasite and NaX zeolite by conventional gravimetric

method and by the new ZLC chromatographic method. Results of both type of measurement are consistent.

Eic and Ruthven (1989), reported the diffusion of benzene and several linear paraffins in large crystals of silicalite. The ZLC data is consistent with recently reported membrane, piezometric and frequency response values. Also they found a trend of decreasing diffusivity with increasing carbon number upto C_6 and thereafter the rate of change is much smaller in all the three, 5A, silicalite and 13X zeolite crystals.

Bulow and Micke (1995), derive a complete solution of ZLC chromatography using a Volterra integral technique. The model includes the effect of nonlinearity, extracolumn broadening and various type of intrinsic sorption kinetics. The model also describes the initial stage of ZLC chromatographic experiment. They also investigate the influence of diffusivity, the carrier gas flow rate and the isotherm non-linearity on the shape of the system response curves.

Cavalcante et al. (2000) investigated sorption and diffusion of p-Xylene and o-Xylene in Aluminophosphate molecular sieve $AlPO_4$-11. Equilibrium data were correlated using Langmuir, Virial and Dubinin plots in order to estimate equilibrium constants, saturation capacity and heat of adsorption at low coverage. Intracrystalline diffusivities at higher temperature (150-180^{0}C) were measured by ZLC method. Diffusivities from both methods agree reasonably well and follow a typical Arrhenius behavior with low activation energy.

Of the zeolites currently in use as adsorbents and catalysis, some have isotropic (three dimensional) pore structures and show the corresponding diffusional behavior (zeolites A, X, Y, erionite and chabazite), whereas others have pore structures that favor diffusion in one direction ($ALPO_4$-5, silicalite, mordenite, and offretite). The difference in behavior should be reflected in the diffusion model and hence in the form in the transient uptake curve, as well as in the critical dimension on which the diffusional time constant is based. Cavalcante et al. (1997) showed a simple method of distinguishing between one-dimensional and three-dimensional diffusion in zero length column based on the expression obtained for the ZLC desorption curves for 'slab' and 'spherical' diffusion models.

Rodrigues et al.(1998) extended the ZLC technique to measure the intraparticle diffusion in ion-exchangers. They develop a mathematical model to describe the response of ZLC ion exchange system. The model allows the use of non-linear ion-exchange equilibrium isotherms, describes ion fluxes with Nernst-Plank equation and includes the resistance to mass transfer both in the particle and in the film. Simulations are carried out to analyze the effect of model parameters on the system response curve. They use several ion exchange systems Na^+-H^+, K^+-H^+, and K^+-Na^+ to measure the validity of the model. They obtain the value of diffusivity of Na^+, K^+ and H^+ using the experimental procedures which are the same order of magnitude of those previously reported.

Duncan and Moller (2000) measured the sorption kinetics of cyclohexane in three samples of ZSM-5, differing in size and morphology using ZLC method. The diffusivities were found to be quite consistent across the sample and agree well with previously published data except that the small zeolite crystals exhibited similar values to those of the large particle. Inconsistencies with the standard model assumptions were partly explained by the effect of Langmuir type adsorption equilibrium known to be a property of the system.

Duncan and Moller (2000) made a systematic comparison of standard model of ZLC to a plug flow model. They analyze the zero length assumption theoretically and developed a simple criterion, which ensures that differential approach is always achieved and the diffusivity is accurately measured. They consider the case of finite dispersion in their model and found it to be intermediate to the two extremes. Using this comparison they developed a criterion by which the two cases can be considered identical for practical purpose. The axial flow pattern in the sorbent bed may be disregarded when the dimensionless parameter $L > 15$, assuming that the interstitial fluid holdup is negligible.

Jan-Baptist et al. (2000) performed ZLC experiments to find out the diffusion coefficient of benzene and ethylbenzene in silicalite in the applicable temperature and flow range. They considered the effect of crystal shape, size distribution and apparatus, which cause ambiguity in the estimated parameters, to estimate realistic zeolite diffusion coefficients. A more widely applicable procedure is used to determine the effect of surface barriers at zeolite pore mouths, crystal shape and anisotropy, crystal size distribution and apparatus

effect on the modeling and estimated parameters. The inclusion of these parameters substantially improves full time fits and leads to more realistic parameter values. In all cases diffusivities are larger than in the literature.

Jiang and Eic (2003) measured the transport properties of ethane, butane, and their binary mixtures in large crystals of silicalite-1, ZSM-5 and MIF zeolite membrane as well as agglomerates (pellet) of silicalite by ZLC method. They found that in large crystal of silicalite-1 and ZSM-5 and the membrane sample desorption of isobutene was controlled by micropore diffusion, while in the case of pelleted silicalite sample it was controlled by macropore diffusion.

Cavalcante et al. (2003) measured the diffusivity of n-C_7, n-C_8, n-C_{10} in dealuminated Y-zeolite using the ZLC method. Dealuminated Y zeolites have a large mesopore. So large hydrocarbon molecules can easily penetrate. ZLC data was analyzed by both long time and short time method and consistency was checked by moment analysis.

2.18 Nomenclature

a	=	External area per unit particle (3/R) (cm^{-1})
c	=	Fluid phase concentration (mole/cm^3)
C	=	Normalized fluid phase concentration
c_o	=	Initial fluid phase concentration (mole/cm^3)
C_p	=	Heat capacity (joule/cm^3.deg)
D , D_c	=	Crystal diffusivity (m^2/sec)
D_m	=	Molecular diffusivity (m^2/sec)
E	=	Activation energy (kcal/mole)
F	=	Carrier gas flow rate (cm^3/min)
h	=	Heat transfer coefficient (joule/cm^2.K.s)
(-ΔH)	=	Heat of adsorption (kcal/mole)
I	=	Integral of desorption curve
I_o	=	Integral of desorption curve for gaseous system
K	=	Dimensionless Henry's law constant
k_c	=	Mass transfer resistance
L	=	Dimensionless ZLC parameter
l	=	Slab half thickness (cm)
L_m	=	Dimensionless ZLC parameter
L_{tracer}	=	Dimensionless ZLC parameter
q	=	Adsorbed phase concentration (mol/cm^3)
$\overline{q}$	=	Average adsorbed phase concentration (mole/cm^3).
q^*	=	Value of q equilibrium with c_o (mole/cm^3)
q_o	=	Initial adsorbed phase concentration (mole/cm^3)
q_s	=	Adsorbed phase concentration, in equilibrium with c_o (mole/cm^3)
R	=	Mean radius (cm)
r	=	Radial coordinate (cm)
R_m	=	log mean radius (cm)
s	=	Laplace parameter
Sh_m	=	Sherwood number
T	=	Temperature (Kelvin)
t	=	Time (sec)
T_o	=	Carrier gas temperature (Kelvin)
V_f / V_s	=	Ratio of fluid volume to solid volume in ZLC cell
V_s	=	Volume of the crystal (cc/gm)
y	=	Mole fraction in the gas phase
y_a , y_b	=	Mole fraction of a and b
y_o	=	Mole fraction in the gas phase at time zero

Greek Characters

β_n	=	Roots of transcendental [eq. 2.5 and 2.16]
γ	=	ratio of the fluid capacity for the sorbate to that of sorbent
λ	=	Nonlinear parameter (q_o/q^*)
μ	=	Mean of the normal distribution; first moment [eq. 2.19]
σ	=	Standard deviation of size distribution particle; Second moment [eq. 2.19]
μ_o	=	$\frac{1}{15}\frac{R^2}{D}\frac{5+L}{L}$
σ_o^2	=	$\frac{1}{15}\left(\frac{R^2}{D}\right)^2\left(\frac{25}{L^2}+\frac{10}{L}+\frac{13}{7}\right)$
ξ	=	Dimensionless radius
ζ	=	Dummy variable for integration
α	=	$\frac{ha}{C_p}\frac{r_c^2}{D_c}$
β	=	$\frac{\Delta H}{C_p}\frac{\partial q}{\partial T}\Big\|_{c_o,T_o}$
τ	=	Normalized time

2.19 References

[1] Brandani, F., Ruthven, D. M., Coe, C. G., "Measurement of Adsorption Equilibrium by Zero Length Column (ZLC) Technique. Part 1: Single Component Systems", Industrial Engineering and Chemical Research, 42(7): 1451-1461 (2003 a).

[2] Brandani, F., Ruthven, D. M., Coe, C. G., "Measurement of Adsorption Equilibrium by Zero Length Column (ZLC) Technique. Part 2: Binary Systems", Industrial Engineering and Chemical Research, 42(7): 1462-1469 (2003 b).

[3] Brandani, S., "Analytical Solution for ZLC Desorption Curves with Bi-Porous Adsorbent Particle", Chemical Engineering Science, 51, 12, 3283-3288 (1996).

[4] Brandani, S., "Effects of Nonlinear Equilibrium on Zero Length Column Experiments", Chemical Engineering Science, 53, 15, 2719-2798 (1998).

[5] Brandani, S., Cavalcante, C. L., Guimaraes, L., Ruthven, D.M., "Heat Effects in ZLC Experiments", Adsorption, 4, 275-285 (1998).

[6] Brandani, S., Jama, M. A , Ruthven, D. M., "ZLC Measurement Under Nonlinear Conditions", Chemical Engineering Science, 55(7): 1205-1212, (2000).

[7] Brandani, S., Jama, M. A., Ruthven, D. M., "Counterdiffusion of p-xylene/o-xylene in silicalite Studied by Zero Length Column", Industrial & Engineering Chemistry Research, 39(3):821-828 (2000).

[8] Brandani, S., Jama, M. A., Ruthven, D. M., "Diffusion, Self Diffusion and Counterdiffusion of Benzene and p-Xylene in Silicalite", Microporous and Mesoporous Material, 35-6: 283-300; (2000).

[9] Brandani, S., Ruthven, D. M., "Analysis of ZLC Desorption Curves", Adsorption, 2, 133-143 (1996).

[10] Brandani, S., Ruthven, D.M., "Analysis of desorption curve for liquid systems", Chemical Engineering Science, 50(13), 2055-2059, (1995).

[11] Brandani, S., Xu, Z., Ruthven, D. M., "Transport Diffusion and Self Diffusion of Benzene in NaX and CaX Zeolite Crystals studied by ZLC Tracer ZLC Methods", Microporous Material, 7, 323-331 (1996).

[12] Bulow, M., Micke, A., "Determination of Transport Coefficient in Microporous Solids", Adsorption, 1, 29-48 (1995).

[13] Caputo, D., Eic, M., Colella, C., "Diffusion and Adsorption of Hydrocarbons from Automative Engine Exhaust in Zeolite Adsorbents", Impact of Zeolites and Other Porous Materials on the New Technologies at the Beginning of the New Millennium, Pts. A and B, 142 : 1611-1618 Part A&B (2002).

[14] Carlos, A. G., Carlos, G., Rodrigues, A. E., "Adsorption of Propane and Propylene in Pellets and Crystals of 5A Zeolites", Industrial Engineering and Chemical Research, 41, 85-92 (2002).

[15] Cavalcante, C. L. Jr., Silva, N. M., Sauza, E. F., Sobrinho E. V., "Diffusion of paraffins in dealuminated Y mesoporous molecular sieve", Adsorption, 9, 205-212, (2003).

[16] Cavalcante, C. L., Jr., Brandani, S., Ruthven, D. M., "Evaluation of the Main Diffusion Path in Zeolites from ZLC Desorption Curves", Zeolites, 18, 282-285 (1997).

[17] Cavalcante, Jr. C. L., Diana, C. S., Azevedo, Irla G. Souza, A. Cristina M. Silva, Odelsia L. S. Alsina and Veronica E. Lima, Antonio S. Araujo, "Sorption and Diffusion of p-Xylene and o-Xylene and in Aluminophosphate Molecular Sieve $AlPO_4$-11", Adsorption, 6, 53-59 (2000).

[18] Cherntonghai, P., Brandani, S., "Liquid phase counter-diffusion of aromatics in silicalite using ZLC method", Adsorption, 9, 197-204, (2003).

[19] Crank, J., "The mathematics of diffusion", Oxford University press, London, 1st edition, (1956).

[20] Da Silva, F. A., Rodrigeus, A. E., "Adsorption Equilibria and Kinetics for Propylene and Propane Over 13X and 4A Zeolite Pellets", Industrial & Engineering Chemistry Research, 38(5):2051-2057 (1999).

[21] Duncan, W. L. Moller, K. P., "On Diffusion of Cyclohexane in ZSM-5 Measured by Zero Length Column Chromatography", Industrial Engineering and Chemical Research, 39, 2105-2113 (2000).

[22] Duncan, W. L., Moller, K. P., "The Effect of a Crystal Size Distribution on ZLC Experiments"; Chemical Engineering Science, 57(14): 2641-2652 (2002).

[23] Duncan, W. L.; Moller, K. P., "A 'Zero Length' Criterion for ZLC Chromatography", Chemical Engineering Science, 55, 5415-5420 (2000).

[24] Eic, M., Micke, A., Kocirik, M., Jama, M., Zicanova, A., "Diffusion and Immobilization in Zeolites Studies by ZLC Chromatography", Adsorption, 8(1): 15-22 (2002).

[25] Eic, M., Goddard, M., Ruthven, D. M., "Diffusion of Benzene in NaX and Natural Faujasite", Zeolites, 8, 327-331 (1988).

[26] Eic, M., Ruthven, D. M, "A New Experimental Technique for Measurement for Intracrystalline Diffusivity", Zeolites, 8, 40-45 (1988).

[27] Eic, M., Ruthven, D. M, "Intracrystalline Diffusion of Linear Paraffins and Benzene in Silicalite Studies by the ZLC Method", Zeolite: Facts, Figures, Future, 897-905 (1989).

[28] Grande, C. A., Rodrigus, A. E., "Adsorption Equilibria and Kinetics of Propane and Propylene in Silica Gel"; Industrial Engineering and Chemical Research, 40(7): 1686-1639 (2001).

[29] Han, M. H., Yin, X. Y., Jin, Y., Chen, S., "Diffusion of Aromatic Hydrocarbon in ZSM-5 Studied by the Improved Zero Length Column Method", Industrial & Engineering Chemistry Research, 38(8):3172-3175 (1999).

[30] Hufton, J. R., Ruthven, D. M., "Diffusion of light alkens in silicalite studied by the zero length column", Industrial & Engineering Chemistry Research, 32, 2379-2386, (1993).

[31] Jan-Baptist, W. P., Verheijen, P. J. T., Moulijn, J. A., "Improved Estimation of Zeolite Diffusion Coefficient from Zero-Length-Column Experiments", Chemical Engineering Science, 55, 51-65 (2000).

[32] Jiang, M., Eic, M., "Transport properties of ethane, butane and their binary mixtures in MFI type zeolite and zeolite membrane samples", Adsorption, 9, 225-234, (2003).

[33] Jiang, M.; Eic, M.; Miachon, S.; Dalmon, J. A.; Kocirik M.; "Diffusion of n-Butane, Isobutene and Ethane in a IMF Zeolite Membrane Investigated by Gas Permeation and ZLC Measurements", Separation and Purification Technology, 25(1-3): 287-295 (2001).

[34] Karger, K., Ruthven, D. M., "Diffusion in Zeolites and Other Microporous Solids", John Willy & Sons, Inc., New York, (1992).

[35] MacDougall, H., Ruthven, D. M., Brandani, S., "Sorption and Diffusion of SF_6 in Silicalite Crystal", Adsorption, 5(4):369-372 (1999).

[36] Malka-Edery, A., Grenier, P., "Diffusion of Benzene in NaX Zeolite, Studied by Thermal Frequency Response"; Journal of Physical Chemistry B, 105(29): 6853-6857 (2001).

[37] Rodrigues, J. F., Valverde, J. L., Rodrigues, A. E. "Measurement of Effective Self Diffusion Coefficient in a Gel Type Cation Exchanger by the Zero Length

Column Method", Industrial Engineering and Chemical Research, 37, 2020-2028 (1998).

[38] Ruthven, D. M., "Principles of Adsorption and Adsorption process", John Wiley & Sons, New York, (1984).

[39] Ruthven, D. M., Stapleton, P., "Measurement of Liquid Phase Counter Diffusion in Zeolite Crystals by ZLC Method", Chemical Engineering Science, 48, 1, 89-98 (1993).

[40] Silva, J. A. C., Da Silva, F. A., Rodrigues, A. E., "An Analytical Solution for The Analysis of Zero-Length-Column Experiments with Heat Effects", Industrial Engineering and Chemical Research, 40(16): 3697-3702 (2001).

[41] Silva, J. A. C., Rodrigues, A. E., "Analysis of ZLC Technique for Diffusivity Measurement in Bidisperse Porous Adsorbent Pellets", Gas Sep. Purif., 10, 4, 207-224 (1996).

[42] Silva, J. A. C., Rodrigues, A. E., "Sorption and Diffusion of n-Pentane in Pellets of 5A Zeolite", Industrial Engineering and Chemical Research, 36, 493-500 (1997).

[43] Wilkenhoner, U., Gammon, D. W., Van Steen, E.; "Intrinsic Activity of Titanium Sites in TS-1 and Al-free Ti Beta", Impact of Zeolites and Other Porous Materials on the New Technologies at the Beginning of the New Millennium, Pts. A and B, 142 : 619-626 Part A&B (2002).

[44] Zhu, W.; Kapteijn, F.; Moulijn, J. A., "Diffusion of Linear and Branched C-6 Alkanes in Silicalite-1 Studied by The Trapped Element Oscillating Microbalance", Microporous and Mesoporous Materials, 47(2-3): 157-171 (2001).

Chapter 3

Investigation of Diffusivities of Benzene, Cumene, 1,3 Di-Isopropyl Benzene and 1,3,5 Tri-Isopropyl Benzene in NaY Zeolite by Zero Length Column Method

3.1 Introduction

Catalysts for Fluid Catalytic Cracking (FCC) processes have been increasingly in demand to provide enhanced thermal and hydrothermal stabilities as well as selectivity towards the product of molecular weight C_7-C_{12}, which have better commercial values. Y type zeolite catalysts are widely used in hydrocarbon conversion process, because of their high activities and selectivity. Their catalytic performance is strongly dependent on the zeolite crystal size and intracrystalline diffusivity. Type Y zeolite is structurally and topologically related to mineral faujasite and frequently referred to as a faujasite type zeolite. It has a network of three dimensional intersecting channels in which minimum free diameter is the same in each direction. The SiO_2/Al_2O_3 ratio is in the range of 3 to 6. It has an array of cavities (supercages) of internal diameter about 1.2 nm. Access to each supercage is through six equispaced necks having a diameter about 0.74 nm formed by the ring comprising 12 oxygen atoms.

Zero length column technique developed by Eic and Ruthven (1988) retains the main feature of conventional fixed bed chromatographic techniques and eliminates the effect of axial dispersion. After its introduction much work has been done on this method to establish it as a convenient method to measure intracrystalline diffusivity. Initially the investigation region was in linear isotherm (Henry's law) region. Later on Brandani (1998) investigated the nonlinear equilibrium effect on ZLC method. Heat effects on ZLC experiments were studied by Brandani et al. (1995). Recently Brandani et al. (2003a) have developed the model to measure adsorption equilibrium for both single component and multi component system. ZLC method also been extended to measure self diffusivity counter diffusion (Brandani et al. 2000b, 2000c), liquid phase measurement (Brandani et al. 1995), liquid phase counter diffusion (Brandani et al. 1995 and Cherntongchai 2003).

In this study we investigate the intracrystalline diffusion of benzene, cumene, 1,3 di-isopropyl benzene and 1,3,5 tri-isopropyl benzene in NaY zeolite crystal by ZLC method. Experimental data are fitted with the appropriate ZLC model equations to measure the diffusivity and activation energy for these hydrocarbons.

3.2 Apparatus and Experimental Procedure

A schematic diagram of the ZLC experiment is shown in the Figure 3.1. The carrier gas (Helium) is introduced in two streams. One is low flow stream and other is high flow stream. Both of the streams are passed through respective mass flow controller (manufactured by Omega Inc). The range of the high mass flow controller is 100 cc/min and low mass flow controller is 20 cc/min. The low flow stream is connected to a three way valve. One way is connected to the high flow stream directly. The other way the low flow stream bubbles through the bubbler, through the hydrocarbon being saturated with the hydrocarbon at the water bath temperature and then rejoins the high flow rate stream. The flow path is controlled by on off switch. The bubbler is made of copper and dipped into a water bath where temperature is kept below the room temperature (>20 $^{\circ}$C). The hydrocarbon height is around 5 inches in the bubbler. There must be enough dead volume over the hydrocarbon to reduce the bubble fluctuation. The height must be sufficient to get the helium bubbles completely saturated with hydrocarbon. The helium bubbles must be small, i.e., less than 1mm in diameter. The ZLC cell is made of ¼'' stainless still coupler. The zeolite crystals are kept between two sintered disks. In order to minimize the intrusion of thermal effect and extra particle resistance to mass transfer the adsorbent quantity should be as small as possible, i.e., 1~10 mg. The ZLC column is kept inside a gas oven. To provide the isothermal condition the gas flows through 2 meters of tube inside the oven before it joins ZLC cell. The outlet of the ZLC cell is connected to a Flame Ionization Detector (FID). The detector reading is sent to a chart recorder.

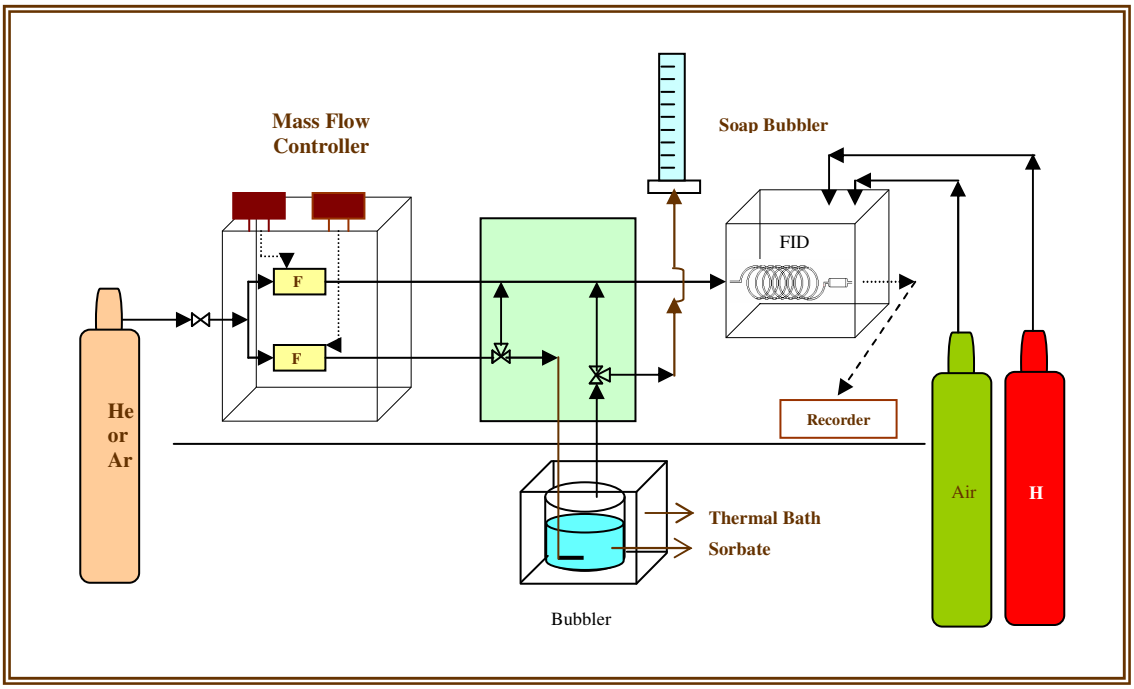

Figure 3.1: Schematic Diagram of experimental setup

Catalyst Regeneration*:* Very small amount of crystal (2mg~4mg) is placed in the ZLC cell. The column is then put inside the oven. The crystals are then regenerated at high temperature, i.e., 300~350 $^{\circ}$C for 16~18 hours at very low flow of the helium purge gas i.e. 12~20 cc/min.

Start of Experiment*:* The temperature of the oven is reduced to the desire temperature of investigation. The water bath is adjusted to the desired temperature to keep the hydrocarbon temperature inside the bubbler constant. The high mass flow controller is set at a high value, i.e. 30~80 cc/min. The low flow controller is set at a low value, i.e. 4~7 cc/min. Start up the FID. Provide enough time to cool down the oven and crystals, inside the ZLC cell, to the desired temperature, i.e. 30~60 minutes. Locate a steady base line for the FID response for pure helium purge.

Adsorption Step*:* Switch on the three way valve. The low flow stream will now bubble through the hydrocarbon and become saturated with hydrocarbon. The saturated helium stream is then mixed with the high flow stream of pure helium. This provides a very low hydrocarbon concentration in the gas stream. The partial pressure of the hydrocarbon can be calculated as we know the bath temperature and the total helium flow rate. Enough time must be provided to achieve the complete equilibrium of the zeolite crystals. One must take care that there must not be any partial equilibrium.

Desorption Step: After attaining a steady adsorption line, the switch of the three way valve must be diverted. Pure helium purges through completely pass the equilibrated

saturated zeolite crystals. The concentration of hydrocarbon reduces with time and the data is recorded on the chart recorder. Again sufficient time to achieve a steady base line for the complete desorption of adsorbed hydrocarbon is provided.

End of Experiment: After attaining the steady baseline for desorption, we have to regenerate the crystals again for the next experiment for another 10~12 hours. Again start from the beginning by selecting another oven temperature or another purge flow rate.

3.3 Mathematical Model

The column is sufficiently short that there is no overall gradient of sorbate concentration through the cell. This is a valid approximation science the Peclet number approaches infinity. The cell is modeled as a perfectly mixed cell. Other basic assumptions are

(1) Equilibrium at the particle surface

(2) Perfect mixing through the cell

(3) The holdup in the fluid phase in comparison with the adsorbed phase hold-up is neglected.

For an isothermal system of uniform spherical particles with linear equilibrium isotherm the dynamic behavior of the system can be described by the following set of equations.

$$\frac{\partial q}{\partial t} = D\left(\frac{\partial^2 q}{\partial r^2} + \frac{2}{r}\frac{\partial q}{\partial r}\right) \tag{3.1}$$

$$\left.\begin{aligned} &\frac{\partial q}{\partial r}(0,t)=0 \\ &q(R,t)=Kc(t) \\ &q(r,0)=q_o=Kc_o \end{aligned}\right\} \tag{3.2}$$

From the mass balance over the cell a further boundary condition must be included.

$$D\frac{\partial q}{\partial r}(R,t)+\frac{1}{3}\frac{FR}{V_s K}q(R,t)=0 \tag{3.3}$$

The solution of these equations, subject to these boundary conditions, is readily obtained by separation of variables or directly from known solutions (Crank, 1965). The resulting expression for the desorption curve is:

$$\frac{c}{c_o}=2L\sum_{n=1}^{\infty}\frac{\exp\left(-\frac{\beta_n{}^2 Dt}{R^2}\right)}{\left[\beta_n{}^2+L(L-1)\right]} \tag{3.4}$$

where, β_n is given by the roots of the following equation:

$$\beta_n\cot\beta_n+L-1=0 \tag{3.5}$$

In this equation, L is given by,

$$L=\frac{1}{3}\frac{FR^2}{KV_s D} \tag{3.6}$$

In the long time region Equation (3.4) reduces to a simple exponential decay curves since only the first term of the summation is significant:

$$\frac{c}{c_o}=\frac{2L}{\left[\beta_1{}^2+L(L-1)\right]}\exp\left(-\frac{\beta_1{}^2 Dt}{R^2}\right) \tag{3.7}$$

Equation 3.7 is the long term solution for ZLC. From a semilog plot of normalized concentration vs time, the slope gives us the value of D/r^2 and from the intercept we can get the value of L.

The assumption of linearity in the adsorption isotherm is generally not valid specially when considering strongly adsorbed species. Brandani (1998) developed the model for ZLC experiments to analyze the effect of nonlinear equilibrium on the resulting apparent diffusivities assuming Langmuir equilibrium and the concentration dependence of zeolitic diffusivity varying according to Darken's relationship.

$$D(q) = D_o \frac{d\ln p}{d\ln q} = \frac{D_o}{1 - q/q_s} = \frac{D_o}{1 - \lambda Q} \tag{3.8}$$

where, D_o is the diffusivity at infinite dilution and q_s is the saturation loading. The extent of nonlinearity is described by the nonlinearity parameter $\lambda = q_0/q_s$ with $Q = q/q_o$ the dimensionless loading. A numerical solution was developed. The solution of these equations for the long time asymptote is given by

$$\ln\frac{C}{C_o} = \ln(1-\lambda) - \lambda + \ln\left(\frac{2L}{\beta_1^2 + L(L-1)}\right) - \beta_1^2 \frac{D_o t}{R^2} \tag{3.9}$$

If $\lambda \rightarrow 0$, the solution reduces to Equation 5 as for the linear isotherm.

The intercept $\ln(1-\lambda) - \lambda + \ln\left(\frac{2L}{\beta_1^2 + L(L-1)}\right)$ decreases due to increase in the nonlinearity parameter λ but the slope remains constant. If such curves are (incorrectly) analyzed on the basis of the linear model, the error in the value of D_0/R^2 will be minimal. However, the error in the apparent Henry constant (derived from the intercept of Equation 3.7) may be very large. From the practical point of view we come to the conclusion that nonlinearity affects the intercept of the $\ln(c/c_o)$ vs t plot [i.e., the equilibrium parameter K] but has little effect on the slope [i.e., the limiting diffusivity].

3.4 Results and Discussion

3.4.1 Molecular size effect

Molecules should not be viewed as rigid spheres. For cases where the molecular diameter is close and similar to the zeolite channel diameter the molecule might experience a net attraction when passing through the channels. If the molecular diameter is much larger than the channel diameter the molecule can no longer enter the zeolite due to the strong repulsive force of the channel. When the diameter of the sorbent molecule is comparable with the pore diameter, significant steric hindrance may occur and the situation becomes more and more complicated. Such effects become large when the ratio of molecular to pore diameter exceeds about 0.1 (Karger and Ruthven, 1992). Molecules smaller than the channel diameter easily penetrate through the zeolite. For NaY zeolite of channel diameter 7.4 Å, benzene of critical kinetic diameter 5.85 Å, can easily penetrate through the pores. Very fast desorption curve is also observed. Cumene, having a larger molecular size 6.8 Å than benzene but with the same critical diameter, does not exceed the pore size of NaY. Hence it is not difficult for it to penetrate through the pores and slower desorption curves are observed. 1,3 di-isopropyl benzene of molecular size 8.4 Å, exceeds the pore channel of NaY zeolite, but can penetrate through the pore as both the pore size and molecular size is not rigid for zeolite NaY because of molecular vibration.. So we observed a very slow desorption curve for 1,3 di-isopropyl benzene in NaY. 1,3,5 tri-isopropyl benzene of critical kinetic diameter 9.3 Å faces great difficulty entering the pores. Molecules having critical diameter 9.5 Å can only penetrate through the pore structure at the ordinary temperature (Karger and Ruthven, 1992) with difficulty Further there is a possibility of being trapped in the zeolite pores and cracking when it tries to

exit from the pores (Al-Khattaf and de Lasa, 2001). Desorption curves are much slower for and the exact diffusivity may be the combine effect of all of the reactant and products diffusing out the pores of NaY.

3.4.2 Diffusivity of hydrocarbons in NaY zeolite

Benzene diffuses very fast as it is expected through NaY. The results are tabulated in Table 3.2 and presented in Figure 3.3. Diffusivity increases with the increase of temperature. Experimental data was analyzed fitting the model equation 3.1. considering the long time solution as an initial guess. The L values ranges from 4.46 to 5.60 and the equilibrium constant (k) values are in range of 6,221 to 40,060. The K values are too high to consider the system in nonlinear region. So the use of linear ZLC model is not valid to evaluate the diffusivities. The diffusivity was hence determined using the asymptotic solution, Equation 3.9 but as we did not have an independent determination of the λ values, it was not possible to determine the true linear Henry's constant, and hence the isosteric heat of adsorption. Use of Equation 3.9 implies that the reported values of diffusivity are for zero loading as this is the basis on which Equation 3.9 is derived. Initial data points don't fit that well to the theoretical curve but fit the long time region. Hufton and Ruthven (1993) revealed that when intracrystalline diffusion is fast compared to the rate at which sorbate is removed by purge gas, the overall desorption process is controlled by equilibrium effect. Investigation temperature range is 50-150 $^{\circ}$C. Diffusivity values are in the range of 10^{-15} m^2/sec, D^* value is 2E-12 m^2/sec. Eic and Ruthven (1989) reported the diffusivity values for benzene in faujasite which is around four order of magnitude higher than our values. Indicating we need much larger crystals

to measure diffusivity for this material. Present values are controlled by the response time of the instrument.

Cumene, being a larger molecule than benzene, diffuses much slower than Benzene. Experimental values are tabulated in Table 3.3 and desorption curves are shown in Figure 3.4. L and K values are also reported using equation 3.7. Apparent values of L range from 4.62 to 5.69 and K values range from 13,636 to 59,292. As the values are in the nonlinear region equation 3.9 is used to calculate the values and reported here. Cumene diffusivity must be much higher than the experimental results reported here. Large crystals are required to measure the diffusivity of this hydrocarbon.

1,3 di-isopropyl benzene, having critical molecular diameter greater than NaY pore opening, takes much longer time to diffuse. Experimental values are tabulated in Table 3.4 and desorption plots are shown in Figure 3.5. Apparent values of L and K, calculated by equation 3.7 are also reported. Apparent L value ranges from 4.46 to 6.23 and apparent K value ranges from 31,939 to 249,119. As these are in the nonlinear range, Equation 3.9 was used to calculate the diffusivities and these are the values reported. Investigation temperature range is 150-210 $^{\circ}$C. Diffusivity values are in the range of 10^{-17} m^2/sec much lower than cumene as it is expected. Moore and Katzer (1972) reported the diffusivity value at 25 $^{\circ}$C is around $2x10^{-17}$ m^2/sec, value is higher than our experimental results.. Mesitylene has same kinetic diameter as of 1,3 diisopropyl benzene, diffusivity reported by Ruthven and Kaul, (1990). If we extrapolate the diffusivity values we can see mesitylene has lower diffusivity values than 1,3 diisopropyl benzene. Mesitylene has

three methyl group at 1,3,5 position thus have less rotational flexibility. But 1,3 diisopropyl benzene may rotate and deform its structure to diffuse more easily through the pores and thus may has higher diffusivity values than mesitylene.

1,3,5 triisopropyl benzene is a big molecule and its structure is unstable above 150°C. There is a possibility of its cracking while measuring its diffusivity. The measured diffusivity may be the combined effect of diffusivity of all reactant and products. The temperature range is 125-190°C. Results are tabulated in Table 3.5 and plots are shown in Figure 3.6. Approximate L value ranges from 3.69 to 14.14 and approximate K values range from 22,627 to 595,142. As these are in the nonlinear range, Equation 3.9 was used to calculate the diffusivities and these are the values reported. At 125°C and 150°C the diffusivity values are lower than 1,3 diisopropyl benzene but above that 1,3,5 triisopropyl benzene has higher diffusivity than 1,3 diisopropyl benzene. That may be because of reaction at higher temperature and the combined diffusivity effect is faster. Another explanation is that tri-isopropyl benzene is not at all successful to penetrate inside the zeolite pore. It just adsorbed on the surface of zeolite which is only 3% of the total area available as most of the adsorbed area is inside the zeolite pores. So it desorbs much faster from the surface. The diffusivity values we get from the experiment are in the range of 10^{-18} -10^{-16} m^2/sec. Triethylebenzene which has the same critical molecular diameter as 1,3,5 triisopropyl benzene but it has much lower diffusivity than 1,3,5 triisopropyl benzene. Trimethyl benzene is a very stable compound even at very high temperature. But 1,3,5 triisopropyl benzene is very unstable compound and it may crack even at 100 °C with the presence of active catalyst. In the experimental temperature range

(125-190 ^{o}C) 1,3,5 triisopropyl benzene can be completely cracked and the products are diisopropyl benzene isomers and propylene. At lower temperature (<150 ^{o}C) reaction is slow and we have lower diffusivity than 1,3 diisopropyl benzene. But at higher temperature (i.e. 190 ^{o}C) diffusivity is higher than 1,3 diisopropyl benzene.

For 1,3,5 triisopropyl benzene initially we have a slow desorption curve, after some time (i.e. 50 sec) the concentration drops suddenly and after that it diffuses slowly. These curves are shown in Figure 3.7. The initial kink in desorption curve may be the effect of surface diffusion which comes out first at the beginning of desorption process which suggests 1,3,5 triisopropyl benzene is adsorbed on the catalyst surface and surface may act as an active catalytic site . Or this may be cause of reaction and counter diffusion of reactant and product or blockage or diffusion path by larger molecule. This region needs more research. Values of diffusivity reported by early works are tabulated in Table 3.6 and values are displayed in Arrhenius plot to compare our results.

3.4.3 Activation energy determination

The diffusion in zeolite is an activated process, described by an Eyring equation $D = D_o e^{-\frac{E}{RT}}$. We calculated both the activation energy E and D_o from the slope and intercept of Arrhenius plot. Calculated activation energies are 24.47, 30.93, 66.14, 77.34 kJ/mol. Eic and Ruthven (1990) reported activation energy of benzene 25 kJ/mol, Karger and Ruthven (1992) reported the value of 1,3,5 tri isopropyl benzene around 58 kJ/mol.

D^* values for these hydrocarbons in NaY crystals are 2E-12, 1E-12, 3E-9 and 7E-10 for benzene, cumene, 1,3 diisopropyl benzene and 1,3,5 tri isopropyl benzene.

3.5 Conclusion

Zero length column experiments carried out with benzene, cumene, 1,3 di-isopropyl benzene and 1,3,5 tri-isopropyl benzene in NaY zeolite crystal. Activation energy also obtained from the Arrhenius plot. These values can be used in modeling cracking reactions.

Table 3.1: Properties of HNaY catalyst

Zeolite Type [44]	Faujasite
Channel geometry [44]	Three dimensional
Cavity size(Å) [44]	12
Number of O atoms in the larger aperture ring [44]	12
Pore size(Å) [44]	7.4
BET surface area (m^2/gm) [1]	583
Hydrated Density (gm/cc) [3]	1.92
Na_2O (wt. %) [1]	0.25
SiO_2/Al_2O_3 (mole/mole) [1]	5.7
Unit cell size (Å) [1]	24.51
Crystal size (μm) [1]	0.9

Table 3.2 : Diffusivity results for benzene in NaY zeolite

Hydrocarbon	Temperature (^oC)	Partial pressure (psi)	D/R^2 (sec^{-1})	D (m^2/sec)	D_o (m^2/sec)	E (kJ/mol)	L	K
Benzene	50	9.71E-03	1.28E-03	2.59E-16	2.00E-12	24.47	5.60	40060.67
	75	9.71E-03	2.61E-03	5.28E-16			4.61	23871.03
	100	9.71E-03	4.23E-03	8.56E-16			4.03	16818.74
	125	9.71E-03	8.43E-03	1.71E-15			3.91	8705.54
	150	9.71E-03	1.03E-02	2.09E-15			4.46	6221.49

Table 3.3 : Diffusivity results for Cumene in NaY zeolite

Hydrocarbon	Temperature (^oC)	Partial pressure (psi)	D/R^2 (sec^{-1})	D (m^2/sec)	D_o (m^2/sec)	E (kJ/mol)	L	K
Cumene	100	6.70E-03	2.98E-04	6.03E-17	1.00E-12	30.93	5.69	59292.62
	125	6.70E-03	5.27E-04	1.07E-16			5.38	35381.10
	150	6.70E-03	9.08E-04	1.84E-16			5.08	21778.17
	175	6.70E-03	1.60E-03	3.23E-16			4.62	13636.52

Table 3.4 : Diffusivity results for 1,3 Di-Isopropyl Benzene in NaY zeolite

Hydrocarbon	Temperature (^oC)	Partial pressure (psi)	D/R^2 (sec^{-1})	D (m^2/sec)	D_o (m^2/sec)	E (kJ/mol)	L	K
1,3 DIPB	150	5.75E-04	8.35E-05	1.69E-17	3.00E-09	66.14	6.23	249119.56
	170	5.75E-04	2.06E-04	4.17E-17			4.61	136287.37
	190	5.75E-04	3.87E-04	7.84E-17			4.88	68501.17
	210	5.75E-04	9.08E-04	1.84E-16			4.46	31939.09

Table 3.5 : Diffusivity results for 1,3,5 Tri-Isopropyl Benzene in NaY zeolite

Hydrocarbon	Temperature (^oC)	Partial pressure (psi)	D/R^2 (sec^{-1})	D (m^2/sec)	D_o (m^2/sec)	E (kJ/mol)	L	K
1,3,5 TIPB	125	2.63E-05	1.74E-05	3.53E-18	3.00E-05	98.33	14.14	595142.80
	150	2.63E-05	8.35E-05	1.69E-17			6.56	286552.25
	170	2.63E-05	3.14E-04	6.35E-17			5.47	91579.29
	190	2.63E-05	1.13E-03	2.30E-16			3.69	22627.97
	75	x	4.87E-05	9.87E-18				x
	125	x	7.75E-05	1.57E-17				x
	150	x	4.46E-04	9.04E-17				x

Table 3.6 : Literature value of benzene diffusivity in NaX

Temperature ^{o}C	Diffusivity (m^2/sec)	D* (m^2/sec)	Activation energy (kJ/mol)	Method	References
77	1.50E-12	x	x	ZLC	Ruthven and Brandani, (2000)
127	4.00E-12				
227	2.00E-11				
130	4.70E-12	1.38E-08	25.08	ZLC	Ruthven and Eic, (1998)
170	8.80E-12				
200	14.3-12				
220	1.86E-11				
250	2.77E-11				

Table 3.7 : Literature value of hydrocarbon diffusivity in NaX

Hydrocarbon name	Crystal size	Temperature	Diffusivity	D^*	Activation energy	Method	References
	µm	^oC	m^2/sec	m^2/sec	Kcal/mol		
1,3 DIPB (8.4 Å)	x	25	1.20E-17	x	x	x	Moor & Katzer (1972)
Mesitylene (8.4 Å)	55	175	6.00E-13	x	25	Gravimetric	Karger & Ruthven, (1992)
	100	300	6.25E-14	x	x	x	Ruthven & Kaul, (1993)
	100	330	8.30E-14				
1,3,5 Triethyl benzene (9.2Å)	30, 50	273	3.00E-17	6.00E-10	76	Gravimetric	Ruthven & Kaul, (1993)
		305	7.00E-17				
		305	6.50E-17				
		335	1.70E-16				
	x	25	1.50E-20	x	x	x	Moor & Katzer (1972)
1,3,5 TIPB (9.3 Å)	x	227	1.00E-13	x	x	Gravimetric	Ruthven et al. (1990)
	55	175	1.50E-13	x	58	Gravimetric	Karger & Ruthven, (1992)

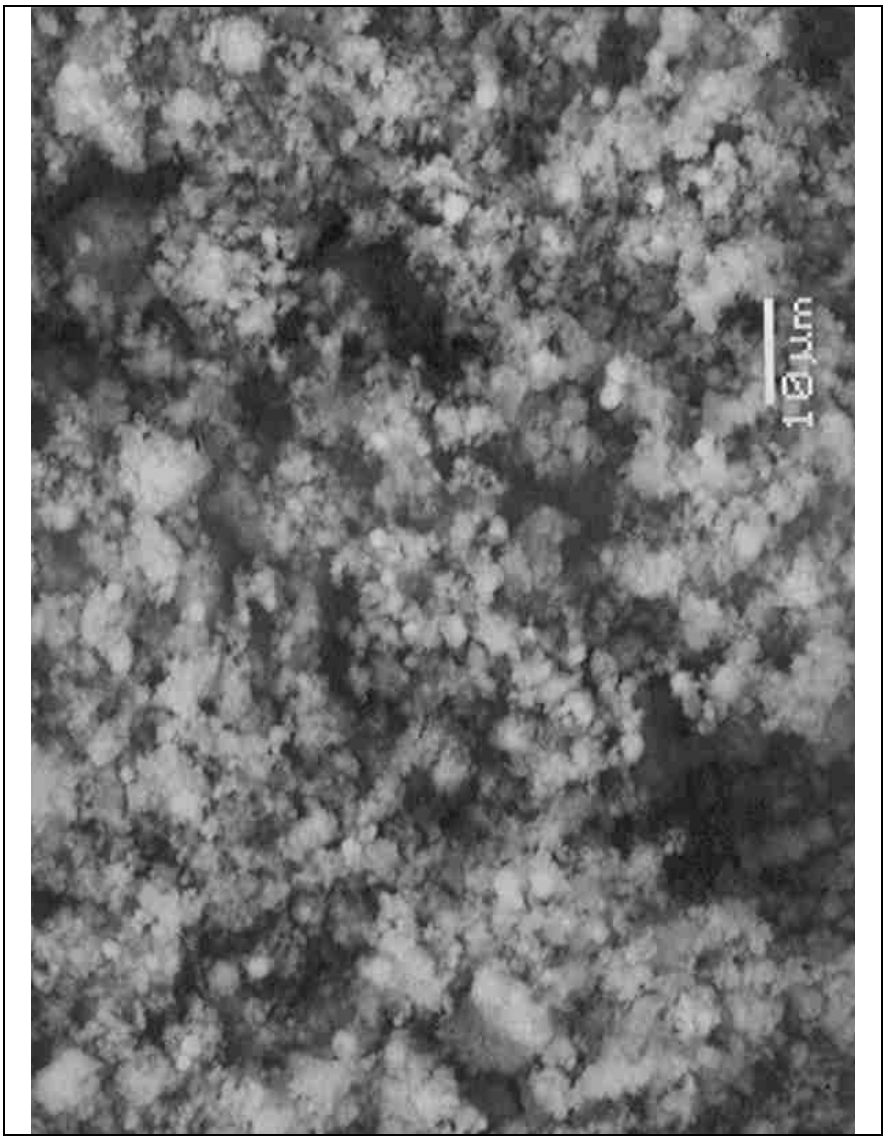

Figure 3.2 : SEM analysis of NaY Crystal

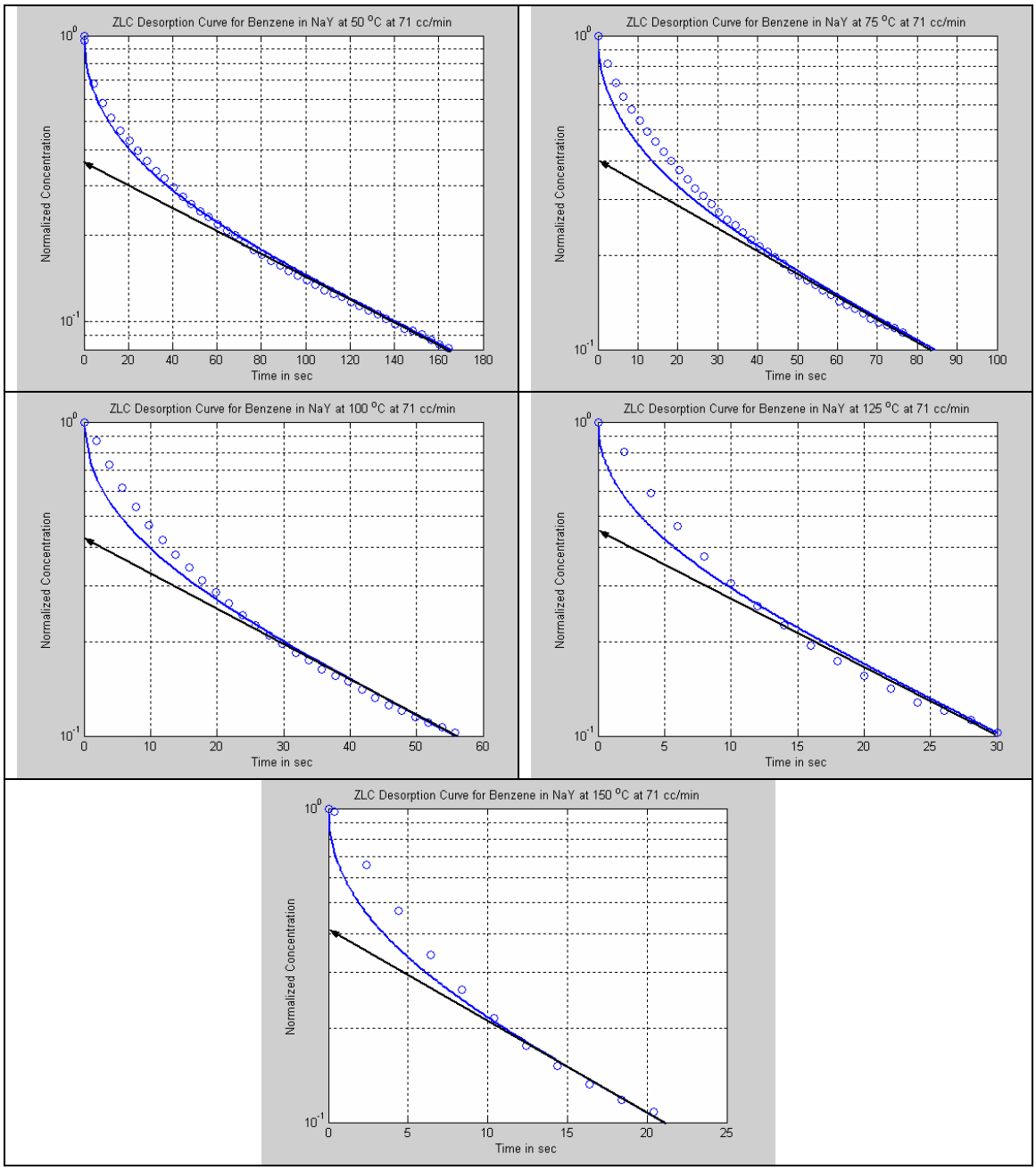

Figure 3.3: ZLC desorption curve for benzene at 71 cc/min for temperature range 150-75 °C

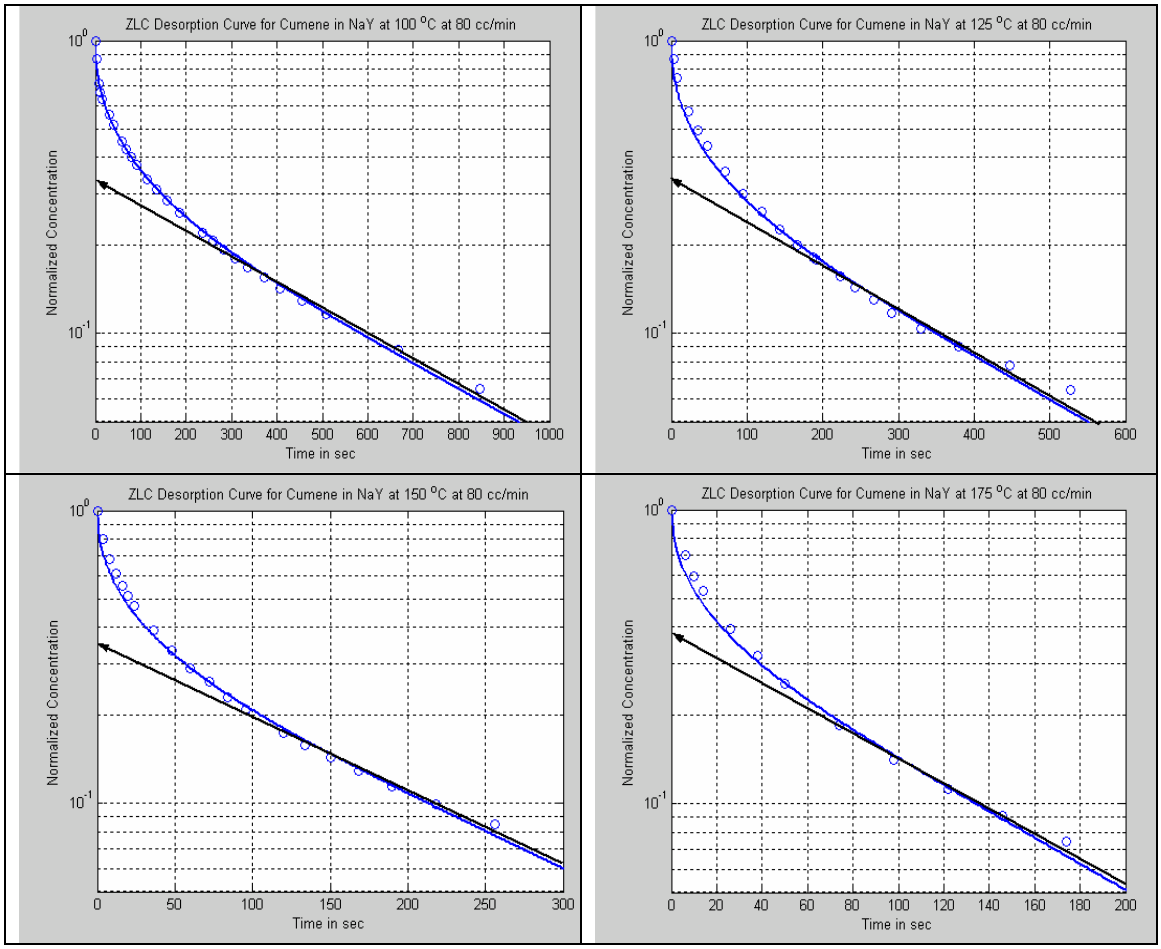

Figure 3.4: ZLC desorption curve for cumene at 80 cc/min for temperature range 175-100 °C

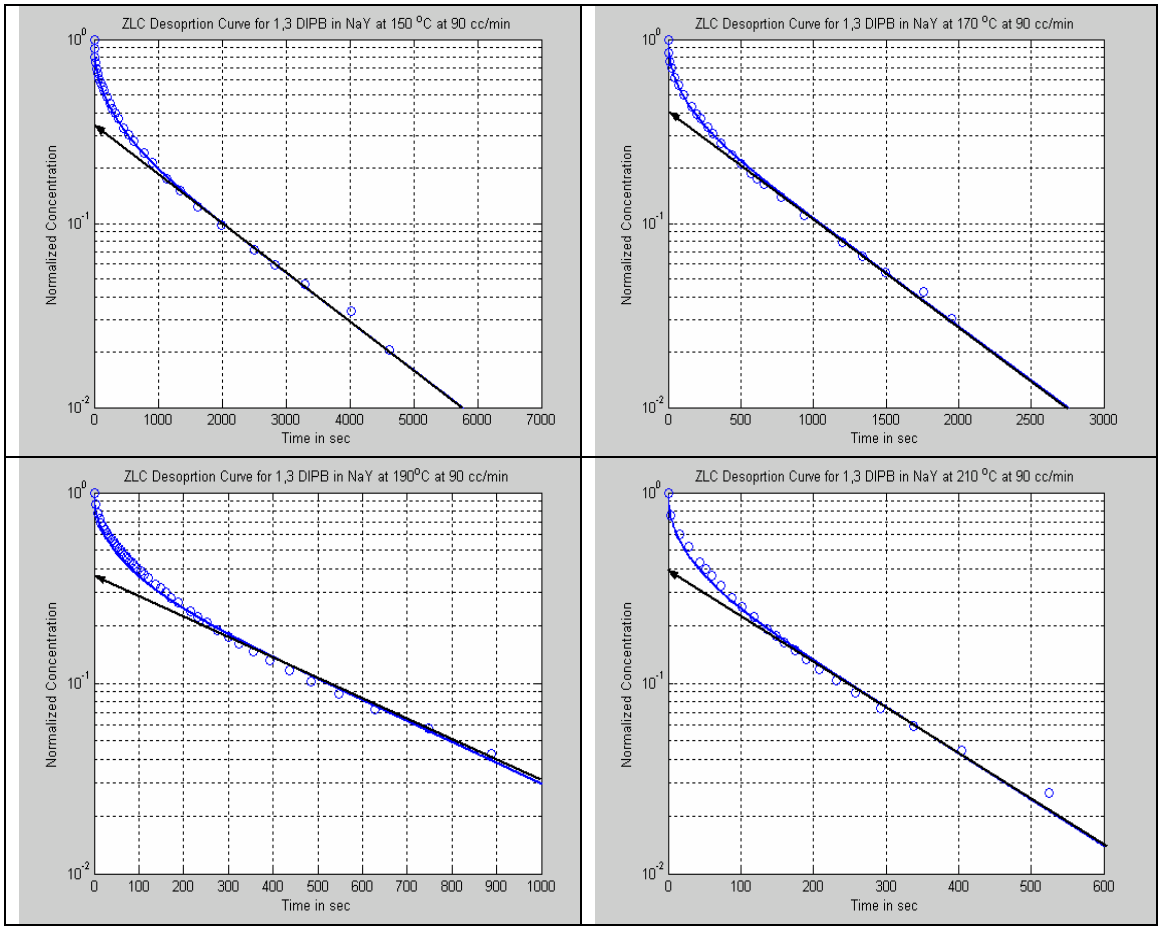

Figure 3.5: ZLC desorption curve for 1,3 di-Isopropyl benzene at 90 cc/min for temperature range 210-150 ^{o}C .

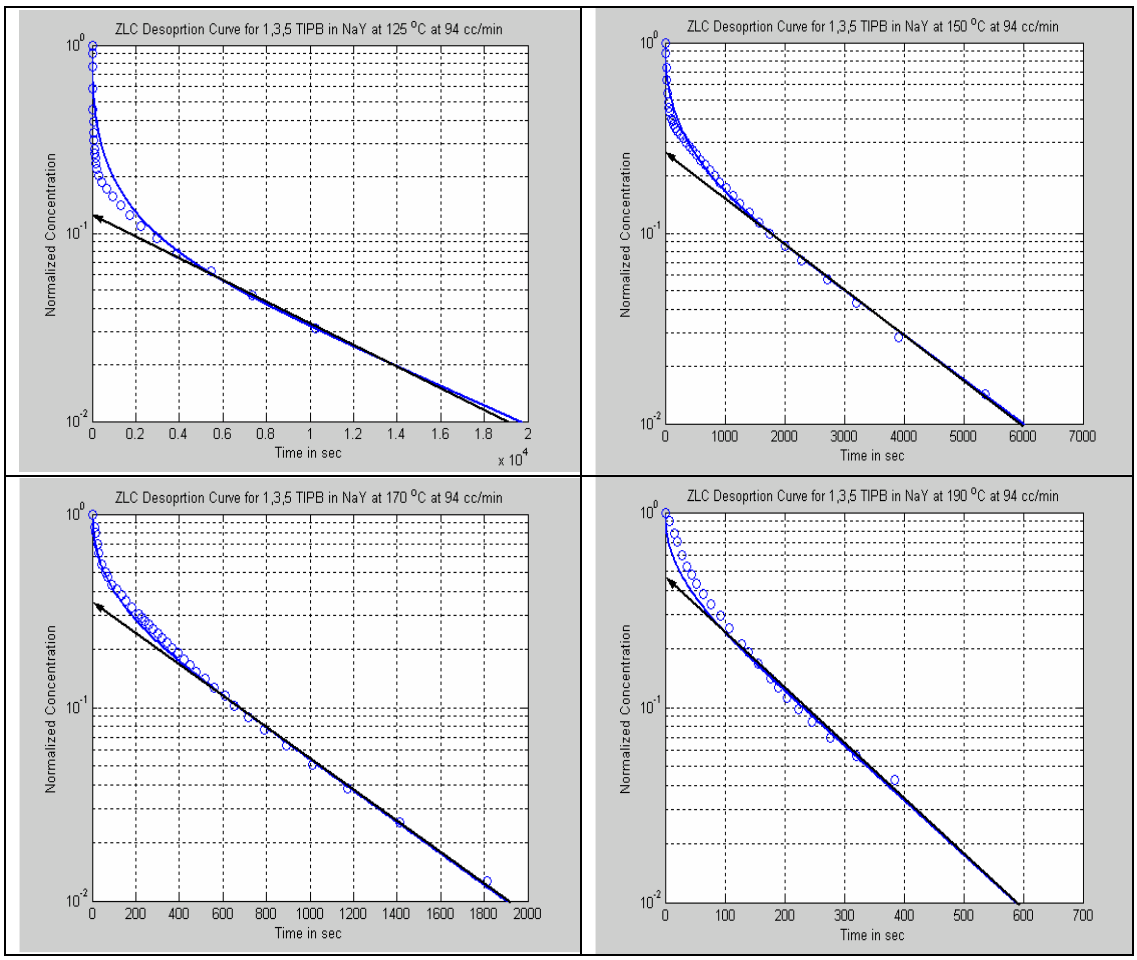

Figure 3.6: ZLC desorption curve for 1,3,5 tri-Isopropyl benzene at 94 cc/min for temperature range 190-125 ^{o}C

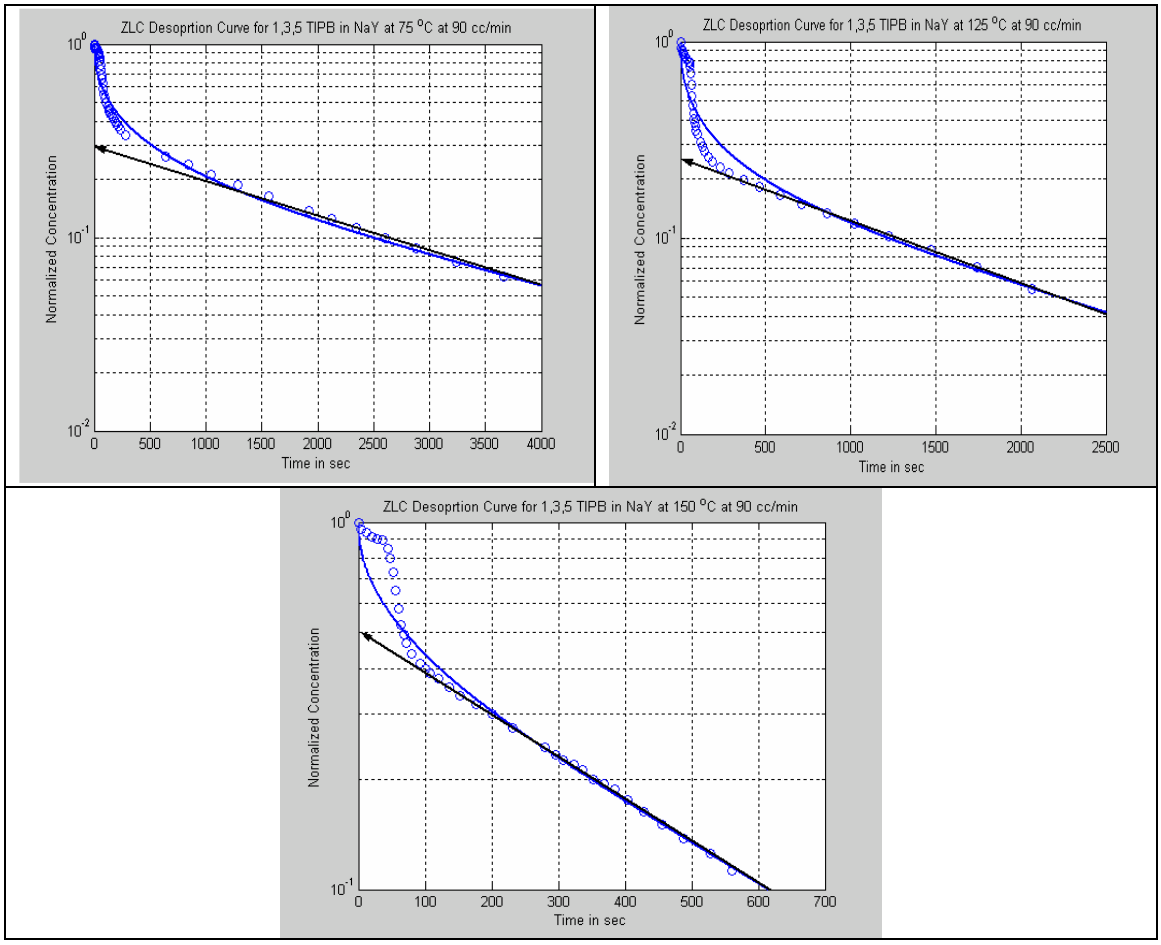

Figure 3.7: ZLC desorption curve for 1,3,5 tri-Isopropyl benzene at 90 cc/min for temperature range 190-125 °C

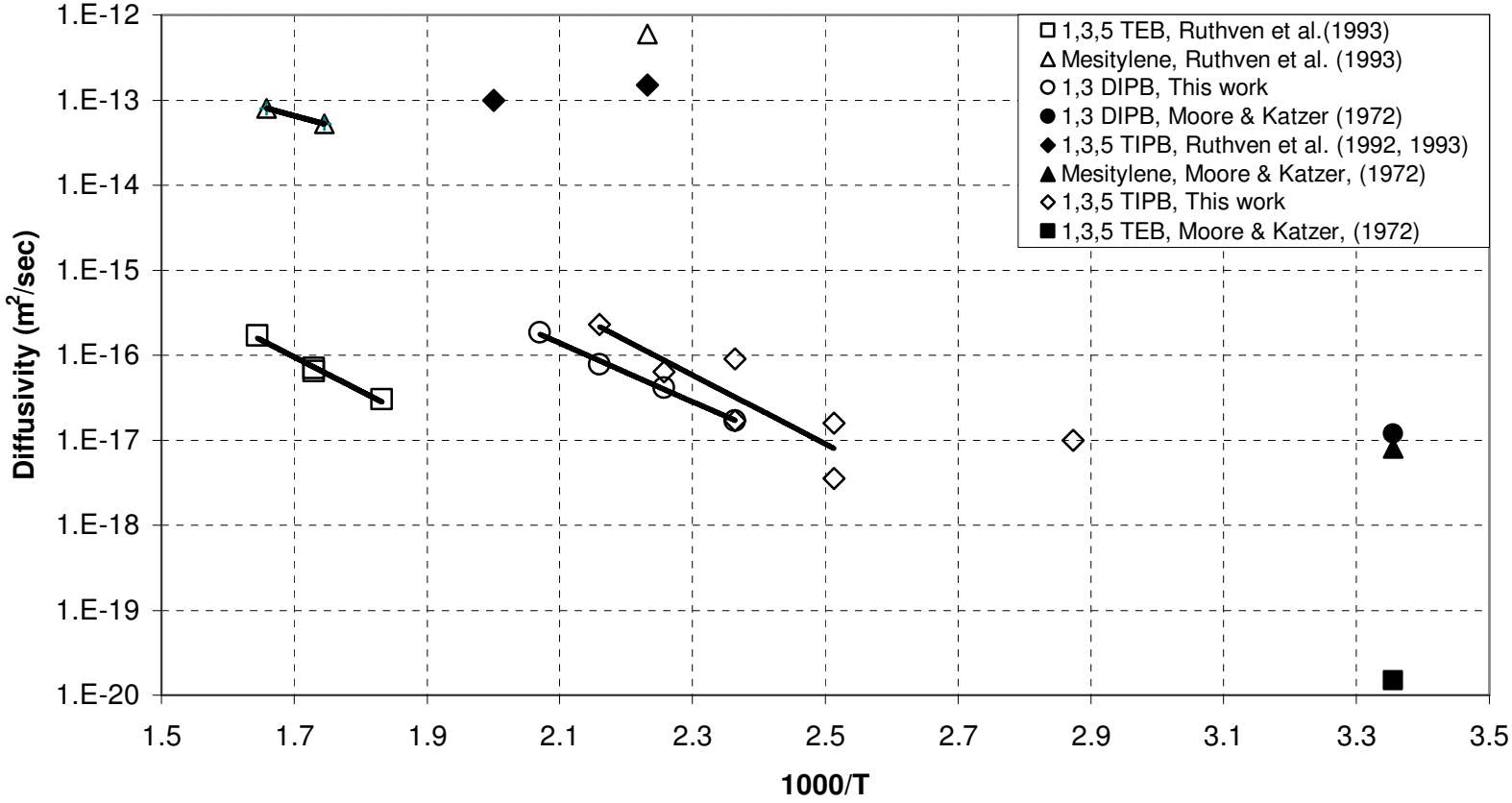

Figure 3.8: Arrhenius plot for benzene, cumene, 1,3 di-isopropyl benzene and 1,3,5 tri isopropyl benzene in NaY crystal

3.6 Nomenclature

C	Fluid phase sorbate concentration (mole/m^3)
C_o	Initial fluid phase sorbate concentration (mole/m^3)
D	Intracrystalline diffusion coefficient (m^2/sec)
F	Volumetric fluid flow of purge fluid (cc/min)
K	Dimensionless Henry's adsorption constant
k_c	Mass transfer coefficient (m/sec)
L	Dimensionless ZLC parameter
q	Adsorbed phase sorbate concentration (mol/m^3)
Q	Dimensionless loading
r	Radial position within sorbent particle (m)
R	Sorbent particle radius (m)
Sh	Sherwood No
t	Time (sec)
V_s	Volume of solid (m^3)
β	Roots of equation 3.5
λ	Isotherm nonlinearity parameter

3.7 References

1. Al-Khattaf, S., de Lasa, H., "The Role of Diffusion in Aalkyl-Benzenes Catalytic Cracking", Applied Catalysis A: General 5855, 1-15 (2001).

2. Beschmann, K., Kokotailo, G. T., Riekert, L., "Kinetics of sorption in zeolite HZSM-5", Chemical Engineering and Processing, 22 (4), 223-9, (1987).

3. Breck, D. W., "Zeolite molecular sieves structure, chemistry and use", John Wiley & Sons Inc., New York (1974).

4. Brandani, F., Ruthven, D. M., Coe, C. G., "Measurement of Adsorption Equilibrium by Zero Length Column (ZLC) Technique. Part 1: Single Component Systems", Industrial Engineering and Chemical Research, 42(7): 1451-1461 (2003a).

5. Brandani, F., Ruthven, D. M., Coe, C. G., "Measurement of Adsorption Equilibrium by Zero Length Column (ZLC) Technique. Part 2: Binary Systems", Industrial Engineering and Chemical Research, 42(7): 1462-1469 (2003b).

6. Brandani, S., "Analytical Solution for ZLC Desorption Curves with Bi-Porous Adsorbent Particle", Chemical Engineering Science, 51, 12, 3283-3288 (1996).

7. Brandani, S., "Effects of Nonlinear Equilibrium on Zero Length Column Experiments", Chemical Engineering Science, 53, 15, 2719-2798 (1998).

8. Brandani, S., Cavalcante C. L., Guimaraes, L., Ruthven, D.M., "Heat Effects in ZLC Experiments", Adsorption, 4, 275-285 (1998).

9. Brandani, S., Jama, M. A , Ruthven, D. M., "ZLC Measurement Under Nonlinear Conditions", Chemical Engineering Science, 55(7): 1205-1212, (2000a).

10. Brandani, S., Jama, M. A., Ruthven, D. M., "Counterdiffusion of p-xylene/o-xylene in silicalite Studied by Zero Length Column", Industrial & Engineering Chemistry Research, 39(3):821-828 (2000b).

11. Brandani, S., Jama, M. A., Ruthven, D. M., "Diffusion, Self Diffusion and Counterdiffusion of Benzene and p-Xylene in Silicalite", Microporous and Mesoporous Material, 35-6: 283-300; (2000c).

12. Brandani, S., Ruthven, D. M., "Analysis of ZLC Desorption Curves", Adsorption, 2, 133-143 (1996).

13. Brandani, S., Xu, Z., Ruthven, D. M., "Transport Diffusion and Self Diffusion of Benzene in NaX and CaX Zeolite Crystals studied by ZLC Tracer ZLC Methods", Microporous Material, 7, 323-331 (1996).

14. Bulow, M., Micke, A., "Determination of Transport Coefficient in Microporous Solids", Adsorption, 1, 29-48 (1995).

15. Caputo, D., Eic, M., Colella, C., "Diffusion and Adsorption of Hydrocarbons from Automative Engine Exhaust in Zeolite Adsorbents", Impact of Zeolites and Other Porous Materials on the New Technologies at the Beginning of the New Millennium, Pts. A and B, 142 : 1611-1618 Part A&B (2002).

16. Carlos, A. G., Carlos, G., Rodrigues, A. E., "Adsorption of Propane and Propylene in Pellets and Crystals of 5A Zeolites", Industrial Engineering and Chemical Research, 41, 85-92 (2002).

17. Cavalcante, C. L. Jr., Silva, N. M., Sauza, E. F., Sobrinho, E. V., "Diffusion of paraffins in dealuminated Y mesoporous molecular sieve", Adsorption, 9, 205-212, (2003).

18. Cavalcante, C. L., Jr., Brandani, S., Ruthven, D. M., "Evaluation of the Main Diffusion Path in Zeolites from ZLC Desorption Curves", Zeolites, 18, 282-285 (1997).

19. Cavalcante, Jr. C. L., Diana, C. S., Azevedo, Irla G. Souza, A. Cristina M. Silva, Odelsia L. S. Alsina and Veronica E. Lima, Antonio S. Araujo, "Sorption and Diffusion of p-Xylene and o-Xylene and in Aluminophosphate Molecular Sieve $AlPO_4$-11", Adsorption, 6, 53-59 (2000).

20. Cherntonghai, P., Brandani, S., "Liquid phase counter-diffusion of aromatics in silicalite using ZLC method", Adsorption, 9, 197-204, (2003).

21. Choudhary, R. V., Nayak, S. V., Choudhary, V. T., "Single component sorption/diffusion of cyclic compounds from their bulk liquid phase in H-ZSM-5 zeolite", Industrial Engineering and Chemical Research, 36, 1812-1818 (1997).

22. Crank, J., "The mathematics of diffusion", Oxford University press, London, 1st edition, (1956).

23. Da Silva, F. A., Rodrigeus, A. E., "Adsorption Equilibria and Kinetics for Propylene and Propane Over 13X and 4A Zeolite Pellets", Industrial & Engineering Chemistry Research, 38(5):2051-2057 (1999).

24. Doelle, H. J., Heering, J., Riekert, L., "Sorption and catalytic reaction in pentasil zeolites. Influence of preparation and crystal size on equilibriums and kinetics", Journal of Catalysis, 71(1), 27-40, (1981).

25. Duncan, W. L., Moller, K. P., "On Diffusion of Cyclohexane in ZSM-5 Measured by Zero Length Column Chromatography", Industrial Engineering and Chemical Research, 39, 2105-2113 (2000).
26. Duncan, W. L., Moller, K. P., "The Effect of a Crystal Size Distribution on ZLC Experiments"; Chemical Engineering Science, 57(14): 2641-2652 (2002).

27. Duncan, W. L.; Moller, K. P., "A 'Zero Length' Criterion for ZLC Chromatography", Chemical Engineering Science, 55, 5415-5420 (2000).

28. Eic, M., Goddard M., Ruthven, D. M., "Diffusion of Benzene in NaX and Natural Faujasite", Zeolites, 8, 327-331 (1988a).

29. Eic, M., Micke, A., Kocirik, M., Jama, M., Zicanova, A., "Diffusion and Immobilization in Zeolites Studies by ZLC Chromatography", Adsorption, 8(1): 15-22 (2002).

30. Eic, M., Ruthven, D. M., "A New Experimental Technique for Measurement for Intracrystalline Diffusivity", Zeolites, 8, 40-45 (1988b).

31. Eic, M., Ruthven, D. M., "Intracrystalline Diffusion of Linear Paraffins and Benzene in Silicalite Studies by the ZLC Method", Zeolite: Facts, Figures, Future, 897-905 (1989).

32. Gates, B. C., Catalytic Chemistry, John Wiley, New York, (1991).

33. Grande, C. A., Rodrigus, A. E., "Adsorption Equilibria and Kinetics of Propane and Propylene in Silica Gel"; Industrial Engineering and Chemical Research, 40(7): 1686-1639 (2001).

34. Han, M. H., Yin, X. Y., Jin, Y., Chen, S., "Diffusion of Aromatic Hydrocarbon in ZSM-5 Studied by the Improved Zero Length Column Method", Industrial & Engineering Chemistry Research, 38(8):3172-3175 (1999).

35. Jan-Baptist, W. P., Verheijen, P. J. T., Moulijn, J. A., "Improved Estimation of Zeolite Diffusion Coefficient from Zero-Length-Column Experiments", Chemical Engineering Science, 55, 51-65 (2000).

36. Jiang, M., Eic, M., "Transport properties of ethane, butane and their binary mixtures in MFI type zeolite and zeolite membrane samples", Adsorption, 9, 225-234, (2003).

37. Jiang, M.; Eic, M.; Miachon, S.; Dalmon J. A.; Kocirik M.; "Diffusion of n-Butane, Isobutene and Ethane in a IMF Zeolite Membrane Investigated by Gas Permeation and ZLC Measurements", Separation and Purification Technology, 25(1-3): 287-295 (2001).

38. Karger, K., Ruthven, D. M., "Diffusion in Zeolites and Other Microporous Solids", John Willy & Sons, Inc., New York, (1992).

39. MacDougall, H., Ruthven, D. M., Brandani, S., "Sorption and Diffusion of SF_6 in Silicalite Crystal", Adsorption, 5(4):369-372 (1999).

40. Malka-Edery, A., Grenier, P., "Diffusion of Benzene in NaX Zeolite, Studied by Thermal Frequency Response"; Journal of Physical Chemistry B, 105(29): 6853-6857 (2001).

41. Moor,R. M., Katzer, J. R., "Counter diffusion of liquid hydrocarbons in type Y zeolite. Effect of molecular size, molecular type and diffusion direction", AIChE J. 18, 876 (1972).

42. Ruthven, D. M., "Principles of Adsorption and Adsorption process", John Wiley & Sons, New York, (1984).

43. Ruthven, D. M., Kaul B. K., "Adsorption of aromatic hydrocarbons in NaX zeolite. 2. Kinetics", Industrial Engineering and Chemical Research, 32, 2053-2057, (1993a).

44. Ruthven, D. M., Stapleton P., "Measurement of Liquid Phase Counter Diffusion in Zeolite Crystals by ZLC Method", Chemical Engineering Science, 48, 1, 89-98 (1993b).

45. Satterfield, C. N., “Heterogeneous Catalysis in Industrial Practice”, McGraw Hill, 2nd edition, (1993).

46. Silva, J. A. C., Da Silva, F. A., Rodrigues, A. E., “An Analytical Solution for The Analysis of Zero-Length-Column Experiments with Heat Effects”, Industrial Engineering and Chemical Research, 40(16), 3697-3702, (2001).

47. Silva, J. A. C., Rodrigues, A. E., “Analysis of ZLC Technique for Diffusivity Measurement in Bidisperse Porous Adsorbent Pellets”, Gas Sep. Purif., 10, 4, 207-224 (1996).

48. Silva, J. A. C., Rodrigues, A. E., “Sorption and Diffusion of n-Pentane in Pellets of 5A Zeolite”, Industrial Engineering and Chemical Research, 36, 493-500 (1997).

49. Wilkenhoner, U., Gammon, D. W., Van Steen E.; “Intrinsic Activity of Titanium Sites in TS-1 and Al-free Ti Beta”, Impact of Zeolites and Other Porous Materials on the New Technologies at the Beginning of the New Millennium, Pts. A and B, 142 : 619-626 Part A&B (2002).

50. Zhu, W.; Kapteijn, F.; Moulijn, J. A., “Diffusion of Linear and Branched C-6 Alkanes in Silicalite-1 Studied by The Trapped Element Oscillating Microbalance”, Microporous and Mesoporous Materials, 47(2-3): 157-171 (2001).

Chapter 4

Investigation of Diffusivities of Xylene Isomers in ZSM-5 Zeolite by Zero Length Column Method

4.1 Introduction

ZSM-5 (Zeolite Socony Mobil) zeolite is a highly active and shape selective catalyst used in many modern petrochemical and hydrocarbon processes. HZSM-5 zeolite possesses channels defined by 10 membered oxygen rings, elliptical in shape. It has two types of channels, a sinusoidal channel having a size of 5.1 x 5.5 Å and straight channels 5.3 x 5.6 Å, (Karger and Ruthven, 1992). This medium pore zeolite is a very important catalyst for a number of catalytic processes. Because of their intermediate channel diameter, configurational restrictions are imposed in the sorption and diffusion of bulky sorbate molecules having comparable size to that of the channels. This results in a shape selective behavior in sorption/diffusion in these zeolites. In these shape selective zeolites, diffusion plays a vital role in deciding the product selectivity in catalytic process through diffusion-reaction interaction. Intracrystalline diffusivity of these molecular species involved in these reactions is frequently the rate controlling factor in the overall kinetics of the process. An accurate knowledge of the transport properties of the reactants and products

in theses catalyzed reactions is indispensable for fully understanding the mechanism of the reaction and also for modeling the complex behavior of the catalytic system.

The worldwide consumption of mixed xylenes is expected to be 32.4 million metric tons in 2004 [Davenport (2001)]. Of this production, approximately 55% is m xylene, 26% is o xylene and 24% is p xylene whereas demand is for 78% p xylene, 4% m xylene and 18% o xylene. Hence there is a worldwide need to isomerize meta to para xylene. The reaction is generally performed in HZSM-5 zeolite, and it is postulated that the kinetics are controlled by the rate of diffusion of the isomers. Accordingly, there is a need to measure the diffusion rates of these isomers in this zeolite.

Although silicalite is similar to HZSM-5 zeolite, only the diffusivities in HZSM-5 are reviewed. Reported diffusivity values indicate that ortho and meta diffuse much more slowly than para. [Choudhury et al. (1997)]. Typical measurement techniques have been gravimetric [Prinz and Riekert (1986), Nayak and Riekert (1985), Doelle et al. (1981), Beschmann et al. (1987)], volumetric [Choudhury et al. (1997)] and ZLC [Han et al. (1999)]. All of the studies have been in the gas phase with the exception of the liquid phase study of Choudhury et al (1997). The diffusion measurements have been measured at zero loading [ZLC], differential or integral steps [gravimetric], or at saturated conditions [liquid, volumetric]. Karger and Ruthven (1992) indicate that the data for p-xylene show a strong (positive) concentration dependence even at loadings less than 2 or 3 wt%. Conversely only limited concentration dependence is observed for o-xylene in the low loading region. Conformity of the uptake curves with the diffusion model has been queried by Beschmann et al (1987) and by Eic and Ruthven for silicalite. In the case of p-xylene Beschmann et al (1987) observed large deviations from the diffusion model with

the uptake curves being slower than expected in the long time region while, in the initial region, the uptake was faster than for benzene under similar conditions [Karger and Ruthven (1992)]. Nakazaki et al. (1992) simulated the dynamic behavior of xylene isomers in the pores of HZSM-5. The activation energies calculated are much higher than the experimentally reported values.

This has resulted in a plethora of diffusion coefficients which lack coherence and the objective of this study is to clarify this situation. In this paper we report on the diffusivity of xylene isomers in HZSM-5 zeolite by ZLC method. Activation energies for the xylene isomers are also reported. Results are compared with the available literature data.

4.2 Mathematical Model

The ZLC, as originally developed by Eic and Ruthven (1988), involved equilibrating a small sample of adsorbent at a known partial pressure of sorbate and then desorbing with a helium purge. For uniform spherical adsorbent particles under linear equilibrium conditions the response curve assuming Fickian diffusion and isothermal operation is given by [Crank (1965)]

$$\frac{c}{c_o} = 2L\sum_{n=1}^{\infty}\frac{\exp\left(-\frac{\beta_n^{\,2} D_0 t}{R^2}\right)}{\left[\beta_n^{\,2} + L(L-1)\right]} \tag{4.1}$$

where, β_n is given by the roots of the following equation:

$$\beta_n \cot \beta_n + L - 1 = 0, \tag{4.2}$$

$$L = \frac{1}{3}\frac{FR^2}{KV_s D} \tag{4.3}$$

L can be expressed as

$$L = \left(\frac{1}{3}\right)\left(\frac{Purge\ flow\ rate}{Crystal\ volume}\right)\left(\frac{R^2}{KD}\right) \tag{4.4}$$

In the long time region Equation (1) reduces to a simple exponential decay curves since only the first term of the summation is significant:

$$\frac{c}{c_o} = \frac{2L}{\left[\beta_1^{\,2} + L(L-1)\right]}\exp\left(-\frac{\beta_1^{\,2} D_0 t}{R^2}\right) \tag{4.5}$$

Under these conditions, D_0/R^2 and L can be determined directly from the slope and intercept of the semi logarithmic plot of c/c_o vs. t. This is known as long time (LT) analysis.

The assumption of linearity in the adsorption isotherm is generally not valid specially when considering strongly adsorbed species. Brandani (1998) developed the model for ZLC experiments to analyze the effect of nonlinear equilibrium on the resulting apparent diffusivities assuming Langmuir equilibrium and the concentration dependence of zeolitic diffusivity varying according to Darken's relationship.

$$D(q) = D_o \frac{d\ln p}{d\ln q} = \frac{D_o}{1 - q/q_s} = \frac{D_o}{1 - \lambda Q} \tag{4.6}$$

where, D_o is the diffusivity at infinite dilution and q_s is the saturation loading. The extent of nonlinearity is described by the nonlinearity parameter $\lambda = q_0/q_s$ with $Q = q/q_o$ the dimensionless loading. A numerical solution was developed. The solution of these equations for the long time asymptote is given by

$$\ln\frac{C}{C_o} = \ln(1-\lambda) - \lambda + \ln\left(\frac{2L}{\beta_1^2 + L(L-1)}\right) - \beta_1^2 \frac{D_o t}{R^2} \tag{4.7}$$

If $\lambda \rightarrow 0$, the solution reduces to Equation 5 as for the linear isotherm.

The intercept $\ln(1-\lambda) - \lambda + \ln\left(\frac{2L}{\beta_1^2 + L(L-1)}\right)$ decreases due to increase in the nonlinearity parameter λ but the slope remains constant. If such curves are (incorrectly) analyzed on the basis of the linear model, the error in the value of D_0/R^2 will be minimal. However, the error in the apparent Henry constant (derived from the intercept of Equation 5) may be very large. From the practical point of view we come to the conclusion that nonlinearity affects the intercept of the ln (c/c_o) vs t plot [i.e., the equilibrium parameter K] but has little effect on the slope [i.e., the limiting diffusivity].

4.3 Apparatus and experimental procedure

The apparatus and procedure are described elsewhere [Zaman et al. (2004)]. Details of the adsorbent used in this study are provided in Table 1. The particle diameter was determined by scanning electron microscope [SEM]. The SEM of the particles used is presented in Figure 1; the mean diameter of the oval shaped particles was determined to be approximately 3 Å. The agglomerates shown in Figure 1 were not considered in the particle size determination.

The critical kinetic properties of xylene isomers [MW = 106] are listed in Table 4.1. The literature differs in the reported minimum critical kinetic diameters for these materials as may be observed in Table 4.2. Probably, the diameters provided by Harrison et al. (1984) are the most reasonable. The minimum kinetic diameter of meta and ortho xylene is greater than the pore size of HZSM-5 zeolite whereas p xylene has a critical kinetic

diameter which approaches that of the pore opening in the zeolite. Fresh adsorbent is used for each run to inhibit coking.

The most severe limitation of the choice of operating conditions for ZLC system is generally that the rate of the process be slow enough to measure without intrusion of extraneous time delay resulting form the inevitable dead volume in the system. A reasonable criterion is $\frac{D}{r_c^2} << 0.05\ \sec^{-1}$ [Karger and Ruthven, 1992]. The fastest inverse time constant measured was that of p-xylene at 150 ºC ($\frac{D_0}{r_c^2} = 0.00128\ \sec^{-1}$) which is approaching the limit mentioned above.

4.4 Results & Discussion

Para xylene has a critical diameter similar to benzene with a methyl group fore and aft. The positioning of these methyl groups does not significantly hinder the diffusion of para xylene in its passage through the ZSM-5 pores. For meta xylene and ortho xylene, the critical kinetic size is larger than the pore opening of ZSM-5 and diffusivity is hindered. Accordingly these two molecules must flex and bend to squeeze through the small pores of HZSM-5. Meta xylene has the larger critical kinetic diameter, and faces the highest resistance to diffusion through the pores.

Para xylene diffuses very fast in HZSM-5 zeolite as it can penetrate through the zeolite pores very easily for its small kinetic molecular diameter. The results are presented in Figures 4.2 and 4.3 for two different sets of data and are tabulated in Table 4.3. Diffusivity increases with the increase of temperature. Experimental data was initially analyzed by fitting the model Equation 4.5 considering the long time solution as an initial guess. The tabulated L values for these curves vary between 6.82 and 12. 9 giving values of equilibrium constant K ranging from 11,996 to 32,777. These values of K are so large as to indicate that this system is non-linear, indicating that use of Equation 4.5 is not appropriate. The diffusivity was hence determined using the asymptotic solution, Equation 4.7 but as we did not have an independent determination of the λ values, it was not possible to determine the true linear Henry's constant, and hence the isosteric heat of adsorption. Use of Equation 4.7 implies that the reported values of diffusivity are for zero loading as this is the basis on which Equation 4.7 is derived.

For ortho-xylene, critical kinetic molecular diameter is greater than p-xylene and consequently diffusion is much slower than for that material. The experimental values of diffusivity are presented in Figures 4.4 and 4.5 and are reported in Table 4.3. Also reported are the apparent values of L and K calculated using Equation 4.5. The first two values reported were found to be coked and are omitted from further consideration. The values of apparent L range from 27.8 to 44.4 and the values of apparent K range from 5204 to 9760. As these are in the nonlinear range, Equation 4.7 was used to calculate the diffusivities and these are the values reported.

Meta-xylene has a critical kinetic molecular diameter just slightly larger than ortho xylene and consequently diffusion is only slower than for that material. The experimental values of diffusivity are presented in Figures 4.6 and 4.7 and are reported in Table 4.3. Also reported are the apparent values of L and K calculated using Equation 4.5. The values of apparent L range from 42.5 to 95.2 and the values of apparent K range from 8356 to 27,595. As these are in the nonlinear range, Equation 4.7 was used to calculate the diffusivities and these are the values reported where possible for this material. In many cases resort to Equation 4.5 had to be employed as the range and accuracy of the measurements did not enable the use of Equation 4.7. A surprising observation is that Equation 4 fits the data so well for this material over the entire range even though the system is nonlinear..

In addition, also tabulated in Table 4.3 are the diffusivity values reported by other workers for para, ortho, and meta xylenes. Included are the various experimental methods used to determine the diffusivity values. The results are also plotted in Figure 4 with the notation p, o or m to indicate para, ortho, and meta respectively.

A pre-condition towards comprehending this Table is to understand the effect of the concentration dependence of diffusivity as expressed in Darken's relationship, Equation 4.6. Consider this effect for, say, a Langmuir isotherm, where the diffusivity is given by

$$D = \frac{D_0}{1 - \lambda Q} \tag{4.8}$$

and the integral diffusivity over the range 0 to q_o is given by

$$\tilde{D} = \frac{1}{q_o}\int_0^{q_o} D(q)dq \tag{4.9}$$

For zero loading ($\lambda = 0$), the diffusivity $D = D_0$ and the intrinsic mobility of the molecule is at its minimum value. For 50% loading ($\lambda = 0.5$), $D \sim 3D_0$ and the effective diffusivity is trebled. For 99% loading, approaching adsorption of a pure liquid, ($\lambda \approx 0.99$), $D \sim 100D_0$ and the mobility of the adsorbing species are two orders of magnitude greater than for the zero loading. The effect then of a positive concentration dependence of diffusivity from pure gas adsorption in the Henry's region to adsorption of a pure liquid is a difference of two orders of magnitude increase. This assumes there is no intrinsic difference between adsorption of a gas or liquid in the zeolitic species. These conclusions were substantiated in a study by Lee and Ruthven (1979) in a study of uptake of cis-2-butene from the gas phase and n-heptane from the liquid phase in a variety of 5A molecular sieve pellets.

The various experimental techniques involve understanding the complexity of these diffusion phenomena. The ZLC technique is the simplest as the values of D measured are those at zero loading, i.e. D_0. This is because in the desorption step the outer shell of the adsorbent is rapidly depleted so that in the long time region, the diffusivity resulting is that of a diffusing species at zero loading (in outer shell). The gravimetric step may be

performed differentially at any point on the isotherm or integrally using large steps. Only when a differential adsorption step is performed at zero loading is D_0 determined. For a large integral step from zero loading to approaching saturation, the overall diffusivity approaches two orders of magnitude greater than for zero loading. Volumetric gas adsorption steps exhibit the same behavior as for the gravimetric steps. Volumetric liquid adsorption steps are analogous to large integral steps and are expected to approach two orders of magnitude diffusivity greater than that at zero mobility. In all cases, extraneous mass or heat transfer effects must be eliminated.

In Figure 4.8, p. o. and m represent para, ortho, and meta xylenes respectively. The results of this ZLC study are shown as (p1), (o1) and (m1) respectively and the reported diffusivities are for D_0 the zero loading diffusivity. The diffusion results of Choudhury et al (1997) for the volumetric measurement of liquid diffusivities are reported as (p2), (o2) and (m2) respectively. These diffusivities are effectively integral diffusivities from zero to saturation loading and are expected to be approximately two orders of magnitude greater than for zero loading. The surprising result is that the data for this study and that of Choudhury et al. (1997) are in agreement as shown by the Arrhenius plot passing through both sets of data. Yet as one diffusivity is effectively the measurement of D_0 (gas, ZLC) and the other a measurement of ~$100D_o$ (liquid, volumetric), they should differ by two orders of magnitude. This is contrary to the results of Chertonghai and Brandani (2003) who reported liquid phase diffusivities approximately two orders of magnitude greater than for gas phase diffusivities for xylene and benzene in silicalite. They qualified their results due to possible leakage around a valve but overall they were convinced that the liquid phase diffusivities were much greater than the gas phase

diffusivities. The experimental gravimetric gas phase results of Beschmann et al. (1987) at 25 ºC are shown as p4 for para-xylene. The lower value is that for an integral differential step of 50% and the higher value that for an integral step of approximately 100%. If both values are extrapolated to zero loading, the relevant data points would lie on an extension of the Arrhenius line for data sets (p1) and (p2), e.g. the diffusivity 1E-14 for 100% loading becomes 1E-16 for zero loading using the two orders of magnitude factor. Similarly, the diffusivity for the gravimetric integral step of Nayak and Riekert (1985) and Prinz and Riekert (1986) when extrapolated to zero coverage will also lie approximately on the same Arrhenius line. The data of Han et al (1999) is two orders of magnitude greater than for this work. They used a Fuller Range technique to extract their diffusivities combining the short time (ST) and (LT) solution. Their LT solution is two orders of magnitude less than the ST solution. Considering that they may have nonlinear adsorption and that the short time solution may be in the zone of reliability of the apparatus (dead volume problem mentioned earlier), it is probable that the long time solution is a more true reflection of the actual diffusivity in which case their results would be close to the results determined in this work.

The ortho xylene results for this work (o1) and for Choudhury et al. (o2) also lie on the same Arrhenius line as shown in Figure 8. Further, the diffusivity for the gravimetric integral step of Nayak and Riekert (1985) (o4) when extrapolated to zero coverage will also lie approximately on the same Arrhenius line but that for Beschmann et al. (1987) (o3) for a similar gravimetric step is inconsistent with the other studies. A possible explanation for the latter result is the existence of a pore mouth resistance for that particular sample.

Similarly, the meta xylene results for this work (m1) and for Choudhury et al. (1997) (m2) also lie on the same Arrhenius line as shown in Figure 8. However, the diffusivity for the gravimetric integral step of Doelle et al. (1981) (m3) when extrapolated to zero coverage is approximately 4 orders of magnitude larger than that anticipated from the extension of the Arrhenius line. As it is also significantly more rapid than for para xylene, this suggests that the intracrystalline diffusivity may not have been the parameter measured.

As these various studies involved use of crystal sizes from 0.3 to 26 μm radius and as most of the studies appear consistent, it appears that intracrystalline diffusion is the rate controlling parameter.

Thus with a few limited exceptions, all the experimental diffusion results for p, o, and m-xylene in HZSM-5 appear compatible. The one exception is the liquid diffusion data of Choudhury et al which even though it matches the other data, the theoretical framework for these diffusion coefficients is not consistent with the other studies.

Diffusion in zeolite is an activated process, described by the Eyring equation $D = D_o e^{-\frac{E}{RT}}$. Both the activation energy E, and D_o can be calculated from the slope and intercept of the Arrhenius plot. The calculated activation energies are 19.49, 30 and 51.1 kJ/mole respectively for this study. The first two are consistent with published data but that for meta is higher than other reported studies. The activation energies reported by Choudhury et al. (1997) are 18.81, 35.65 and 39.38 kJ/mol for para, ortho and meta respectively. The activation energy value for meta is lower than that reported for this study. The D_o values are 9×10^{-8}, 2×10^{-12} and 2×10^{-10} m^2/sec for para, ortho and meta

xylene respectively. Karger and Ruthven (1992) reported very little difference between the activation energies, E = 20-30 kJ/mole, for these three isomers in silicalite crystals containing a very small amount of aluminum. Our meta xylene results differ from this conclusion.

The activation energies of the combined data of this work and of Choudhury et al. are also tabulated in Table 4.3. The calculated activation energies are 19.62, 33.28 and 56.981 kJ/mole respectively for both combined.

4.5 Conclusion

Transport properties of xylene isomers in HZSM-5 zeolite crystal were measured experimentally using the ZLC technique. However, the asymptotic form of the diffusion model for the non linear isotherm must be used to derive the correct diffusivities. The diffusivity sequence is p-xylene > o-xylene > meta xylene. This indicates that we can get improved p-xylene selectivity using HZSM-5 catalyst which is the desired industrial product The measured results are mainly consistent with the reported literature data when analyzed using the correct theoretical framework...

Table 4.1: Properties of HZSM-5 catalyst

Zeolite Type [19]	MFI
Channel geometry [19]	Two dimensional
Number of O atoms in the larger aperture ring [19]	10
Pore size (Å) [19]	5.1x5.5 tube interconnecting with zigzag 5.3x5.6 tube
BET surface area (m^2/gm) [20]	361
Hydrated Density (gm/cc) [20]	2.12
SiO_2/Al_2O_3 (mole/mole)[20]	31
Crystal size (μm) [20] [SEM analysis, RI-KFUPM]	3

Table 4.2 : Properties of Xylene isomers

	Molecular Size (nm)				Purity**
	Maximum	Minimum Kinetic (Critical size)			
Para Xylene	0.99	0.67*,	0.513+	0.58##	99.9%
Meta Xylene	0.92	0.74*	0.538++		99.9%
Ortho Xylene	0.87	0.73*	0.564+	0.68##	99.9%

- * Choudhary et al. (1997)
- + Gates (1991)
- ++ Cherntongchai and Brandani (2003)
- ## Harrison et al (1984)
- *** Xylene Isomers were supplied by FLUKA INC; Purity was also tested in the laboratory using FID.*

Table 4.3: Diffusivity Results for Xylenes in HZSM-5

Data for Para Xylene

Temperature (°C)	r_C (μm)	1000/T	D/r^2	Diffusivity (m^2/sec)	D_o (m^2/sec)	E (kJ/mol)	L	Apparent K	Comments	Reference
75	1.5	2.873563	5.698E-04	1.282E-15	9E-08	19.49	12.9	32777.	ZLC nonlinear	This work
100	1.5	2.680965	8.293E-04	1.866E-15			10.2	24711.	"	
125	1.5	2.512563	1.067E-03	2.4E-15			9	17618.	"	
150	1.5	2.364066	2.076E-03	4.67E-15			6.82	11996.	"	
75	1.5	2.873563	5.422E-04	1.22E-15			12.5	30007.	"	
100	1.5	2.680965	7.964E-04	2.107E-15			9.5	24795.	"	
125	1.5	2.512563	1.084E-03	2.44E-15			10	17087.	"	
35		3.246753	x	5.13E-16	9E-13	18.81	x	x	Volumetric Liq.	Choudhury et al.
45		3.144654		8E-16					"	
64		2.967359		1E-15					"	
100	26	2.680965	x	4.00E-13	x	x	x	x	ZLC	Han M. et al. ZLC method
150	26	2.364066		5.20E-13					"	
200	26	2.114165		6.80E-13					"	
25	1.5,4	3.355705		3e-15					Gravimetric $0.5< \theta <1.0$	Beschmann et al
25	1.5,4	3.355705		~E-14					Gravimetric $0.0< \theta <1.0$	Beschmann et al
25	1.8	3.355705		6E-15					Gravimetric Integral Step	Prinz and Riekert
25	0.3	3.355705		3E-15					Gravimetric Integral Step	Nayak and Riekert
25	0.5	3.355705		~E-20					Chromatographic Extrapolation	Forni and Viscardi
x		x	x	x	1E-12	19.62	x	x		Combined data from Choudhary et al. and this work

Data for Meta Xylene

Temperature (^oC)	r_C (μm)	1000/T	D/r^2	Diffusivity (m^2/sec)	D_0 (m^2/sec)	E (kJ/mol)	L	K	Reference	
150	1.5	2.364066	3.956E-05	8.9E-17	2E-10	51.1	95.2	27595.	ZLC nonlinear	This work
175	1.5	2.232143	7.467E-05	1.68E-16			74.1	17723.	"	
200	1.5	2.114165	2.049E-04	4.61E-16			60.6	10372.	"	
220	1.5	2.028398	3.076E-04	6.92E-16			42.5	8356.	"	
150	1.5	2.364066	4.064E-05	9.143E-17			95.2	26541.	"	
150	1.5	2.364066	4.320E-05	9.72E-17			91	27001.	"	
175	1.5	2.232143	9.333E-05	2.1E-16			66.7	17051.	"	
200	1.5	2.114165	1.920E-04	4.32E-16			66.6	11384.	"	
35		3.246753	x	2.5E-19	1E-12	39.38	x	x	Gravimetric Liq.	Choudhury et al.
50		3.095975	x	5E-19					"	
80		2.832861	x	1.77E-18					"	
25	14	3.55705	x	2.00E-14	x	x	x	x	Gravimetric Integral Step	Doelle et al.
x		x	x	x	9E-10	56.98	x	x		Combined data from Choudhary et al. and this work

Data for Ortho Xylene

Temperature (°C)	r_C (μm)	1000/T	D/r^2	Diffusivity (m^2/sec)	D_o (m^2/sec)	E (kJ/mol)	L	K		Reference
180	1.5	2.207506	4.951E-05	1.114E-16	2E-12	30	118.	27949.	Coked	This work
200	1.5	2.114165	1.137E-04	2.558E-16			83	17253.	Coked	
220	1.5	2.028398	3.920E-04	8.82E-16			42.6	9760.	ZLC, nonlinear	
240	1.5	1.949318	7.667E-04	1.725E-15			40.8	5204.	"	
125	1.5	2.512563	9.961E-05	2.241E-16			44.4	x	"	
150	1.5	2.364066	1.437E-04	3.233E-16			41	x	"	
180	1.5	2.207506	3.019E-04	6.793E-16			40	x	"	
200	1.5	2.114165	6.250E-04	1.406E-15			27.8	x	"	
25	1.5	3.355705	x	1.00E-19	x	x	x	x	Gravimetric Integral Step	Beshman et al.
35		3.246753	x	9E-18	1E-11	35.65	x	x	Gravimetric Liq.	Choudhury et al.
50		3.095975		1.9E-17					"	
80		2.832861		5.4E-17					"	
25	0.5	3.355705	x	1.00E-16	x	x	x	x	Gravimetric Integral Step	Nayak and Reikert
x		x	x	x	4E-12	33.28	x	x		Combined data from Choudhary et al. and this work

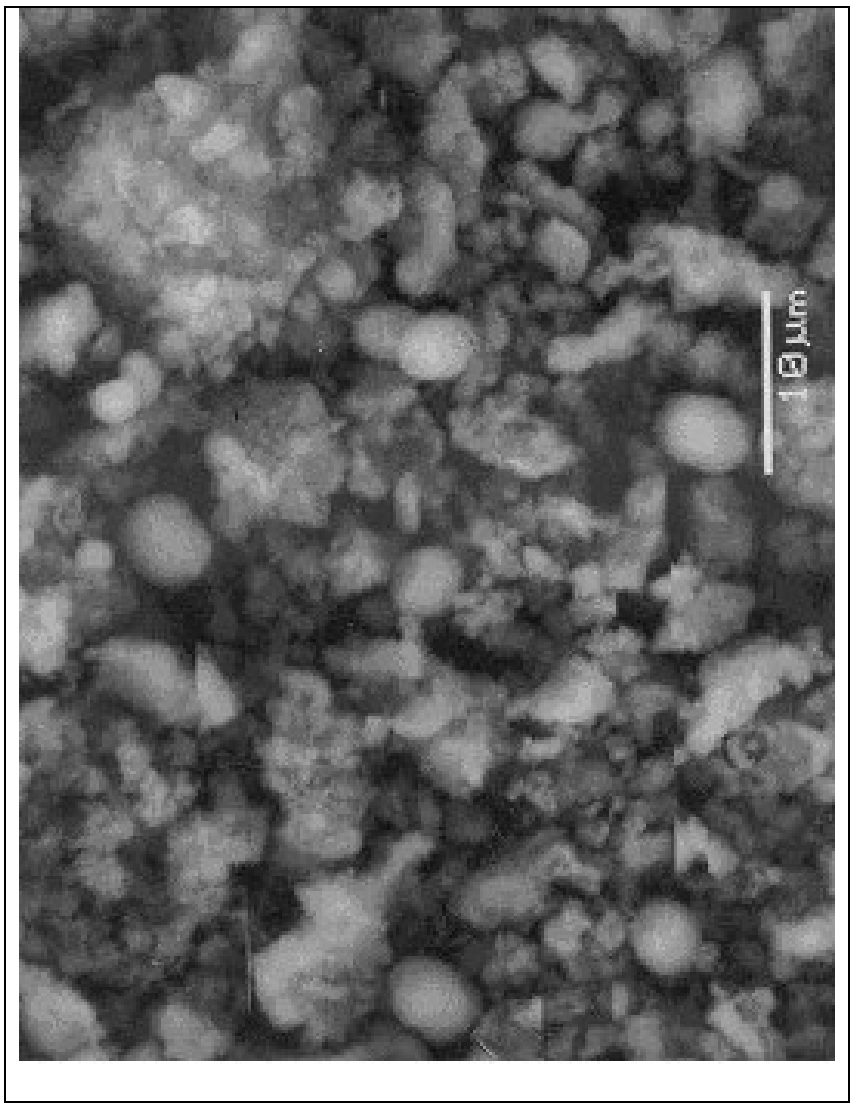

Figure 4.1 : SEM picture of HZSM-5 crystal

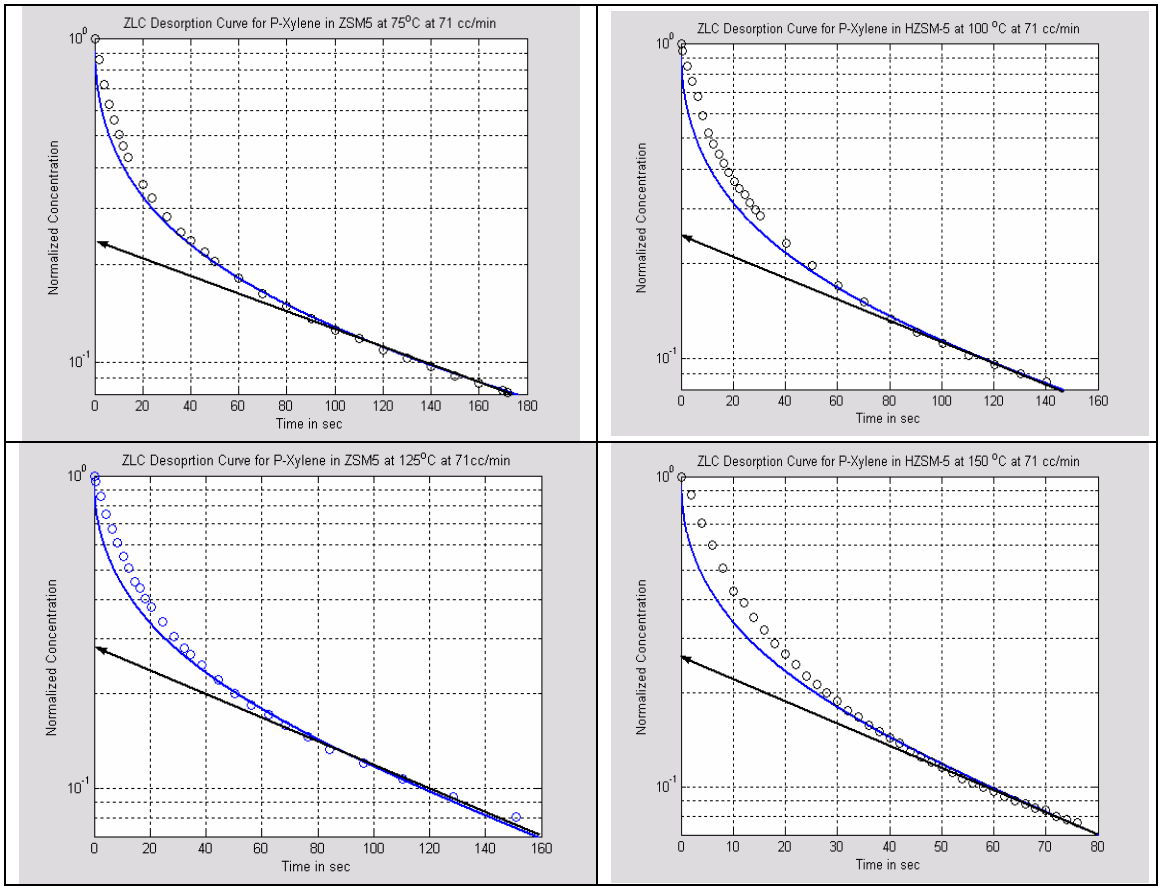

Figure 4.2: ZLC Desorption Curve for Para Xylene in H-ZSM5 at 71 cc/min purge flow rate (1st data set)

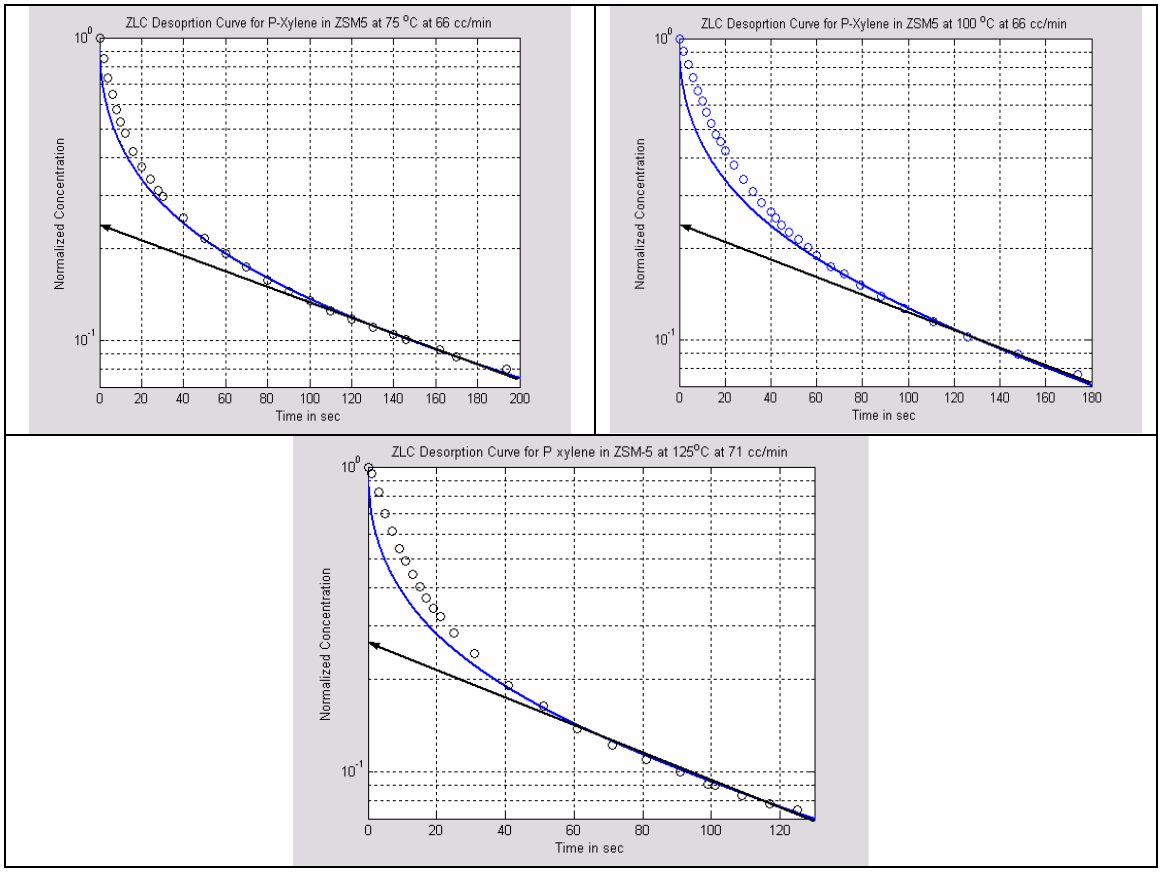

Figure 4.3: ZLC Desorption Curve for Para Xylene in H-ZSM5 at 71 cc/min purge flow rate (2nd data set)

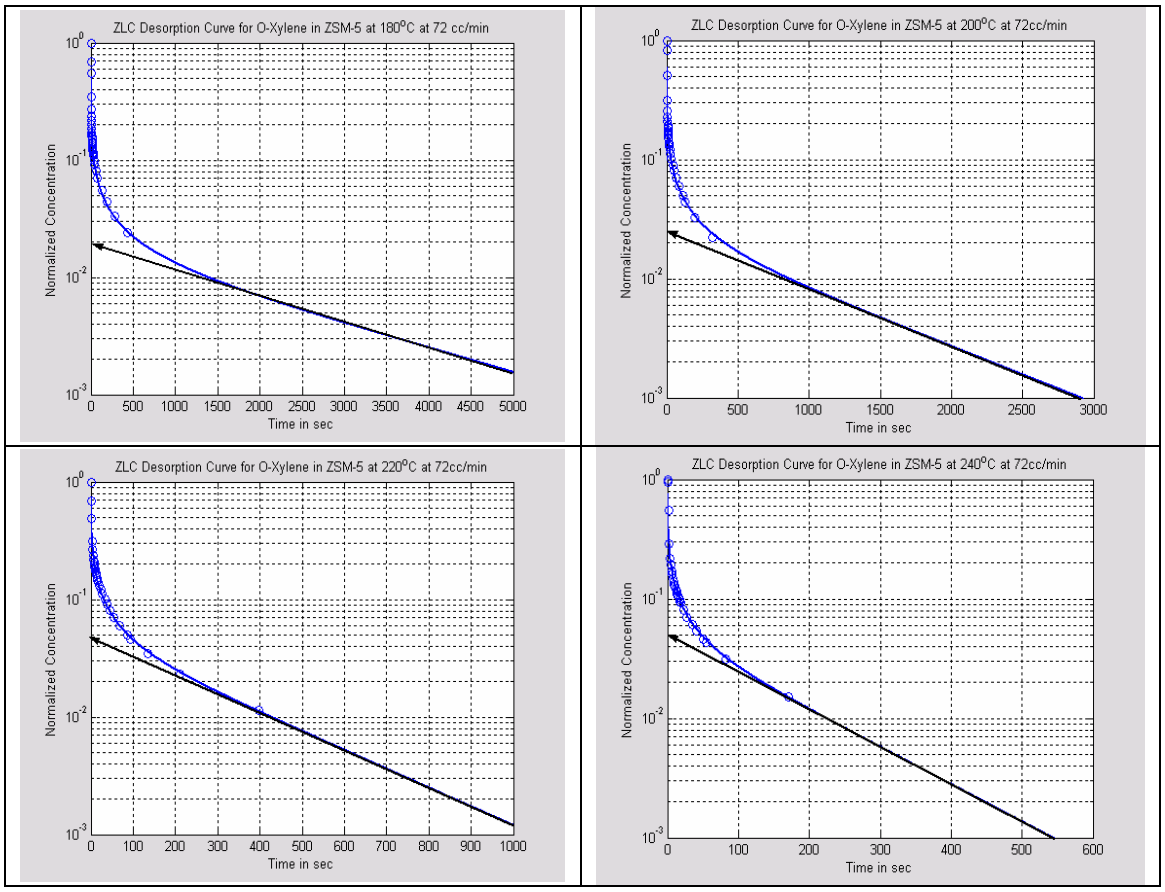

Figure 4.4: ZLC Desorption Curve for Ortho Xylene in H-ZSM5 at 72cc/min purge flow rate (1st data set)

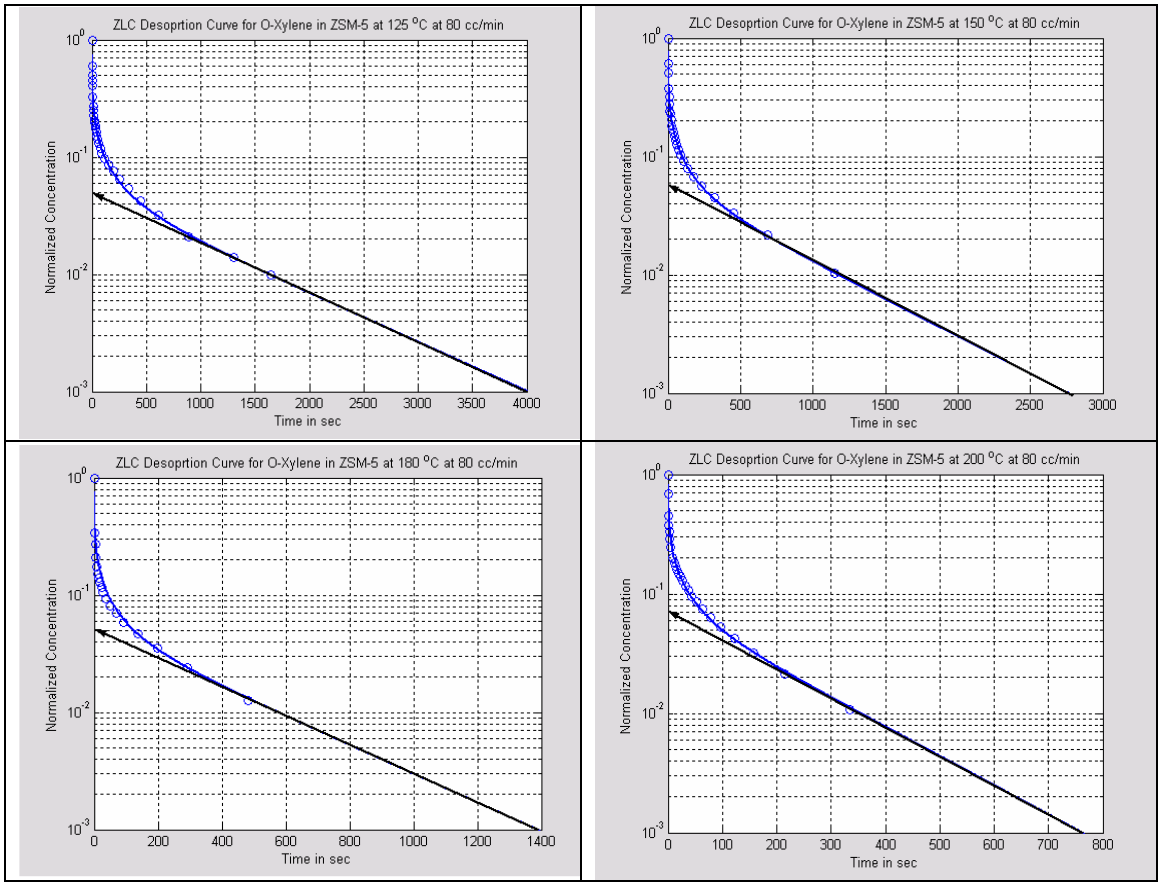

Figure 4.5: ZLC Desorption Curve for Ortho Xylene in H-ZSM5 at 80cc/min purge flow rate (2nd data set)

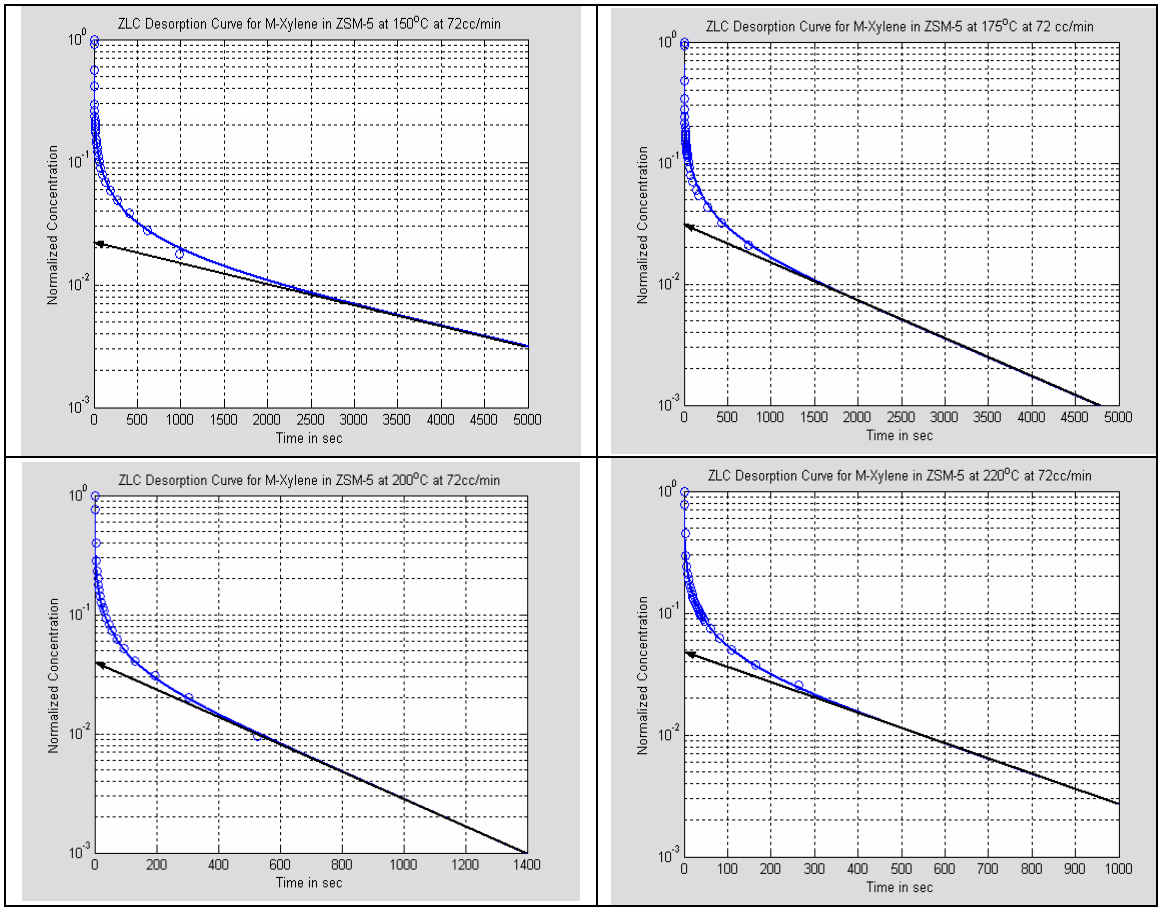

Figure 4.6: ZLC Desorption Curve for Meta Xylene in H-ZSM5 at 72 cc/min purge flow rate (1st data set)

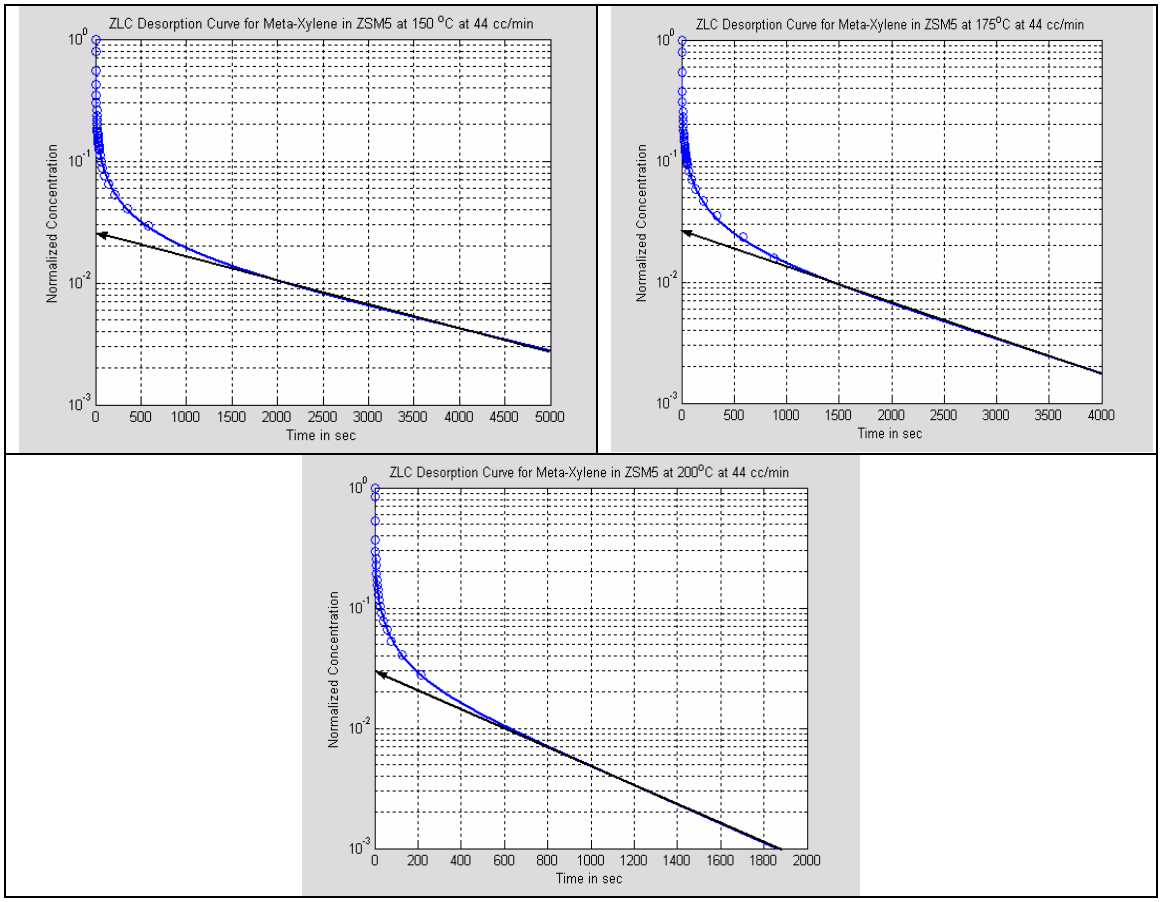

Figure 4.7: ZLC Desorption Curve for Meta Xylene in H-ZSM5 at 72 cc/min purge flow rate (2nd data set)

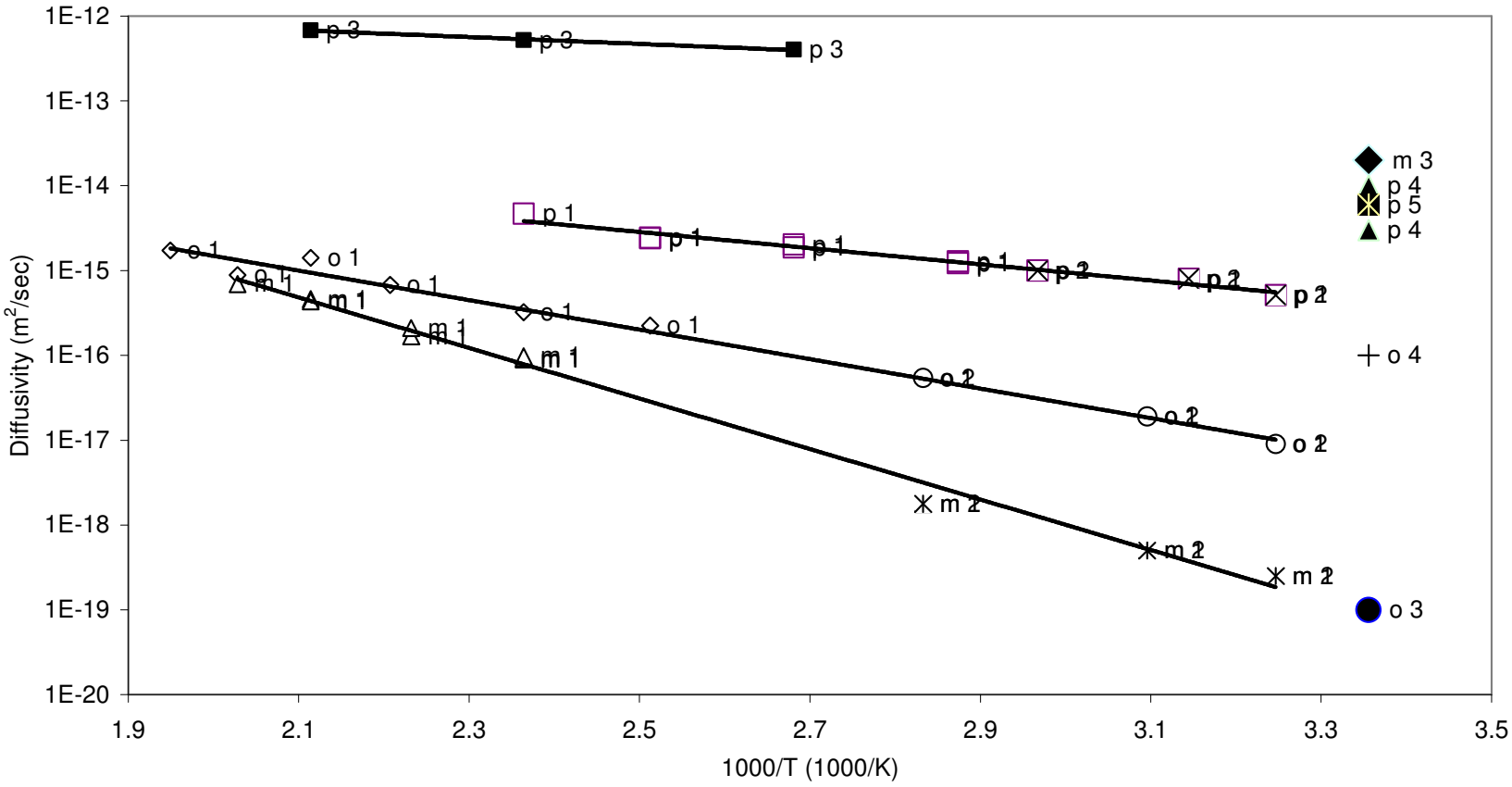

Figure 4.8: Arrhenius plot for Xylene isomers in H-ZSM5

Legend: [p, o and m are para, ortho, and meta xylene respectively; p1, o1, m1 this work; p2, o2, m2, data of Choudhury et al.; p3, data of Han et al.; p4, o3, data of Beschmann et al.;p5, o4, data of Nayak and Riekert; m3, data of Doelle et al.]

4.6 Nomenclature

c	Fluid phase sorbate concentration (mole/m^3)
c_o	Initial fluid phase sorbate concentration (mole/m^3)
D	Intracrystalline diffusion coefficient (m^2/sec)
D_0	Zero loading diffusivity (m^2/sec)
$\tilde{D}$	Integral diffusivity from 0 to q_0, (m^2/sec)
D_m	Molecular diffusion coefficient (m^2/sec)
F	Volumetric fluid flow of purge gas (cc/min)
K	Dimensionless Henry's adsorption constant
L	Dimensionless ZLC parameter
p	gas pressure
q	Adsorbed phase sorbate concentration (mol/m^3)
q_o	Adsorbed phase sorbate concentration to this loading (mol/m^3)
q_s	Saturation adsorbed phase sorbate concentration (mol/m^3)
Q	dimensionless loading
r	Radial position within sorbent particle (m)
r_c, R	Crystal radius (m or μm)
t	Time (sec)
V_s	Volume of solid (m^3)

Greek Letters

β_n	Roots of transcendental equation.
λ	isotherm nonlinearity parameter

4.7 References

51. Beschmann, K., Kokotailo, G. T., Riekert, L., "Kinetics of sorption in zeolite HZSM-5", Chemical Engineering and Processing, 22 (4), 223-9, (1987).

52. Brandani, S., "Effects of Nonlinear Equilibrium on Zero Length Column Experiments", Chemical Engineering Science, 53, 15, 2719-2798 (1998).

53. Brandani, S., Jama, M. A , Ruthven, D. M., "ZLC Measurement Under Nonlinear Conditions", Chemical Engineering Science, 55(7): 1205-1212, (2000a).

54. Brandani, S., Ruthven, D. M., "Analysis of ZLC Desorption Curves", Adsorption, 2, 133-143 (1996).

55. Cherntonghai, P., Brandani, S., "Liquid phase counter-diffusion of aromatics in silicalite using ZLC method", Adsorption, 9, 197-204, (2003).

56. Choudhary, R. V., Nayak, S. V., Choudhary, V. T., "Single component sorption/diffusion of cyclic compounds from their bulk liquid phase in H-ZSM-5 zeolite", Industrial Engineering and Chemical Research, 36, 1812-1818 (1997).

57. Crank, J., "The mathematics of diffusion", Oxford University press, London, 1st edition, (1956).

58. Doelle, H. J., Heering, J., Riekert, L., "Sorption and catalytic reaction in pentasil zeolites. Influence of preparation and crystal size on equilibriums and kinetics", Journal of Catalysis, 71(1), 27-40, (1981).

59. Eic, M., Ruthven, D. M., "A New Experimental Technique for Measurement for Intracrystalline Diffusivity", Zeolites, 8, 40-45 (1988b).

60. Eic, M., Ruthven, D. M., unpublished data.

61. Gates, B. C., Catalytic Chemistry, John Wiley, New York, (1991).

62. Han, M. H., Yin, X. Y., Jin, Y., Chen, S., "Diffusion of Aromatic Hydrocarbon in ZSM-5 Studied by the Improved Zero Length Column Method", Industrial & Engineering Chemistry Research, 38(8):3172-3175 (1999).

63. Karger, K., Ruthven, D. M., "Diffusion in Zeolites and Other Microporous Solids", John Willy & Sons, Inc., New York, (1992).

64. Lee, L-K., Yucel, H., Ruthven D. M., "Kinetics of Adsorption in Biporous Molecular Sieves. Part II: Comparison of Theory and Experiment for Batch Systems", Can. J. Chem. Eng., 57(1), 71-77 (1979)

65. Nakazaki, Y., Goto, N., Inui T.; "Simulation of dynamic behaviors of simple aromatic hydrocarbons inside the pores of a pentasil zeolite", Journal of catalysis, 136, 141-148 (1992).

66. Nayak, V. S., Riekert, L., "Factors influencing sorption and diffusion in pentasil zeolites", Acta Physical et Chemica, 31 (1-2) 156-66, (1985).

67. Prinz, D., Riekert, L., "Observation of rates of sorption and diffusion in zeolite crystals at constant temperature and pressure", Phys. Chem., 90 (5), (1986).

68. Ruthven, D. M., "Principles of Adsorption and Adsorption process", John Wiley & Sons, New York, (1984).

69. Satterfield, C. N., "Heterogeneous Catalysis in Industrial Practice", McGraw Hill, 2nd edition, (1993).

70. Shakeel, A., personal communication, (2003).

71. Silva, J. A. C., Rodrigues, A. E., "Sorption and Diffusion of n-Pentane in Pellets of 5A Zeolite", Industrial Engineering and Chemical Research, 36, 493-500 (1997).

72. Zaman, Sharif F., Loughlin, Kevin F., and Al-Khattaf, Sulaiman A., "Investigation of Diffusivities of 1,3 di-isopropyl benzene and 1,3,5 tri-isopropyl benzene in NaY Zeolite by Zero Length Column Method", For submission to Ind. Eng. Chem. Res., Sep. (2004)

Chapter 5

Investigation of Diffusivities of 1,3 di-Isopropyl Benzene and 1,3,5 tri-Isopropyl Benzene in Alumina by Zero Length Column Method

5.1 Introduction

In FCC catalysis, large bulky molecules of heavy oil crack into smaller molecules. Zeolites are widely used in these cracking reactions. Zeolite crystals have small pore opening and don't permit large molecules to penetrate inside the zeolite cage. The outer surface of zeolite, which is only 3% of the total active site, is available for the larger molecules. Therefore zeolites are commonly combined with an amorphous matrix that cracks the larger molecules into smaller ones, which are then able to access the micropore system. Alumina is commonly used as a catalyst binder for FCC pellets. It has large pores and allows the larger molecules to penetrate inside the pellet and reach the micropore system. Diffusivity of large molecule through this macropore system is important to understand the cracking mechanism of larger molecules.

ZLC, a well established method to measure the intracrystalline diffusivity, was introduced by Eic and Ruthven (1988). Diffusivity and equilibrium constants can be

found following the slope and intercept of the long time region of the desorption curve. Later on Brandani et al. (1996) and Hufton et al. (1994) came up with short time and intermediate time solution of the desorption curve. Xu and Ruthven (1993) applied ZLC method to measure the pore diffusivity in pellets. Rodrigues et al. (1996, 1997, 1998, 2001, 2002) derived the model to the bidisperse system and applied this method for pellet system. Recently Silva et al (2003) investigated the mesopore diffusivity using this method and got consistent data with other methods.

In this study we used ZLC method to investigate the diffusivity of 1,3 di isopropyl benzene and 1,3,5 tri isopropyl benzene in the macropores of alumina for different temperatures. The activation energy was also established.

5.2 Apparatus and experimental details

The apparatus and experimental procedure is described in chapter 3. Alumina crystals are analyzed by SEM, Figure 5.1, to find the crystal size. A wide range of crystal distribution with crystal diameters varies from 50 to 360 micron is observed. Using statistical analysis, taking approximately 114 samples, the mean diameter of the crystals is determined. The analysis results are tabulated in Table 6.1. Two types of analysis, normal distribution and log normal distribution are examined. Standard deviation, skewness, and goodness of fit suggest that log normal distribution is more appropriate to determine the mean particle diameter. In Figure 6.2 two types of distribution curves a normal distribution density curve and a log normal probability density curves are plotted. From the log normal probability curve, the mean diameter is 104.58 microns.

5.3 Results and Discussion

5.3.1 Molecular Size Effect

The molecular size of 1,3 di isopropyl benzene is 8.4 Å and for 1,3,5 tri isopropyl benzene is 9.4 Å. The pore diameter of alumina is around 500 Å. So in this case there is no steric hindrance. These molecules can easily go through the pores. But the larger size 1,3,5 tri isopropyl benzene takes longer time to diffuse out than 1,3 di-isopropyl benzene and this was observed the same in the experiments. 1,3 di-isopropyl benzene diffuses 100 times faster than tri isopropyl benzene.

5.3.2 Diffusivity of 1,3 di-isopropyl benzene and 1,3,5 tri isopropyl benzene

The theory of calculation of diffusivities for various size distributions for crystals has been formulated for gravimetric experiments by Ruthven and Loughlin (1971) and for ZLC experiments by Duncan and Moller (2002). It is shown in both studies that such a distribution introduces tailing into the normally linear long time region of the desorption curve. Duncan and Moller state that analyzing such a curve with the standard ZLC model causes the diffusional time constant to be underpredicted, whereas the adsorption related parameter (L) is overpredicted, and that the error increases with increasing distribution width. For linear adsorption, Duncan and Moller (2002) solved the problem in the Laplace Domain using the expression:

$$\frac{\hat{C}}{C_o} = \frac{1}{s} \frac{\int_{-\infty}^{\infty} \left[\left(e^{\sqrt{2}\sigma\varsigma} \sqrt{s} \right) \coth\left(e^{\sqrt{2}\sigma\varsigma} \sqrt{s} \right) - 1 \right] e^{\sqrt{2}\sigma\varsigma - \varsigma^2} d\varsigma}{\sqrt{\pi} L_m e^{4.5\sigma^2} + \int_{-\infty}^{\infty} \left[\left(e^{\sqrt{2}\sigma\varsigma} \sqrt{s} \right) \coth\left(e^{\sqrt{2}\sigma\varsigma} \sqrt{s} \right) - 1 \right] e^{\sqrt{2}\sigma\varsigma - \varsigma^2} d\varsigma} \tag{5.1}$$

where

$$\left. \begin{aligned} L_m &= \frac{FR_m^2}{3V_s KD} \\ R_m &= e^{\mu} \end{aligned} \right\} \tag{5.2}$$

This equation can be solved numerically using the Fast Fourier Transform technique, with the indicated integral being evaluated by Gauss-Hermite quadrature. The author attempted to solve Equation 5.1 using a Fast Fourier Transform technique but could not derive a solution. Further, based on the earlier work in chapter 3, the system is expected to be nonlinear and so this attempt was not pursued. A further investigation was undertaken by summing the desorption curves of the individual, discrete size fractions, weighted by their volume fraction, but this also proved extremely difficult as the intercept L_m for each size fraction m varies.

From an examination of the papers of Ruthven and Loughlin (1971) and Duncan and Moller (2002), it was decided to fit the experimental data for the size distribution in the region $0.02 \langle \left(1 - \frac{m_t}{m_\infty} \right) \rangle 0.08$ by solving numerically the normalized linear ZLC model at the mean particle diameter R_m and assume that this gives a reasonable representative value of the diffusion coefficient. Also, as no analysis appears to have been made for the nonlinear asymptotic solution for a crystal size distribution for the ZLC, the value of the diffusivity calculated by the above procedure is assumed to not vary significantly from

the value that the nonlinear asymptotic solution gives as is true for the linear case [Brandani (1998), Brandani et al. (2000)].

ZLC desorption curves and theoretical fits for 1,3 di-isopropyl benzene are shown in Figure 5.3 and the results are tabulated in Table 5.2. The temperature range is 125 ^{o}C to 190 ^{o}C. Diffusivity value ranges from 1.08E-11 m^2/sec to 3.5E-11 m^2/sec, L_m values from to and K values from 38,200 to 84,900 which of course is highly nonlinear. For 1,3,5 tri-isopropyl benzene, ZLC desorption curves and theoretical fits are shown in the Figure 5.4 and the results are tabulated in Table 5.3. As 1,3,5 tri-isopropyl benzene is a very unstable compound at higher temperature, a lower temperature range for diffusivity investigation was employed. The temperature range is 75 $^{\circ}$C to 150 $^{\circ}$C. Diffusivity value ranges from 2.36E-13 m^2/sec to 1.26E-12 m^2/sec, L_m values from to and K values from 181,000 to 792,000 which of course is highly nonlinear. Strong temperature dependency is observed in both cases. It should be noticed in all plots that the tail end the desorption curve tends to be curved due to the effect of crystal size distribution. The tailing effect increase with the increase of temperature as more adsorbent comes out initially and then it starts to come out from the inner pores of the large crystals. The Figures shows decreasing of tailing effect with decrease of temperature.

5.3.3 Activation energy determination

The diffusion in zeolite is an activated process, described by an Eyring equation $D = D_o e^{-\frac{E}{RT}}$. The Arrhenius plot for 1,3 di and 1,3,5 tri isopropyl benzene is presented in Figure 5.5. The activation energy E, and pre-exponential factor D_o are calculated from the slope and intercept of Arrhenius plot. The data points are linear within the temperature

range. Activation energy for1,3 di-isopropyl benzene is 27.8 kJ/mol and for 1,3,5 tri-isopropyl benzene is 32.43 kJ/mol. 1,3,5 tri isopropyl benzene needs higher activation energy than 1,3 di isopropyl benzene in order to diffuse through the pores for its big molecular size. Still the activation energy is much less than for the NaY zeolite crystal where they face steric hindrance.

The final question that arises is what kind of diffusion exists? Is it molecular, Knudsen, surface, or intracrystalline diffusion. The effective diffusivity for a homogeneous particle for linear equilibrium is given by

$$D = \frac{\varepsilon_P D_P}{\varepsilon_P + (1-\varepsilon_P)K} \tag{5.3}$$

where

$$\frac{1}{D_P} = \tau_P \left(\frac{1}{D_m} + \frac{1}{D_k} \right) \tag{5.4}$$

and ε_P is the particle voidage, D_P is the pore voidage, K is the linear equilibrium constant, D_m is the molecular diffusivity, D_k is the Knudsen diffusivity, and τ_P is the particle tortuosity. Calculations of D_P indicate it is of the order of magnitude of 10^{-7} m^2/sec. However, the problem is the nonlinear term which is of the order of magnitude of 10^{-5} for 1,3 di isopropyl benzene and 10^{-6} for 1,3,5 tri isopropyl benzene. Dividing D_P by K gives effective diffusion coefficients of the order of magnitude of 10^{-12} and 10^{-13} m^2/sec for the two compounds respectively which is the order of the coefficients. This implies that the reported activation energy is really the negative of some form of the heat of adsorption.

5.4 Conclusion

Diffusivity of 1,3 di and 1,3,5 tri isopropyl benzene is investigated by ZLC method. These two large molecules easily diffuse through the big macropores of alumina. Initial region is equilibrium control as sorbate comes out faster than it can be removed by purge gas stream. Due to the particle size distribution (log normal distribution of particles was found) the original model does not fit the experimental data, suggests the need of a nonlinear model to fit the tailing effect. Duncan and Moller's (2002) model could not be used because it applies to linear system.

Table 5.1: Statistical analysis for particle size distribution of alumina crystal

	Normal Distribution	Log Normal Distribution
Mean diameter (μm)	116.667	4.65
Standard deviation (σ)	68.95	0.64
Skewness (SK)	0.72	0.22
Goodness of fit	2.94	2.7

Table 5.2: Diffusivity results for 1,3 di isopropyl benzene in alumina crystal

Temperature (K)	D/R_m^2 (1/sec)	L_m	Equilibrium Constant x 10^{-4} (K)	Activation Energy (Kcal/mole)	D_o/R_m^2 (1/sec)
398.15	0.0013	4.93	8.49	27.8	5.70
423.15	0.002	4.46	6.10		
443.15	0.0032	3.56	4.34		
463.15	0.004	3.91	3.82		

R_m = Mean radius of particle size distribution.

Table 5.3: Diffusivity results for 1,3,5 tri isopropyl benzene in alumina crystal

Temperature (K)	D/R_m^2 x10^4 (1/sec)	L_m	Equilibrium Constant x 10^{-5} (K)	Activation Energy (Kcal/mole)	D_o/R_m^2 (1/sec)
348.15	0.876	8.05	7.92	32.43	6.66
373.15	1.72	6.56	4.22		
398.15	3.62	7.41	2.08		
423.15	4.69	7.69	1.81		

R_m = Mean radius of particle size distribution.

Table 5.4 : Numerical Calculation of effective diffusivity of 1,3 di-isopropyl benzene in alumina crystal.

Temp (^oC)	Molecular Diffusivity D_{ab} (cm^2/sec)	Knudsen Diffusivity D_{ka} (cm^2/sec)	Pore Diffusivity D_p (cm^2/sec)	Henry's Equilibrium Constant (K)	Effective Diffusivity (m^2/s)
150	1.25E-01	3.92E-02	4.97E-03	8.49E+04	3.15E-12
170	1.36E-01	4.01E-02	5.16E-03	6.10E+04	4.55E-12
190	1.47E-01	4.10E-02	5.34E-03	4.34E+04	6.63E-12
210	1.58E-01	4.19E-02	5.52E-03	3.82E+04	7.77E-12

Table 5.5 : Numerical Calculation of effective diffusivity of 1,3,5 tri-isopropyl benzene in alumina crystal**.**

Temp (^oC)	Molecular Diffusivity D_{ab} (cm^2/sec)	Knudsen Diffusivity D_{ka} (cm^2/sec)	Pore Diffusivity D_p (cm^2/sec)	Henry's Equilibrium Constant (K)	Effective Diffusivity (m^2/s)
125	9.81E-02	3.39E-02	4.20E-03	7.92E+05	2.85E-13
150	1.09E-01	3.49E-02	4.41E-03	4.22E+05	5.63E-13
170	1.18E-01	3.57E-02	4.57E-03	2.08E+05	1.18E-12
190	1.28E-01	3.65E-02	4.74E-03	1.81E+05	1.41E-12

* Porosity = 0.35, Tortuosity = 6, Pressure = 3 atm., $MW_{1,3DIPB}$ = 162 gm/mol, $MW_{1,3,5\ TIPB}$ = 204 gm/mol, d_{pore} = 500 Å.

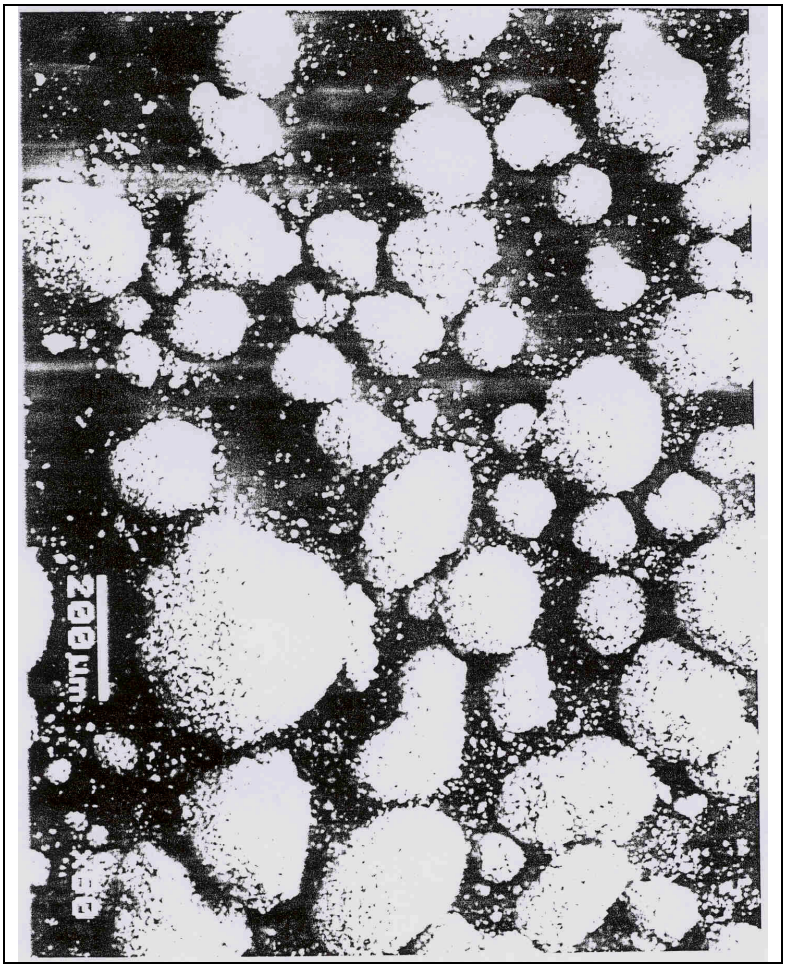

Figure 5.1: SEM analysis of alumina crystal

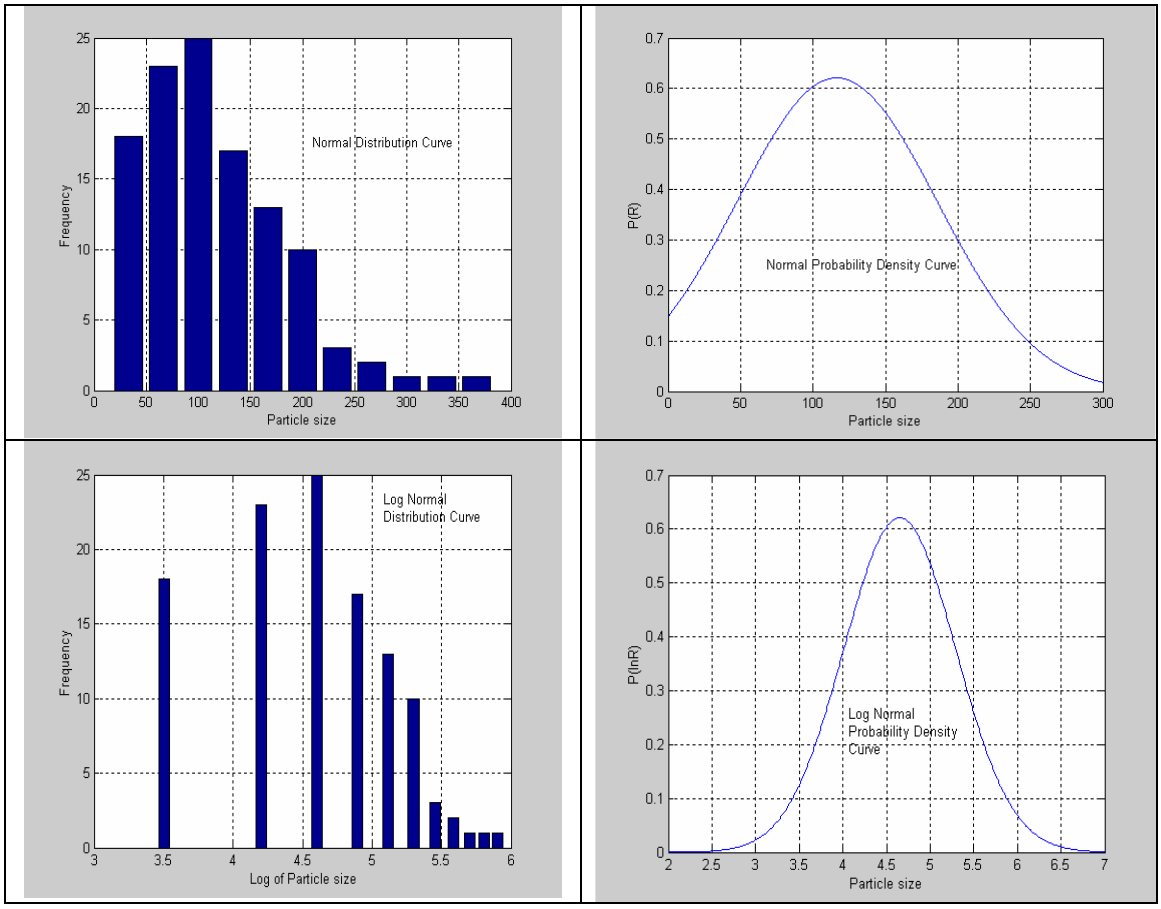

Figure 5.2: Particle size distribution curve for alumina crystal

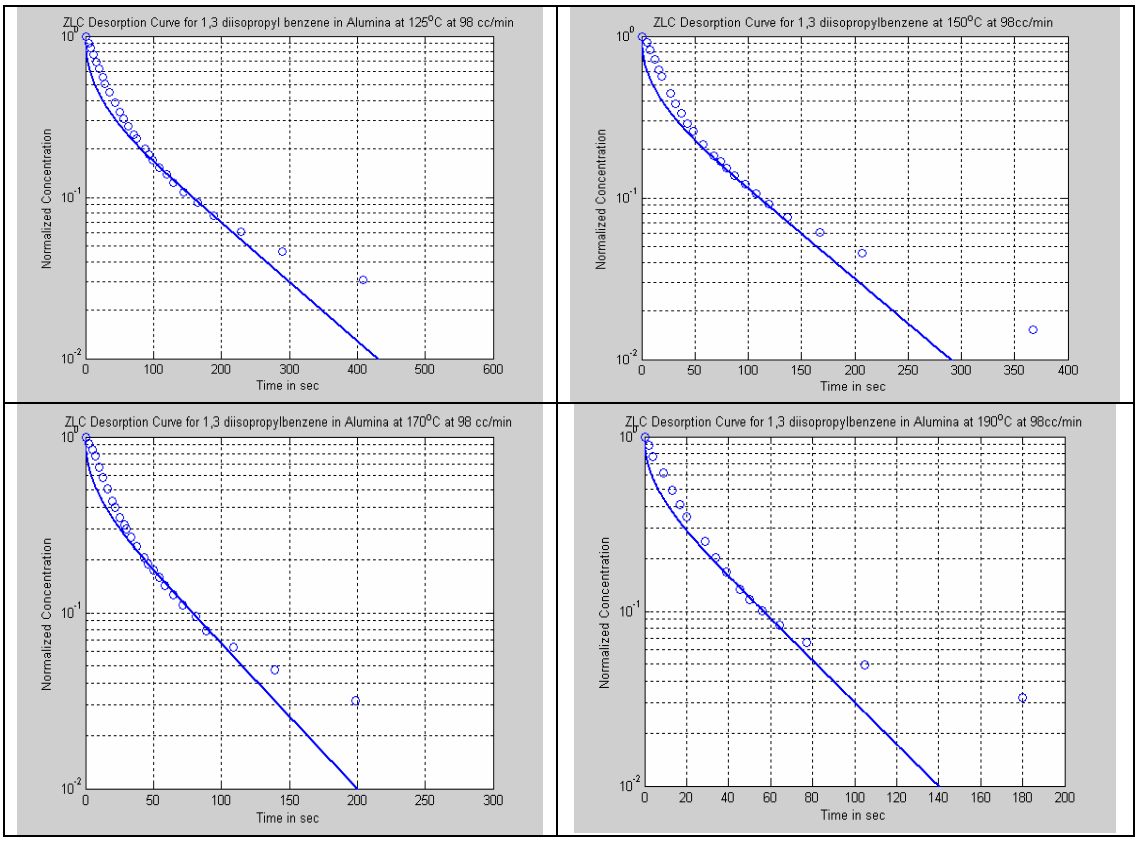

Figure 5.3: ZLC desorption curves for 1,3 di-isopropyl benzene in Alumina crystals at 98 cc/min

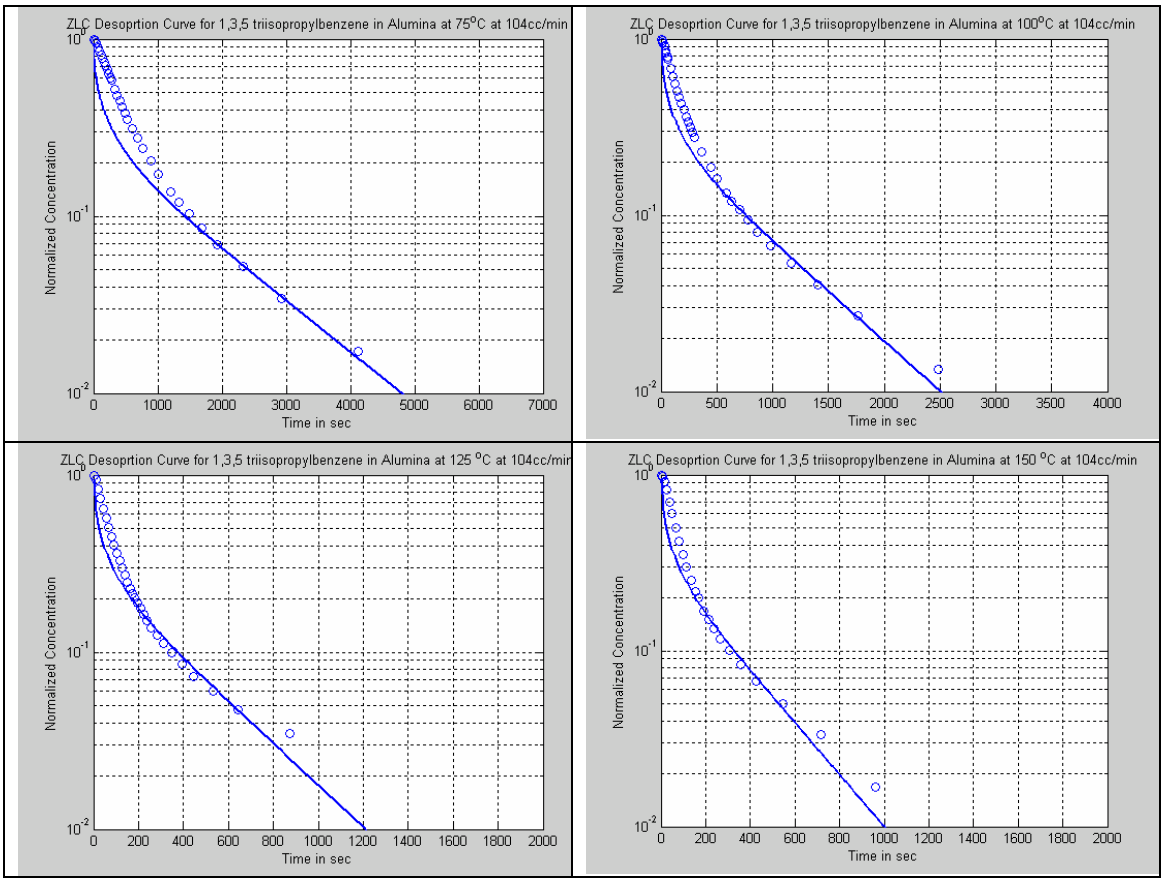

Figure 5.4: ZLC desorption curves for 1,3,5 tri-isopropyl benzene in Alumina crystals at 104 cc/min

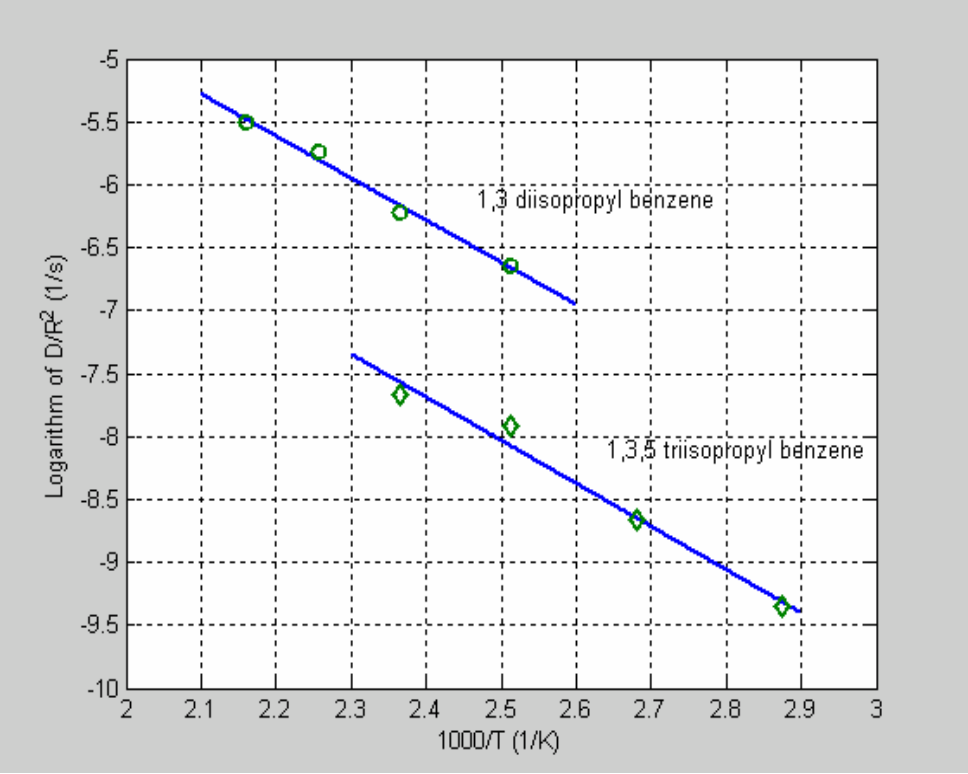

Figure 5.5: Arrhenius plot for 1,3 diisopropyl and 1,3,5 triisopropyl benzene alumina crystal.

5.5 References

1. Brandani, Douglas M. Ruthven, “Analysis of ZLC Desorption Curves”, Adsorption, 2, 133-143 (1996).

2. Brandani, S. “Analytical Solution for ZLC Desorption Curves with Bi-Porous Adsorbent Particle”, Chemical Engineering Science, 51, 12, 3283-3288 (1996).

3. Brandani, S. “Effects of Nonlinear Equilibrium on Zero Length Column Experiments”, Chemical Engineering Science, 53, 15, 2719-2798 (1998).

4. Brandani, S., Xu, Z., Ruthven, D, M., “Transport Diffusion and Self Diffusion of Benzene in NaX and CaX Zeolite Crystals studied by ZLC Tracer ZLC Methods”, Microporous Material, 7, 323-331 (1996).

5. Brandani, S; Jama, M. A.; Ruthven, D. M.; “Diffusion, Self Diffusion and Counterdiffusion of Benzene and P-Xylene in Silicalite”, Microporous ans Mesoporous Material, 35-6: 283-300; (2000a).

6. Brandani, S; Jama, M. A.; Ruthven, D. M.; “ZLC Measurement Under Nonlinear Conditions”, Chemical Engineering Science, 55(7): 1205-1212, (2000b).

7. Bulow, M., Micke, A., “Determination of Transport Coefficient in Microporous Solids”, Adsorption, 1, 29-48 (1995).

8. Cavalcante, C. L. Jr., Diana C.S. Souza, A. I G., A. Silva, C. M., Alsina, L. S., and Lima, V. E., Araujo, A. S., “Sorption and Diffusion of p-Xylene and o-Xylene and in Aluminophosphate Molecular Sieve AlPO4-11”, Adsorption, 6, 53-59 (2000).

9. Cavalcante, C. L., Jr., Brandani, S., Ruthven, D. M., “Evaluation of the Main Diffusion Path in Zeolites from ZLC Desorption Curves”, Zeolites, 18, 282-285 (1997).

10. Duncan, W. L., Moller, K. P., “A Zero Length Criterion for ZLC Chromatography”, Chemical Engineering Science, 55, 5415-5420 (2000a).

11. Duncan, W. L., Moller, K. P., “On Diffusion of Cyclohexane in ZSM-5 Measured by Zero Length Column Chromatography”, Industrial Engineering and Chemical Research, 39, 2105-2113 (2000b).

12. Duncan, W. L.; Moller, K. P.; “The Effect of a Crystal Size Distribution on ZLC Experiments”; Chemical Engineering Science, 57(14): 2641-2652 (2002).

13. Eic, M., Ruthven, D. M., “A New Experimental Technique for Measurement for Intracrystalline Diffusivity”, Zeolites, 8, 40-45 (1988).

14. Eic, M., Ruthven, D. M., “Intracrystalline Diffusion of Linear Paraffins and Benzene in Silicalite Studies by the ZLC Method”, Zeolite: Facts, Figures, Future, 897-905 (1989).

15. Han M. H.; Yin, X. Y.; Jin, Y.; Chen, S.; “Diffusion of Aromatic Hydrocarbons in ZSM-5 Studied by the Improved Zero Length Column Method”, Industrial & Engineering Chemistry Research, 38(8):3172-3175 (1999).

16. Jan-Baptist W.P. Loos, Peter, J. T., Jacob A. Moulijn, “Improved Estimation of Zeolite Diffusion Coefficient from Zero-Length-Column Experiments”, Chemical Engineering Science, 55, 51-65 (2000).

17. Jose A. C. Silva, Alirio E. Rodrigues, “Analysis of ZLC Technique for Diffusivity Measurement in Bidisperse Porous Adsorbent Pellets”, Gas Sep. Purif., 10, 4, 207-224 (1996).

18. Jose A. C. Silva, Alirio E. Rodrigues, “Sorption and Diffusion of n-Pentane in Pellets of 5A Zeolite”, Industrial Engineering and Chemical Research, 36, 493-500 (1997).

19. MacDougall, H; Ruthven, D. M. ; Brandani, S; “Sorption and Diffusion of SF_6 in Silicalite Crystal”, Adsorption, 5(4):369-372 (1999).

20. Ruthven, D. M., Loughlin, K. F., “Effect of crystal size distribution on diffusion measurements in molecular sieves”, Chem. Eng. Sci. 26(5), 577-84 (1971).

21. Zhu, W.; Kapteijn, F.; Moulijn, J. A.; “Diffusion of Linear and Branched C-6 Alkanes in Silicalite-1 Studied by The Trapped Element Oscillating Microbalance”, Microporous and Mesoporous Materials, 47(2-3): 157-171 (2001).

Chapter 6

Investigation of diffusivity of 1,3 di-isopropylbenzene and 1,3,5 tri-isopropylbenzene in FCC catalyst pellet by Zero Length Column method

6.1 Introduction

The successful application of zeolites as an industrial sorbent depends on the appropriate development sorption cycle (Barrer 1981) and this requires an intensive study of phenomena like equilibria and kinetics of adsorbent. Adsorption equilibrium isotherms can be analyzed from a thermodynamic point of view using virial isotherm (Kiselev 1971, Ruthven et al. 1974), molecular model based on localized adsorption (e.g. Langmuir 1918, Nitta et al. 1984) and empirical correlations (Yans 1987). Kinetics of sorption in bidisperse porous adsorbent generally includes macropore and micropore diffusion, and both can significantly influence the rate of mass transfer.

In practice zeolite solids are available in pellet form by compressing zeolite crystal together with a small amount of binder to form pellets. The void between microparticles contributes to the mesopore and macropore of the particle. These pores act as a conduit to transport molecules from the surroundings to the interior of the particle. Molecules adsorb at the pore mouth of the microparticles and thence the adsorbed molecule diffuse into the interior of the crystal. Micropores within the crystal provide the adsorption space to accumulate adsorbate molecules. The dynamics into this particle is affected by the interplay between the two diffusion processes (macropore & micropore) as well as the capacity accommodated by micropores.

Zero Length Column (ZLC) technique is a well developed method to investigate both crystal and pellet diffusivities. ZLC technique, developed by Eic and Ruthven (1988), retains the main feature of conventional fixed bed chromatographic techniques (e.g. axial dispersion, external mass transfer resistance). ZLC is a differential bed of porous particles which is first saturated with the fluid mixture containing the adsorbable component. At time zero the carrier gas flows through the ZLC at sufficiently high flow rate and desorption curve is analyzed in terms of concentration of adsorbate vs time.

In this study we measured the diffusivity of 1,3 di-isopropyl benzene and 1,3,5 tri-isopropyl benzene in FCC catalyst pellet (0.9 micron NaY zeolite) by ZLC method. The objective is to determine the apparent diffusivity and pore diffusivity for the system and attempt to identify the controlling mechanism of mass transfer in the FCC catalyst pellet.

6.2 Literature Review

The Zero Length Column technique is widely used for investigating adsorption kinetic data, i.e., intracrystalline diffusion, Henry's law constant, equilibrium isotherms, for hydrocarbons in zeolite crystals. Eic and Ruthven (1988) proposed this method. A very small sample of crystal is loaded with adsorbate then purged with high velocity inert gas, and diffusivity data is investigated by following the desorption curve. This method is also applicable to the study of macropore diffusion and useful when sorption diffusion rates are too fast to follow easily by traditional methods, Ruthven et al. (1993). Ruthven and Xu (1993) came with the first paper using ZLC method to find diffusivity data for O_2 and N_2 in 5A commercial adsorbent pellets. For a spherical macroporous particle with rapid intracrystalline diffusion within the microparticle, the basic differential mass balance equation is given by

$$\varepsilon_p \frac{\partial C}{\partial t} + (1-\varepsilon_p)\frac{\partial q}{\partial t} = \frac{1}{R^2}\frac{\partial}{\partial R}\left[\varepsilon_p D_p R^2 \frac{\partial C}{\partial R}\right] \tag{6.1}$$

q(is assumed)=KωC (Linear equilibrium) between the adsorbed phase within the microparticles and the gas within the macropores, and the pore diffusivity (D_p) is independent of concentration. Thus the model equation reduces to

$$\frac{\partial C}{\partial t} = \frac{\varepsilon_p D_p}{\varepsilon_p + (1-\varepsilon_p)K\omega}\left[\frac{\partial^2 C}{\partial R^2} + \frac{2}{R}\frac{\partial C}{\partial R}\right] \tag{6.2}$$

This is identical with the standard form of the diffusion equation for a spherical particle. The effective diffusivity is given by

$$D_e = \frac{\varepsilon_p D_p}{\varepsilon_p + (1-\varepsilon_p)K\omega} \tag{6.3}$$

where ε_p is the porosity of the pellet, *w* represents the fraction of zeolite in the solid matrix and K is the equilibrium constant expressed on a crystal volume basis. The values of Henry's equilibrium constant, K, must be evaluated by another method, i.e., moment analysis, gravimetric methods.

For the measurement of diffusivities of O_2 and N_2 in 5A pellet, the effective diffusivity is higher for oxygen than for nitrogen but for the pore diffusivity the reverse is true. The temperature dependence of pore diffusivity shows a well defined minimum at around 250 K for nitrogen and 190 K for oxygen. this pattern suggests that surface diffusion is probably important particularly at lower temperature. At higher temperature, strong temperature dependence of diffusivities suggests that molecular diffusion rather than Knudsen diffusion is the dominant transport mechanism.

The increase in $\varepsilon_p D_p$ with decreasing temperature at the low temperature region is attributed to an increasing contribution of surface diffusion resulting from a relatively strong temperature dependence of K_s. Xu and Ruthven (1993) assume that the fluxes of molecular diffusion (large pores) and surface diffusion (in small pores) are additive

$$\varepsilon_p D_p = \varepsilon_p D_p^{'} + K_s a D_s \tag{6.4}$$

Temperature dependence of the surface diffusion contribution depends on the difference between the adsorption energy (-ΔU) and the diffusional activation energy (E):

$$K_s D_s \infty \exp\left[\frac{(-\Delta U - E)}{R_g T}\right] \tag{6.5}$$

From the low temperature asymptote we can fine the value of (-ΔU-E). At higher temperature contribution of surface diffusion is negligible and molecular diffusion predominates.

Later on most the work on investigating pellets diffusivity by ZLC method has been done by Rodrigues *et al*. Silva and Rodrigues (1996), developed the model for the ZLC accounting for macropore and micropore (crystal) diffusivity. They also derived the analytical solution for the model equation and investigated the effect of model parameters on the desorption curves and derive a methodology to obtain diffusional parameter from the long time straight line and intercept in the semi-log plots. Brandani (1996), also derived a model for bi-porous adsorbent particles and provides the analytical and numerical solution for it. Both of them ended with the similar criterion for defining the controlling mechanism.

6.3 Mathematical model

Mathematical model describing ZLC system is based on the following assumptions.

(1) The adsorbent pellet has a bidisperse porous structure containing macropores and micropores.

(2) Fick's law of diffusion is valid for macropore and micropore diffusion.

(3) Macropore and micropore diffusion are in series.

(4) Adsorption in macropores is negligible.

(5) The adsorption equilibrium isotherm is linear.

(6) There is a film resistance at the adsorbent external surface.

(7) The ZLC cell is equivalent to a continuous stirred tank adsorber.

(8) The pellets and microparticles have spherical geometry.

(9) There is isothermal operation.

Mass balance for the adsorbable components in crystals (micropore)

$$\frac{\partial C_s}{\partial t} = D_c \frac{1}{r_c} \frac{\partial}{\partial r}\left(r^2 \frac{\partial C_s}{\partial r} \right) \tag{6.6}$$

Boundary conditions are given by

$$r = 0; \qquad \frac{\partial C_s}{\partial r} = 0 \tag{6.6a}$$

$$r = r_c; \qquad C_s = HC_p \tag{6.6b}$$

$$t = 0; \qquad C_{so} = HC_{po} \tag{6.6c}$$

Equations (6.6a) and (6.6b) are the symmetry condition at the center of the microsphere and the adsorption equilibrium at the macropore/crystal interface, respectively. H is the dimensionless equilibrium constant.

Mass balance for the adsorbable component in a volume element of the pellet:

$$\varepsilon_p \frac{\partial C_p}{\partial t} + \left(1 + \varepsilon_p\right) \frac{\partial \overline{C_s}}{\partial t} = \varepsilon_p D_p \frac{1}{R^2} \frac{\partial}{\partial R}\left(R^2 \frac{\partial C_p}{\partial R} \right) \tag{6.7}$$

where C_s is the average adsorbed concentration in the crystal, R is the radial coordinate in the pellet, ε_p is the macropore porosity, C_p is the concentration in the macropores and D_p is the diffusivity in the macropores. The boundary and initial conditions are given by

$$R = 0, \qquad \frac{\partial C_p}{\partial R} = 0 \tag{6.7a}$$

$$R = R_p, \qquad \varepsilon_p D_p \frac{\partial C_p}{\partial R}\bigg|_{R=R_p} = k(C_{out} - C_p\big|_{R=R_p}) \tag{6.7b}$$

$$t = 0, \qquad C_p = C_0 \tag{6.7c}$$

Equations (6.7a) and (6.7b) represents the symmetric condition and the equality of fluxes at the pellet surface respectively.

Mass balance of the ZLC cell

Neglecting the accumulation in the interparticle void fraction, the mass balance for the adsorbate in the ZLC cell is:

$$vC_{in} = vC_{out} + \frac{1-\varepsilon_b}{\varepsilon_b} l\varepsilon_b D_p \frac{3}{R_p} \frac{\partial C_p}{\partial R}\bigg|_{R=R_p} \tag{6.8}$$

where v is the interstitial velocity, C_{in} is the fluid phase concentration at the ZLC inlet, C_{out} is the fluid phase concentration at the ZLC outlet, ε_b is the void fraction of ZLC and l is the length of the ZLC cell. The initial condition is given by

$$t = 0, \quad C_{out} = C_0, \quad C_{in} = 0 \tag{6.9}$$

Normalization

Introducing dimensionless variables for concentration in the macropore and crystal, and the average concentration in the crystal, respectively,

$$C_p^a = \frac{C_p}{C_o}; \quad C_s^a = \frac{C_s}{C_{so}}; \quad \overline{C_s^a} = \frac{\overline{C}_s}{C_{so}} \tag{6.10}$$

and for time and space coordinate in the crystal and pellet, respectively

$$\theta = \frac{D_p t}{R_p^2}; \quad x = \frac{r}{r_c}; \quad y = \frac{R}{R_p} \tag{6.11}$$

The dimensionless model equations now follow

Mass Balance in microsphere

$$\frac{\partial C_s^a}{\partial \theta} = \gamma \frac{1}{x} \frac{\partial}{\partial x}\left(x^2 \frac{\partial C_s^a}{\partial x} \right) \tag{6.12}$$

with boundary and initial conditions:

$$x = 0, \quad \frac{\partial C_s^a}{\partial x} = 0 \tag{6.12a}$$

$$x = 1, \quad C_s^a = C_p^a \tag{6.12b}$$

$$\theta = 0; \quad C_s^a = 1 \tag{6.12c}$$

Mass balance in the adsorbent pellet

$$\frac{\partial C_p^a}{\partial \theta} + K \frac{\partial \overline{C_p^a}}{\partial \theta} = \frac{1}{y^2} \frac{\partial}{\partial y}\left(y^2 \frac{\partial C_p^a}{\partial y} \right) \tag{6.13}$$

with boundary and initial condition

$$y = 0; \quad \frac{\partial C_p^a}{\partial y} = 0 \tag{6.13a}$$

$$y = 1; \quad \left. \frac{\partial C_p^a}{\partial y} \right|_{y=1} = l\left(C_{in}^a - C_p^a \big|_{y=1} \right) \tag{6.13b}$$

$$\theta = 0; \quad C_p^a = 1 \tag{6.13c}$$

The model parameters are as follows

(i) Adsorption equilibrium parameter K (capacity factor)

$$K = \left(\frac{1-\varepsilon_p}{\varepsilon_p} \right) H \tag{6.14}$$

(ii) Diffusion controlling mechanism γ, (ratio of time constant for macropore and crystal diffusivities); $\gamma = \frac{\left(\frac{D_c}{r_c^2} \right)}{\left(\frac{D_p}{R_p^2} \right)}$. Crystal diffusivity is the controlling mechanism for $\gamma(1+K)<0.1$; macropore diffusivity is controlling for $\gamma(1+K)>10$; if $0.1 < \gamma(1+K) < 10$ then both macropore and crystal diffusivity should be taken into account.

(iii) ZLC parameter L:

$$\frac{1}{L} = \frac{3(1-\varepsilon_b) l \varepsilon_p D_p}{v \varepsilon_b R_p^2} + \frac{\varepsilon_p D_p}{R_p k} \tag{6.15}$$

the first term of the right hand side of the above equation is the ratio of space time in the ZLC, $\tau = \frac{(1-\varepsilon_b) l}{\varepsilon_b v}$, and macropore diffusion time constant. The second term in the right hand side is the ratio of the film mass transfer time constant and macropore diffusion time constant, i.e., the reciprocal of the Biot number.

This model equation can be solved analytically for linear isotherm, which is the case for ZLC experiments. For negligible film mass transfer resistance, the outlet concentration of ZLC is given by :

$$\frac{C_{out}}{C_o} = 2L\sum_{m=1}^{\infty}\sum_{n=1}^{\infty}\frac{1}{\beta_{n,m}}\frac{\exp\left(-\gamma\beta_{n,m}^2\theta\right)}{\left(\frac{\lambda_n^2 + L(L-1)}{\lambda_n}\right)\left.\frac{d\lambda}{d\beta}\right|_{\beta=\beta_{n,m}}} \tag{6.16}$$

where $\beta_{n,m}$ and λ_n are obtained from the transcendental equations

$$\lambda_n \cot\lambda_n + L - 1 = 0 \tag{6.17}$$

$$\lambda_n = \sqrt{\beta_{n,m}^2\gamma + 3K\gamma(1 - \beta_{n,m}\cot\beta_{n,m}} \tag{6.18}$$

and

$$\left.\frac{d\lambda}{d\beta}\right|_{\beta=\beta_{n,m}} = \frac{\gamma}{2\lambda_n}\left(2\beta_{n,m} + 3K\times\left(\cot\beta_{n,m}\left(\beta_{n,m}\cot\beta_{n,m-1}\right) + \beta_{n,m}\right)\right) \tag{6.19}$$

Numerical solution for the model equation is done using matlab ODE solver.

Data analysis for pellets in ZLC experiments

ZLC analysis of macropore and micropore systems is well documented in literature. Analytical solution for the bidisperse pellet model equations is also done. *Silva et al* (1997) had reported the method of analyzing ZLC data similar to the micropore system.

For crystals the equation that describe the change of gas concentration in the desorption steps is, Eic et al. (1988)

$$\frac{C}{C_0} = 2L\sum_{n=1}^{\alpha}\frac{\exp\left(-D_c\beta_n^2 t/R_c\right)}{\beta_n^2 + L(L-1)} \tag{6.20}$$

$$\beta_n\cot(\beta_n) + L - 1 = 0 \tag{6.20a}$$

$$L = \frac{Q_p R_c^2}{3KV_s D_c} \tag{6.20b}$$

where D_c is the crystal diffusivity, Q_p is the purge flow rate, R_c is the crystal radius, V_s is the solid volume inside the cell, K is the equilibrium constant, and L is the ZLC parameter.

For the case of the macroporous pellet with macropore diffusion control, similar equation can be derived,

$$\frac{c}{c_0} = 2L\sum_{n=1}^{\alpha}\frac{\exp\left(-D_{ap}\beta_n^2 t/R_p\right)}{\beta_n^2 + L(L-1)} \tag{6.21}$$

$$\beta_n \cot(\beta_n) + L - 1 = 0 \tag{6.21a}$$

$$L = \frac{\varepsilon_c Q_p R_c^2}{3(1-\varepsilon_c)\left[\varepsilon_p + (1-\varepsilon_p)K\right]V_c D_{ap}} \tag{6.21b}$$

$$L = \frac{1}{2}\frac{Purge\ flow\ rate}{Pellet\ vloume}\frac{R_p^2}{\varepsilon_p D_p} \tag{6.21c}$$

where D_{ap} is the apparent diffusivity, ε_c is the porosity of the cell, ε_p is the porosity of the pellet, V_c is the volume of the cell. The apparent diffusivity is expressed by

$$D_{ap} = \frac{\varepsilon_p D_p}{\varepsilon_p + (1-\varepsilon_p)K} \tag{6.22}$$

where, D_p, the pore diffusivity, is related to Knudsen and molecular diffusion by Bosanquet equation.

$$\frac{1}{D_p} = \tau_p\left(\frac{1}{D_m} + \frac{1}{D_k}\right) \tag{6.23}$$

where D_m and D_k are the molecular and Knudsen diffusivity, respectively, and τ_p is the pore tortuosity.

According to Eic and Ruthven (1988), an easy way to determine the model parameters is the use the information of desorption curve at long times. Equation 6.21 reduces to

$$\ln\left(\frac{c}{c_o}\right) = \ln\left[\frac{2L}{\beta_1^2 + L(l-1)}\right] - \frac{\beta_1^2 D_{ap}}{R_p^2} t \tag{6.24}$$

From the slope of the desorption curve we can get the value of D_{ap} and hence the value of D_p is calculated from equation 6.22.

(6.25)

Molecular diffusion, D_m, can be estimated by Chapman-Enskog equation. Knudsen diffusion, D_k, can be calculated by the equation

$$D_K = \frac{2r}{3}\sqrt{\frac{8R_g T}{\pi M}} \tag{6.26}$$

Hence we can estimate the tortuosity factor, τ_p for the pellet.

For the case of pellets of a bidisperse adsorbent, the simplest analysis to determine whether control is by macropore diffusion is to use pellets with different sizes (different R_p but same r_c). If the desorption curve is dependent on the square of the pellet size (R_p^2 dependence), the controlling mechanism is macropore diffusion. If it is independent of R_p then controlling mechanism is crystal diffusion. In the intermediate region desorption curve is sensitive to the pellet size and controlling mechanisms are both macropore and crystal diffusion. Another way, for same pellet size but with variation in crystal size, if the desorption curves are insensitive the controlling resistance to mass transfer is the macropore diffusion.

In bidisperse porous adsorbents such as zeolite pellets there are two diffusion mechanisms: the macropore diffusion with time constant $R_p^2 K / D_p$ and the micropore

time constant r_c^2 / D_c . Ruckenstein et al. (1971) developed a bidisperse porous model applied to the measurement of transient diffusion in system with linear isotherm taking diffusion mechanism in series. Based on the model Ruthven and Loughlin (1972) developed a criterion for the relative importance of the diffusion mechanisms, which is given by γ:

$$\gamma = \frac{\left(D_c / r_c^2 \right)(1+K)}{D_p / R_p^2} \tag{6.27}$$

where $K = \frac{(1-\varepsilon_p) H_{ad}}{\varepsilon_p}$, the capacity factor and $H_{ad} = \frac{\rho_s RTH}{M_w}$ is the dimensionless Henry's constant or local slope of the isotherm. Macropore diffusivity is the controlling mechanism for $\gamma > 10$; crystal diffusivity is controlling for $\gamma < 0.1$. If $0.1 < \gamma < 10$, both macropore and micropore diffusivity should be taken into account.

Silva et al. (1997) carried out a study, an extension of diffusivities in pellets made by Ruthven and Xu (1993). They dealt with experimental and modeling studies of equilibria and diffusion of n-pentane in commercial adsorbents of 5A zeolite, used in the n/iso paraffin separation process. Adsorption equilibrium isotherms were generated by gravimetric method and measured the diffusivity data by both ZLC and gravimetric method. For one solution they assumed pellets and crystals are spheres and used the limiting form of ZLC model for bi-disperse pellet, given by Brandani (1996) and Silva and Rodrigues (1996). Another approach for the solution was to consider the pellets as an infinite cylinder, and took the long time solution for the ZLC system in a macropore controlled system, using the values of slope and intercept from the experimental data to

find the parameters. They concluded that both ways should give the same values for the parameters.

Equilibrium, diffusion and fixed bed adsorption of n-hexane in 5A zeolite pellets was studied by Silva et al. (1997). ZLC method was used to measure the diffusivity values taking the long time solution of the desorption curve. Controlling resistance to mass transfer was macropore found by changing the crystal size.

The deactivation of adsorbents is a problem for process industries using adsorption technology. The adsorbents are subjected to many cycles leading to a drift in their effectiveness due to the deposit of carbon rich compound, i.e., coking. The adsorption capacity and diffusivity are largely affected in coked component. Silva et al. (2000) studied the effect of coke on the adsorption capacity and diffusivity in 5A zeolite pellet. Probe molecule was n-pentane. They used the gravimetric method to measure the equilibrium isotherm and ZLC technique to measure the diffusivity. In fresh pellet the controlling mechanism is the macropore resistance (Silva and Rodrigues, 1997). Macroporosity does not changed for the coked pellets but the capacity factor, K, decreases over the fresh one, which may result a higher reciprocal time constant, $\left(\frac{D_p}{R^2}(1+K)\right)$, for the macropore control system. But the study found that the reciprocal time constant is rather small in coked pellets, which in turn implies micropore control resistance in coked pellet. The activation energy for the coked pellet is much lower than the fresh pellet.

Propane and propylene separation is the most energy consuming separation process in the petrochemical industries. For modeling of adsorptive process such as pressure swing adsorption (PSA) or vacuum swing adsorption (VSA), equilibrium and kinetic data are needed to solve the material and energy balance. Carlos et al. (2001), investigated the equilibrium and kinetic data of propane and propylene over two samples of silica gel. Diffusivity data was investigated by ZLC method. The diffusivity in both samples was well defined by Knudsen diffusion (macropore control).

Equilibrium and kinetic data for propane and propylene adsorption in pellets and crystals of 5A zeolite was investigated by *Carlos et al.* (2002). Long time solution of ZLC data was used to investigate diffusivity data. Mass transport in zeolite pellets is controlled by macropore diffusion.

Carlos et al. (2003) reported the equilibrium and kinetic data for adsorption of propane and propylene on carbon molecular sieve. Zero length column technique was used to measure the diffusivity. Transport of both hydrocarbons in the pellet is controlled by macropore diffusion.

6.4 Results and discussion

Commercial FCC catalysts consist of an alumina matrix and NaY zeolite pellet. These pellets consist of a combination of macropores, mesopores and micropores in an interconnecting network framework. The determination of the controlling resistance in the reaction cracking system in this network is the objective of this work.

The adsorption of 1,3 di-isopropyl benzene and 1,3,5 tri-isopropyl benzene in both alumina and NaY zeolite is nonlinear as determined earlier. If the pellet system is micropore controlled, the nonlinear asymptotic solution to the ZLC model may be used to calculate the zero diffusivity. For a macropore controlled system, the nonlinear asymptotic solution has not been derived for the ZLC system. If we assume for both cases that the long time slope of the linear model for the ZLC is equal to the zero loading diffusivities of the non-linear cases, then we can easily extract the diffusivity from the data using the linear model. This approximation has been shown to be valid for the micropore ssytem [Brandani (1997), Brandani et al. (2000)].

The theoretical effective diffusivity may be calculated taking into consideration only macropore system using equation . The molecular diffusivity (D_m) is calculated by Fuller, Schettler and Giddings correlation $D_{AB} = \frac{10^{-3} T^{1.75} \left(\frac{1}{M_A} + \frac{1}{M_B} \right)^{\frac{1}{2}}}{P\left[(V)_A^{1/3} + (V)_B^{1/3} \right]}$, and the Knudsen diffusion (D_K) by using equation $D_K = 4850\, d_{pore} \sqrt{\frac{T}{M_A}}$. Theoretical pore

diffusivity is found using $D_p = \frac{1}{\tau\left(\frac{1}{D_M} + \frac{1}{D_K}\right)}$, taking porosity, d_{pore} = 500 Å, ε = 0.5 and tortuosity, τ = 6 which are common for FCC systems.

6.4.1 Diffusivity of hydrocarbons

Experimental data points are fitted with the model equation (6.21) and from the long time slope of the desorption curve, the diffusivities for pellet system are calculated. Benzene diffuses very fast through the pellets because of its small molecular size. The desorption curves are presented in Figure 6.1 and the apparent diffusivity values are reported in Table 6.1. For temperature range 100-175°C, experimental values for benzene lies in the range of 10^{-13} m^2/sec. Cumene molecule is larger than benzene and diffuses slower than benzene. Investigated temperature range is 150–225°C. The desorption curves are shown in Figure 6.2 and results are reported in Table 6.2. Effective diffusivity lies in the range of 10^{-13} m^2/sec. Theoretical apparent diffusivity for macropore is the region in 10^{-10} m^2/sec.

However, for both benzene and cumene, diffusivity is so fast that the results are controlled by the operating response of the system and hence the reported values have limited significance.

1,3 di-isopropyl benzene diffuses slower than cumene. The desorption curves are shown in Figure 6.3 and the results are reported in Table 6.3. Equilibrium constant ($K_{Overall}$) values ranges from $1.1x10^4$ to $9.8x10^4$, indicates it's in nonlinear region. Theoretical apparent macropore diffusivities are in the range of $5x10^{-11}$ to $5x10^{-12}$ m^2/sec, whereas

experimental values lie between $6.11x10^{-13}$ to $5.14x10^{-14}$ m^2/sec. This suggests macropore is not the controlling resistance here.

In the earlier analysis on the diffusivity of 1,3,5 tri-isopropyl benzene in NaY crystals, a kink was observed on the desorption curve and the reported measured desorption diffusivity was hypothesized to be the diffusivity of reacted products1,3 di-isopropyl benzene and propylene. Accordingly, it is anticipated that the diffusivity from the NaY crystals in the FCC pellets will be primarily by diffusion of these two products. However, the pellets consist of 80% alumina matrix, in which the diffusion of unreacted 1,3,5 tri-isopropyl benzene is expected to occur. Accordingly exiting the pellet initially will be three species, 1,3,5 tri-isopropyl benzene, 1,2 di-isopropyl benzene and propylene. With the passage of time, the exodus of 1,3,5 tri-iso-propyl benzene will finish earlier than the exodus of 1,3 di-iso propyl benzene and propylene. In effect in the later stages of the desorption cycle, all we are measuring is the diffusivity of these two compounds from the zeolite matrix. As the long time solution of the ZLC technique is only relevant to the last stages of the desorption cycle, the diffusivity of the material measured is basically that of the co-diffusion of di-isopropyl isomers and propylene. In the paragraph that follows, when we speak of the diffusivity of 1,3,5 tri-iso propyl benzene in the long time region, it is really the co-diffusion of these two species that is occurring.

The largest molecule, 1,3,5 tri-isopropyl benzene, has an effective diffusivity in the range of $8.75x10^{-13}$ to $8.31x10^{-15}$ m^2/sec whereas theoretical macropore diffusivity values lie in the range of $1.7x10^{-11}$ to $2.8x10^{-12}$ m^2/sec. These values suggests that diffusion is not macropore controlled. The desorption curves are presented in Figure 6.4 and the results

are reported in Table 6.4. The $K_{Overall}$ values in this case indicates that the system is in nonlinear region.

6.4.2 Determination of controlling resistance

One of the ways to determine whether the system is macropore or micropore controlled is by comparing the diffusivity data for both crystal and pellet system. For a micropore control system pellet must have the same diffusivity values as in crystals, for the same crystal particle size. For 1,3 di-isopropyl and 1,3,5 tri-isopropyl benzene both pellet and crystal desorption curves have same slope in the long time region, which suggest they have same diffusion time constant. For pellets there is a rapid drop of concentration initially. This is due to desorption of the hydrocarbons from the alumina matrix macropores which depletes faster than the zeolite at the start of desorption. Later on when the alumina matrix is nearly depleted, the sorbate mainly exits from the crystal pores. Simulations have been undertaken taking the crystal diffusivity value as the diffusivity and correct the L value for pellet system. The figures are presented in Figure 6.5 and 6.6. Simulation line fits the long time pellet data perfectly; hence for 1,3 di and 1,3,5 tri-isopropyl benzene, crystal and pellet have the same diffusion time constant. So they are micropore controlled system.

6.4.3 Arrhenius plot

Figure 6.7 presents Arrhenius plot for 1,3 di-isopropyl benzene and 1,3,5 tri-isopropyl benzene. Diffusional time constant is plotted against 1000/T. It is clear that for both

systems, crystal and pellet diffusional time constant values are close to each other. The activation energy for 1,3 di-isopropyl benzene is 66 kJ/mol and 1,3,5 tri-isopropyl benzene is 77.35 kJ/mol.

6.5 Conclusion

Diffusivity values of benzene, cumene, 1,3 di-isopropyl benzene, 1,3,5 tri-isopropyl benzene in FCC pellet were measured by ZLC method. Diffusion of 1,3 di-isopropyl benzene and 1,3,5 tri-isopropyl benzene are micropore controlled. The effective diffusivity data can be used in modeling reaction kinetics of the catalytic cracking reactions (i.e., in Thiele modulus).

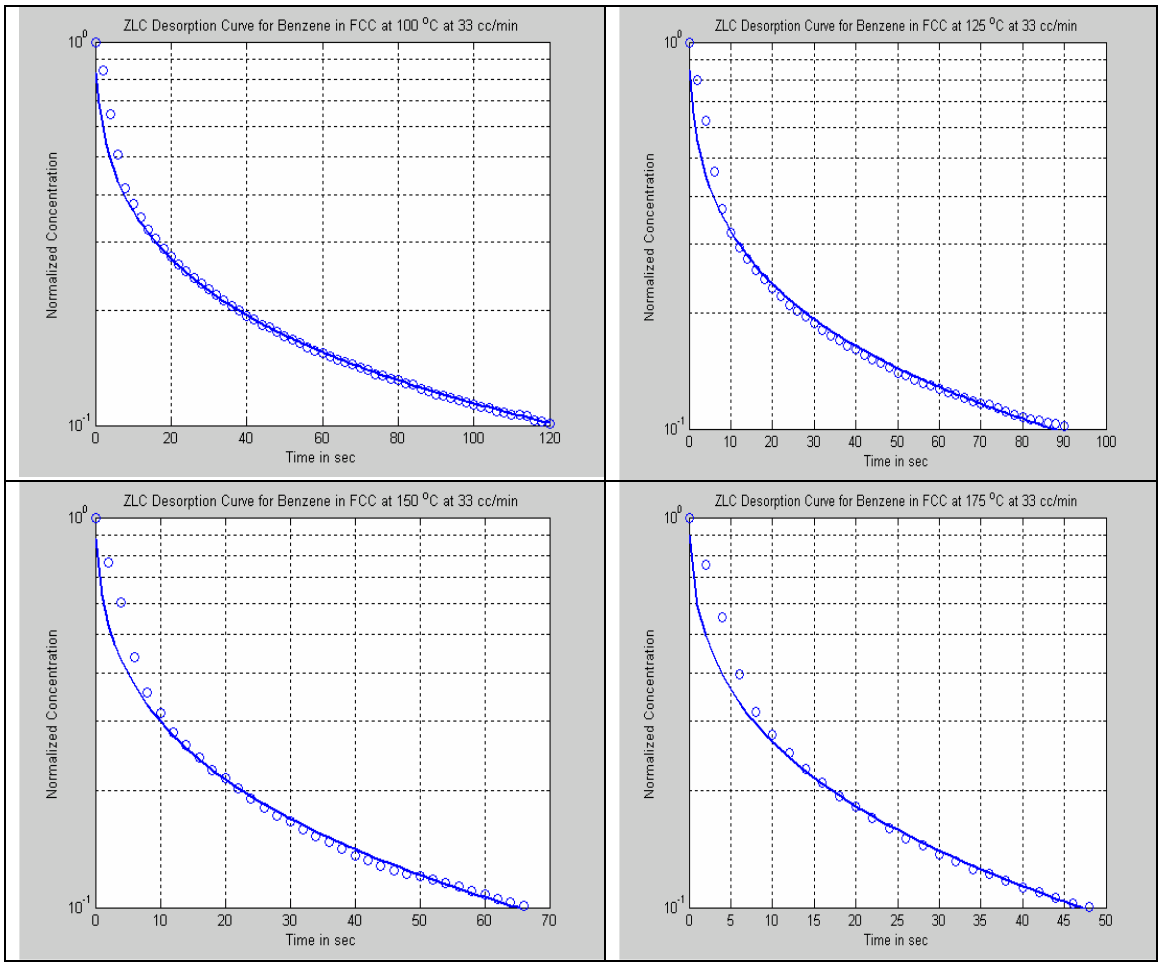

Figure 6.1: ZLC desorption curve for Benzene in FCC pellet (55-45 micron pellet size, 0.9 micron NaY crystal) at 33 cc/min purge flow rate.

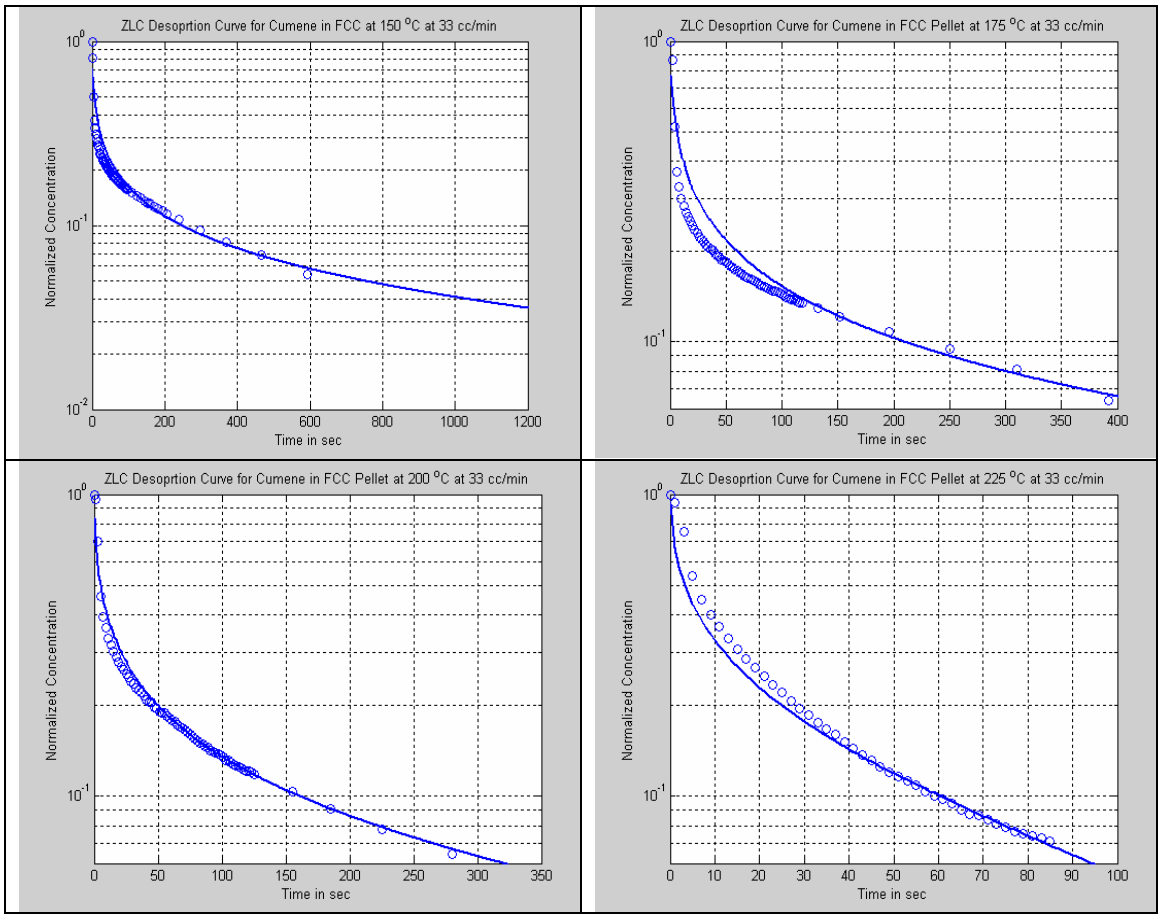

Figure 6.2: ZLC desorption curve for cumene in FCC pellet (55-45 micron pellet size, 0.9 micron NaY crystal) at 33 cc/min purge flow rate.

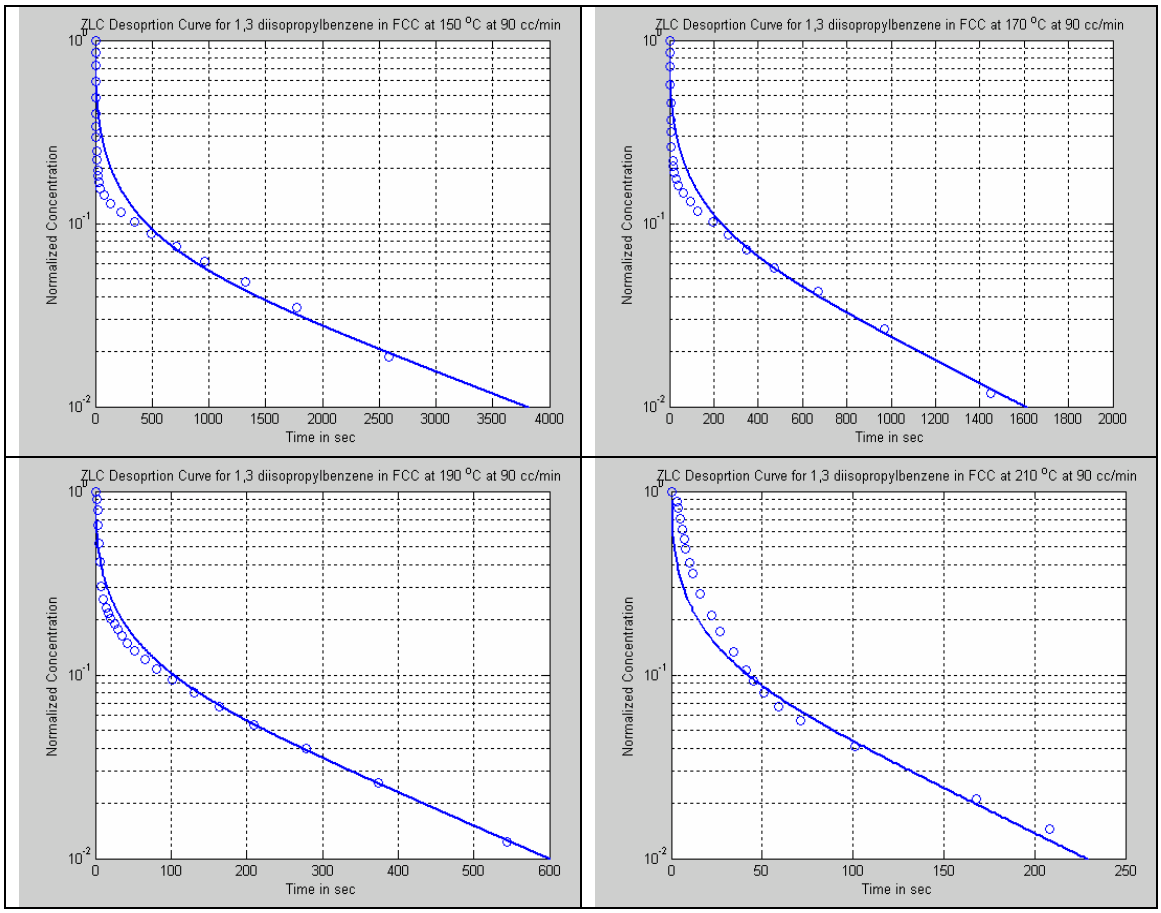

Figure 6.3: ZLC desorption curve for 1,2 di -iopropyl benzene in FCC pellet (55-45 micron pellet size, 0.9 micron NaY crystal) at 90 cc/min purge flow rate.

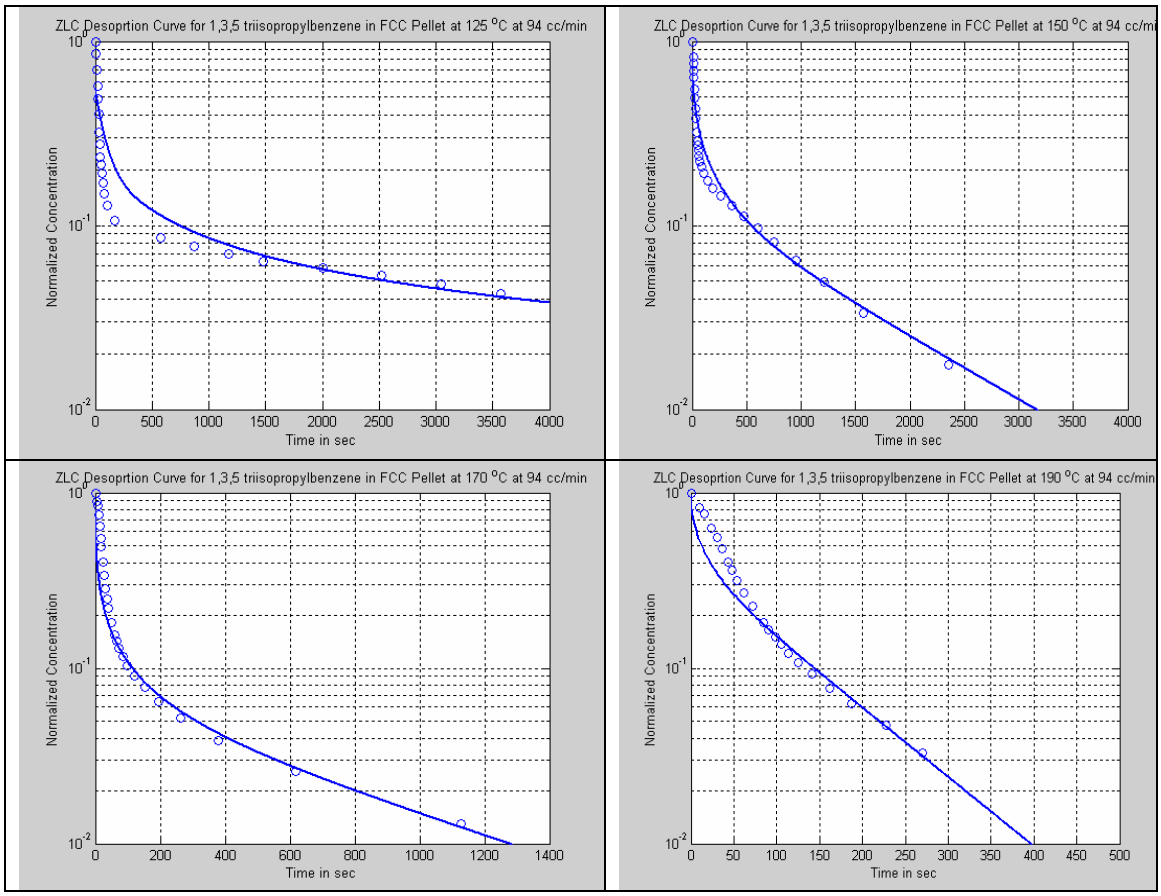

Figure 6.4: ZLC desorption curve for 1,3,5 tri-isopropyl benzene in FCC pellet (55-45 micron pellet size, 0.9 micron NaY crystal) at 90 cc/min purge flow rate

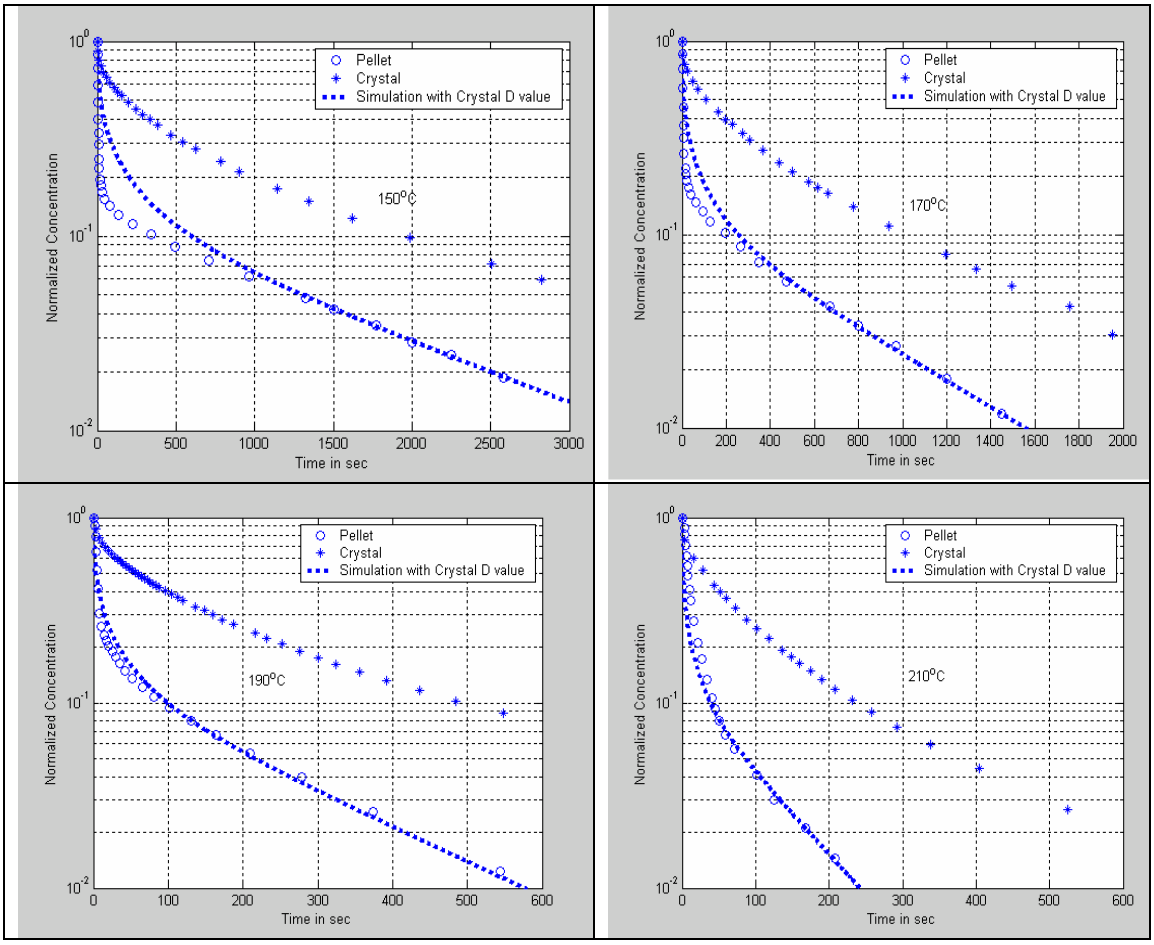

Figure 6.5: Comparison curve for pellet and crystal data for 1,3 di-isopropylbenzene

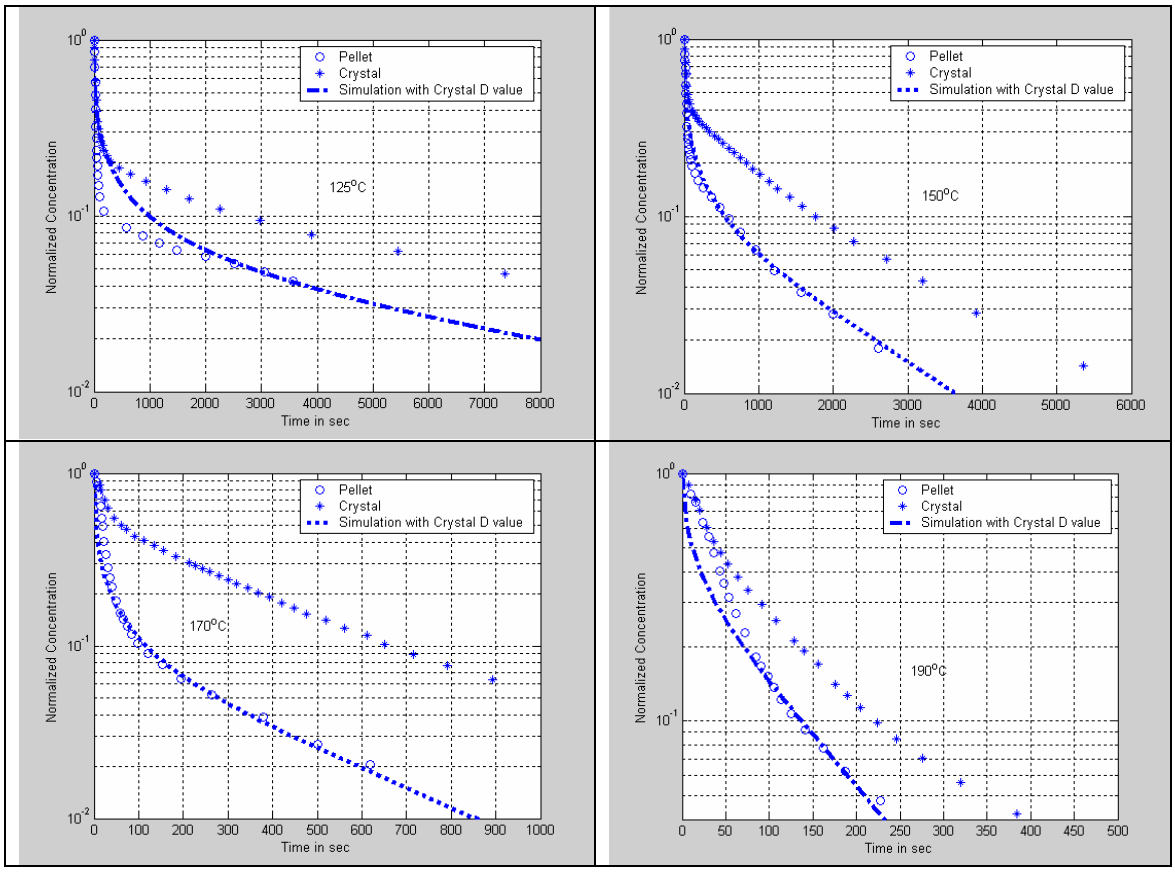

Figure 6.6: Comparison plot for pellet and crystal data for 1,3,5 tri-isopropyl benzene

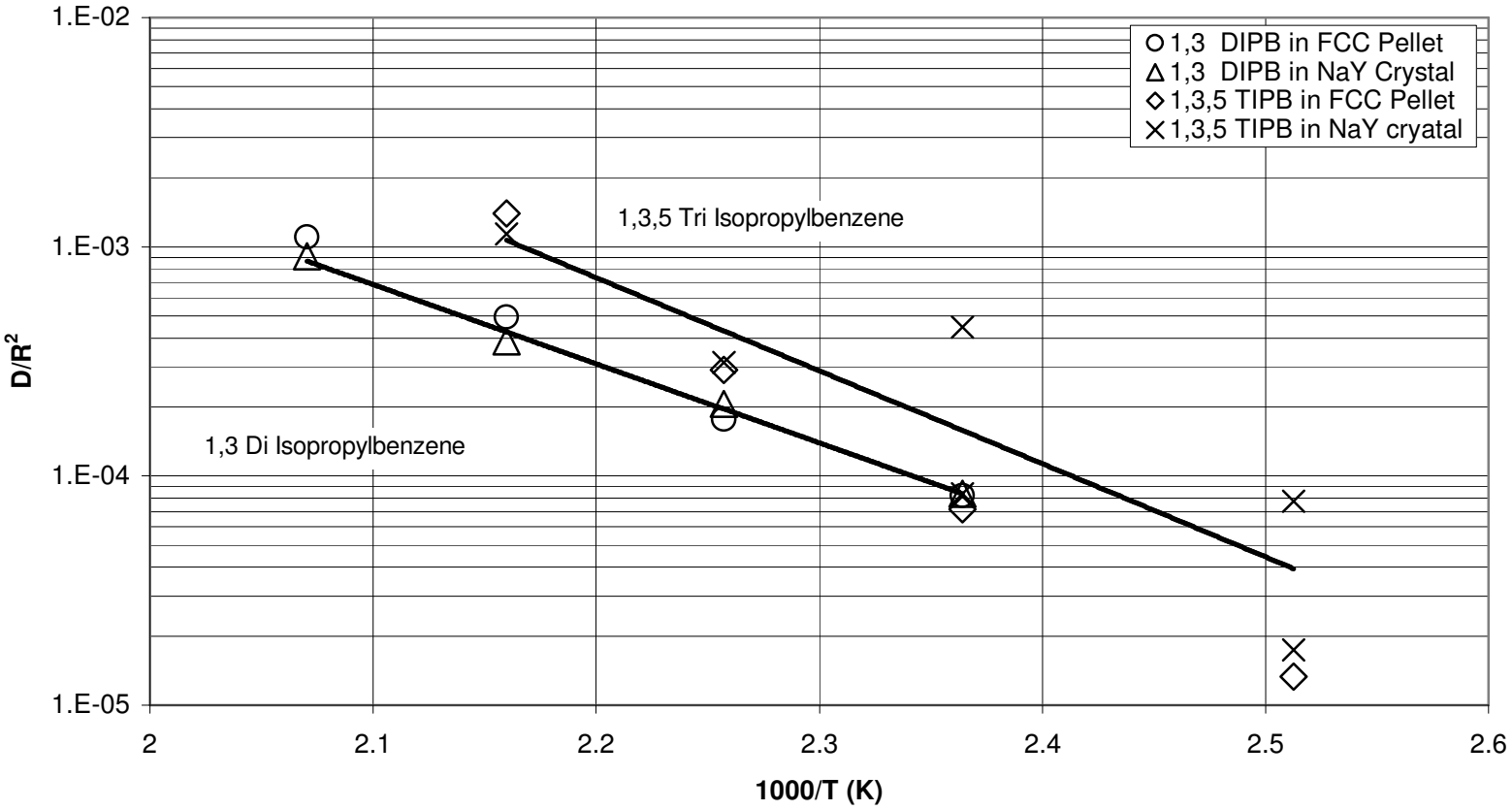

Figure 6.7: Arrhenius plots of 1,3 di-isopropyl benzene and 1,3,5 tri-isopropyl benzene in both FCC pellets and NaY crystal

Table 6.1: Diffusivity of benzene in FCC pellet (0.9 micron NaY Crystal) 50μm pellet diameter (55-45 μm pellet size distribution) purge gas velocity 33cc/min.

Temperature (^oC)	1000/T	D_{ap}/R^2	Apparent diffusivity D_{ap} (m^2/sec)	Theoretical apparent diffusivity D_{ap} (m^2/sec)	L	$K_{overall}$
100	2.68	2.17E-04	1.36E-13	6.64E-11	25.62	9.98E+03
125	2.51	3.89E-04	2.43E-13	1.08E-10	22.06	6.46E+03
150	2.36	7.99E-04	4.99E-13	1.73E-10	16.39	4.24E+03
175	2.23	1.40E-03	8.75E-13	2.72E-10	14.09	2.81E+03

Table 6.2: Diffusivity of cumene in FCC pellet (0.9 micron NaY Crystal) 50μm pellet diameter (55-45 μm pellet size distribution) purge gas velocity 33cc/min.

Temperature (^oC)	1000/T	D_{ap}/R^2	Apparent diffusivity D_{ap} (m^2/sec)	Theoretical apparent diffusivity D_{ap} (m^2/sec)	L	$K_{overall}$
150	2.36	1.38E-04	8.62E-14	9.15E-11	52.09	6.37E+03
175	2.23	2.88E-04	1.80E-13	1.42E-10	37.09	4.28E+03
200	2.11	7.16E-04	4.48E-13	2.46E-10	24.69	2.59E+03
225	2.00	6.85E-03	4.28E-12	9.36E-10	9.48	7.05E+02

Table 6.3: Diffusivity of 1,3 di-isopropyl benzene in FCC pellet (0.9 micron NaY Crystal) 50μm pellet diameter (55-45 μm pellet size distribution) purge gas velocity 90cc/min.

Temperature (^oC)	1000/T	D_{ap}/R^2	Apparent diffusivity D_{ap} (m^2/sec)	Theoretical apparent diffusivity D_{ap} (m^2/sec)	L	$K_{overall}$
150	2.36	8.22E-05	5.14E-14	5.48E-12	25.61	9.08E+04
170	2.25	1.77E-04	1.11E-13	9.81E-12	20.51	5.26E+04
190	2.15	4.93E-04	3.08E-13	2.35E-11	17.09	2.27E+04
210	2.07	1.10E-03	6.88E-13	5.00E-11	15.76	1.10E+04

Table 6.4: Diffusivity of 1,3,5 tri-isopropyl benzene in FCC pellet (0.9 micron NaY Crystal) 50μm pellet diameter (55-45 μm pellet size distribution) purge gas velocity 94cc/min.

Temperature (^oC)	1000/T	D_{ap}/R^2	Apparent diffusivity D_{ap} (m^2/sec)	Theoretical apparent diffusivity D_{ap} (m^2/sec)	L	$K_{overall}$
125	2.51	1.33E-05	8.31E-15	2.80E-12	100	1.50E+05
150	2.36	7.17E-05	4.48E-14	2.71E-12	17.09	1.63E+05
170	2.25	2.90E-04	1.81E-13	2.26E-11	34.04	2.02E+04
190	2.15	1.40E-03	8.75E-13	1.71E-11	5.14	2.77E+04

6.6 Nomenclature

C_o	Initial concentration in the bulk fluid phase in the ZLC cell (mol/m^3)
C_{so}	Adsorbed phase concentration in equilibrium with C_o (mol/m^3)
C_{in}	Fluid phase concentration at the ZLC inlet (mol/m^3)
C_{out}	Fluid phase concentration at the ZLC outlet (mol/m^3)
C_p	Concentration of fluid phase in macropore (mol/m^3)
C_s	Concentration of fluid phase in micropore (mol/m^3)
$\overline{C_s}$	Average adsorbed phase concentration in micropores (mol/m^3)
$\overline{C_s^a}$	Dimensionless average micropore concentration
C_s^a	Dimensionless micropore concentration
C_p^a	Dimensionless macropore concentration
D_c	Intracrystalline diffusivity (m^2/s)
D_p	Diffusivity in macropores (m^2/s)
D_m	Molecular diffusivity (m^2/s)
D_k	Knudsen diffusivity (m^2/s)
D_{ap}	Apparent diffusivity (m^2/s)
D_s	Surface Diffusivity (m^2/s)
E	Activation energy (kjoul/mole)
H	Henry's law constant
k	Film mass transfer constant (m/sec)
K	Capacity factor (=$(1-\varepsilon_p)H/\varepsilon_p$)
K_s	Surface adsorption equilibrium constant
l	length of ZLC cell (m)
L	ZLC parameter
M	Molecular weight (gm/mole)
Q_p	Purge flow rate (m/s)
r	Radial co-ordinate inside crystal (m)
r_c	Crystal radius (m)
R	Radial co-ordinates in macropores (m)
R_p	Pellet radius (m)
R_g	Gas constant
t	Time (s)
T_p	Tortuosity
T	Temperature (Kelvin)
$(-\Delta U)$	Internal energy of sorption (kcal/mole)
V_c	Volume of crystal in ZLC
v	Fluid velocity in the ZLC (m/s)
w	Fraction zeolite in pellet
x	Dimensionless radial coordinate in microspheres
y	Dimensionless radial coordinate in pellet

Greek Symbols

λ_n	Roots of the transcendental equation
$\beta_{n,m}$	Roots of the transcendental equation
ε_b	Void fraction of ZLC
ε_p	pellet macroporosity
γ	Ratio of micropore and macropore diffusional time constant ($\frac{D_c / r_c^2}{D_p / R_p^2}$)
θ	Reduced time ($\frac{D_p t}{R_p^2}$)
ρ_s	Density of the pellet, (kg/m3)

6.7 References

1. Brandani S., " Analytical solution for desorption curves with bi-porous adsorbent particles, Chemical Engineering Science, Vol 51, No 12, pp 3283-3288, (1996).

2. Carlos A. G., Carlos G., Rodrigues A.E,, "Adsorption of propane and propylene in pellets and crystals of 5A Zeolite", Industrial Engineering and Chemical Research, Vol 41, pp 85-92, (2002).

3. Carlos A. G., Rodrigues A.E., "Adsorption equilibira and kinetics of propane and propylene in silica gel", Industrial Engineering and Chemical Research, Vol 40, pp 1687-1693, (2001).

4. Carlos A G., Silva V., Carlos G., Rodrigues A. E., "Adsorption of propane and propylene onto carbon molecular sieve", Carbon, Vol 41, Issue 13 pp 2533-2545, (2003).

5. Eic M., and Ruthven D. M.,"A new experimental technique for measuring intracrystalline diffusivity", Zeolite, Vol 8, No 40,(1988).

6. Silva A. C., Rodrigues A. E., "Equilibrium and kinetics of n-Hexane sorption in pellets of 5A Zeolite:, AIChE journal, Vol 43, No 10, October (1997).

7. Silva A. C., and Rodrigues A. E., "Sorption and diffusion of n-Pentane in pellets of 5A zeolite, Industrial Engineering and Chemical Research, Vol 36, pp 493-500, (1997).

8. Silva A. C., and Rodrigues A. E., "Analysis of ZLC technique for diffusivity measurement in bidisperse porous adsorbent pellets, Gas Separation Purification, Vol 10, No 4, pp 207-224, (1996).

9. Silva A. C., Mata V. G., Malden M. D., Lopes C. B., and Rodrigues A. E., "Effect of coke in the equilibrium and kinetics of sorption on 5A Molecular sieve zeolite, "Industrial Engineering and Chemical Research, Vol 39, pp 1030-1034, (2000).

10. Karger J., and Ruthven D. M., “Diffusion in zeolite and other microporous solids", Chap 9-11, Wiley. New York,(1992).

11. Ruthven D. M., and Xu Z., "Diffusion of oxygen and nitrogen in 5A zeolite and commercial 5A pellets", Chemical Engineering science, Vol 48, No 18, pp 3307-3312, (1993).

Chapter 7

Conclusions and recommendations

7.1 Conclusions

The diffusivity of 1,3 di isopropyl benzene and 1,3,5 tri isopropyl benzene in NaY crystals (r_c = 0.45 μm), alumina (r_{mean} = 104 μm) and FCC catalysts particles (R_p = 25 μm), and the diffusivity of para, ortho and meta xylene in HZSM-5 crystals has been measured using the ZLC method.

The equilibrium constant measured for all systems was exceedingly large indicating that all the systems were nonlinear. The theory of ZLC uptake for nonlinear systems has only been developed for intracrystalline diffusion, and the long time asymptotic solution was applied in the analysis of the NaY crystal system. It should that this gives the zero loading diffusivity. However, the theory of nonlinear uptake on the ZLC system for macropore systems is not developed. For these systems it was assumed that the long time solution for linear macropore systems could be applied to the nonlinear systems, as this has been proved applicable to micropore systems. A further complication, is that the nonlinear ZLC analysis for a size distribution of particles has not bee developed. For this system, the diffusivity was determined by applying the linear model in the intermediate region [$0.02 < (1 - m_t/m_\infty) < 0.08$], and assuming that the nonlinear model would give equivalent results in this region.

In NaY crystals, the uptake curve of 1,3,5 tri isopropyl benzene was observed to have a kink in it. Initially a slow desorption curve was observed, and after approximately 50 sec the diffusivity suddenly increased. It is postulated that the initial kink in desorption curve is due to the desorption of unreacted 1,3,5 tri-isopropyl benzene. The unreacted material is postulated to occupy the outer shell of the crystal. In the interior of the crystal, all the 1,3,5 tri-isopropyl benzene is believed to have reacted to produce isomers of di isopropyl benzene and propylene, and it is postulated that there is no more unreacted material in the central core. As soon as the ZLC is switched to desorption, the desorption rate is controlled by the outer shell where the majority of the unreacted 1,3,5 tri-isopropyl benzene resides. In this outer shell three phenomena are presumed to occur simultaneously. These are 1) diffusion of 1,3,5 tri-isopropyl benzene out of the crystal, 2) diffusion of 1,3,5 tri-isopropyl benzene into the crystal due to the existence of a concentration gradient, and 3) reaction of 1,3,5 tri-isopropyl benzene to produce isomers of di isopropyl benzene and propylene The diffusivity in the first 50 seconds is then probably controlled by the diffusion of 1,3,5 tri-isopropyl benzene and thereafter by the co-diffusion of isomers of di isopropyl benzene and propylene. It is not possible to estimate this diffusivity at the initial time as this is the region which is controlled by the time constant of the apparatus. The reported diffusivity values of the long time nonlinear asymptotic solution of the ZLC model for 1,3,5 tri-isopropyl benzene appear to be for the co-diffusion of isomers of di isopropyl benzene and propylene

The measured diffusivity of 1,3,5 tri-isopropyl benzene (critical molecular diameter 9.3Å), the largest molecule, has a higher diffusivity than 1,3 di-isopropyl benzene. This is due the hypothesis that it is actually the nonlinear co-diffusion of isomers of di-isopropyl

benzene and propylene that it is actually been measured. The activation energies for both 1,3 di isopropyl benzene and 1,3,5 tri isopropyl benzene in NaY crystals are to be similar.

Alumina is commonly used as a binder for the FCC pellet. It provides the macropore for transport to the NaY crystals in the pellet system.. The alumina particles used had a wide range of particle size distribution. Statistical analysis was performed to find the mean radius and the standard deviation. Tailing of desorption curve at lower concentration is the main effect of particle size distribution. High values of equilibrium constant suggests the system is in nonlinear region It is suggested that a model incorporating the crystal size distribution must be utilized for analysis. We fit the experimental data in the region of [$0.02 < (1 - m_t/m_\infty) < 0.08$] to calculate the diffusivity. Experimental data are in good agreement with theoretical macropore diffusivity data, suggesting the system is macropore controlled.

In industrial process pellets are used rather than pure crystals. Pellets are combined network of macropores, mesopores and micropores. The effective diffusivities of 1,3 di-isopropyl and 1,3,5 tri-isopropyl benzene in FCC pellet (20 wt% of 0.7 μm HNaY crystal, 80% alumina matrix) are measured by ZLC method. The system is also nonlinear. Slope of the long time tail is used to evaluate diffusivity values. For 1,3 di-isopropyl benzene and 1,3,5 tri-isopropyl benzene the inverse diffusion time constants are similar to the values as for pure NaY crystals. This implies diffusion of these two larger molecules in FCC pellets is controlled by micropore diffusion. The diffusion time constants of 1,3,5 tri-isopropyl benzene is higher than that of 1,3 di-isopropyl benzene, which is similar to

NaY crystal system, suggesting cracking of 1,3,5 tri isopropyl benzene and measured diffusivity is the co-diffusion of isomers of di-isopropyl benzene and propylene.

HZSM-5 is used in the isomerization of xylene isomers. P-xylene is the main desired product as it is used in many industrial processes. Other two isomers m-xylene and o-xylene has limited commercial importance and need to be converted into p-xylene. ZLC method is used to investigate the intracrystalline diffusivity of xylene isomers in HZSM-5 crystal. Activation energies are also calculated. Equilibrium constant value indicate that in investigation region is nonlinear and experimental data is analyzed taking the long time slope of the system. Experimental data was also fitted with the linear ZLC diffusion model. Para xylene diffuses much faster than the other two isomers. Ortho xylene has higher diffusivity than meta xylene. The results are in good agreement with literature values when extrapolated to a zero loading basis.

Also the uptake of benzene and cumene in NaY crystals and FCC catalyst particles was measured using the ZLC system. Unfortunately, it was found that these systems uptake was so rapid for the crystals used that the ZLC system criteria were not met, i.e., for valid diffusivity measurements the inverse time constant (D/r_c^2) must be much less than 0.05 sec^{-1}.

7.2 Recommendations

In our study we investigate in the linear region of isotherm (Henry's law region) i.e. very low concentration of adsorbent. However, the results are mostly nonlinear. Accordingly, the nonlinear isotherms for benzene, cumene, 1,3 di isopropyl benzene and 1,3,5 tri isopropyl benzene in NaY crystals, alumina and FCC catalysts particles, and the isotherms of para, ortho and meta xylene in HZSM-5 crystals need to be measured on an Intelligent Gravimetric Analyzer (IGA). Multi component isotherms should also be generated by use of an Intelligent Gravimetric Analyzer (IGA) as it is postulated that the 1,3,5 tri isopropyl benzene adsorption system is really a multicomponent system of isomers of di isopropyl benzene and propylene.

The theory of ZLC uptake for nonlinear systems has been developed for intracrystalline diffusion, and the long time asymptotic solution applied in the analysis of the NaY crystal system. However, the theory of nonlinear uptake on the ZLC system for macropore systems needs to be developed.

The theory of ZLC uptake for nonlinear systems analysis for a size distribution of particles needs to be developed for both micropore and macropore systems.

Diffusion of a single component was examined in this study. But most industrial processes involve multi-component systems. Gas phase counter diffusion can also be investigated by ZLC method but the theory for nonlinear systems needs to be developed.

Complete isotherm for both single component and multi component also can be generated by ZLC method and also by use of an Intelligent Gravimetric Analyzer (IGA).

Effect of reaction in ZLC system can be a new area of research. This system can be utilized to model reaction kinetics for reactive systems.

Appendix A

Calculation of partial pressure of hydrocarbon in the stream

Antoine's equation

$$\ln(p) = a + \frac{b}{(T+c)} + d\ln(T) + e * T^{f}$$

where T is temperature in Kelvin p is pressure in kpa.

Antoine's coefficient for hydrocarbons are listed below

Hydrocarbon name	**a**	**b**	**c**	**d**	**e**	**f**
Benzene	1.6965e2	-1.03148e4	0	-2.35895e1	2.09442e-5	2
Cumene	1.36712e2	-9.6877e3	0	-1.9305e1	1.7703e-2	1
1,3 DIPB	7.13e1	-8.77e3	0	-7.898	1.87e-6	2
1,3,5 TIPB	1.727e2	-1.483e4	0	-2.271e1	1.0037e-5	2
P-xylene	9.125e1	-8.12125e3	0	-1.13188e1	7.3055e-6	2
M-xylene	7.7839e1	-7.5941e3	0	-9.257	5.55e-6	2
O-xylene	8.376e1	-7.9608e3	0	-1.0126e1	6.015e-6	2

- Antoine's coefficients are taken from HYSIS database.

Table for partial pressure, vapor pressure

Hydrocarbon name	Bath temperature (^{o}C)	System pressure (psi)	Low flow rate (sccm)	High flow rate (sscm)	Vapor pressure at bubbler (psi)	Partial pressure of the mixed stream (psi)
Benzene	8	44.7	6	60	0.0970	9.71e-3
Cumene	18	44.7	9.6	66	0.0525	6.7e-3
1,3 DIPB	20	39.7	10	80	5.17e-3	5.75e-4
1,3,5 TIPB	20	39.7	14	80	3.42e-4	5.0989e-5
P-xylene	12	39.7	6.5	60	0.0772	7.6e-3
M-xylene	12	39.7	8	60	0.0734	8.6e-3
O-xylene	12	39.7	8	60	0.1005	1.18e-2

Sample calculation

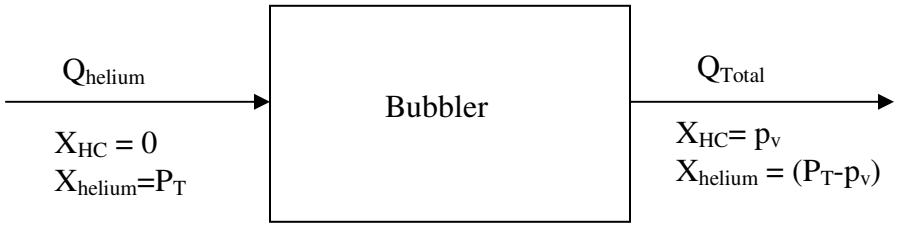

Total amount out of bubbler is

$$Q_T = Q_{helium}\left(\frac{P_T}{P_T - p_v}\right)$$

P_T = Total pressure in psi.

P_v = Vapor pressure of hydrocarbon in psi at bath temperature.

Q_T = Total volume out from the bubbler.

Q_{helum} = Volume of helium in to the bubbler.

Calculation of vapor pressure and partial pressure of hydrocarbon

Example: 1,3 di isopropyl benzene

$$\ln(p) = a + \frac{b}{(T+c)} + d\ln(T) + e*T^f$$

Bath temperature = 20 ^oC (293K)

System pressure = 39.7 psi (absolute pressure)

Low flow rate of helium through bubbler = 10 sccm

High flow rate helium stream = 80 sccm

$$\ln(p) = 71.3 + \left(\frac{-8.77\times10^{3}}{293+0}\right) + (-7.898)\ln(293) + (1.87\times10^{-6})(293)^{2}$$

$$p = 0.035668 \quad kPa$$

$$p = 5.174\times10^{-3} \quad psi$$

Partial pressure of helium out of the system

P_{helium} = (39.7-5.174x10^{-3}) =39.6948 psi

Total volume of gas (Helium+HC) out from bubbler

$$Q_T = Q_{helium}\left(\frac{P_T}{P_T - p_v}\right) = 10.0013036 \; sscm$$

Volume of HC in the stream = 10-10.0013036 = 1.3036x10^{-3} sscm

Total mixed stream = 80+10.0013036 = 90.0013036 sscm

Volume fraction of hydrocarbon, $x = \frac{1.3036\times10^{-3}}{90.0013036} = 1.4482\times10^{-5}$

Partial pressure of HC in gas stream

$$p_{HC} = P_{Total}\times x = 39.7\times1.4482\times10^{-5} = 5.7502\times10^{-4} \; psi$$

Appendix B

Tabulated data for ZLC experiments

Diffusion of benzene in NaY crystals

[Catalyst weight 4.8 mg, Flow rate 71 cc/min]

50 ℃		75 ℃		100 ℃		125 ℃		150 ℃	
Time (sec)	Norm. Conc..	Time (sec)	Norm. Conc..	Time (sec)	Norm. Conc..	Time (sec)	Norm. Conc..	Time (sec)	Norm. Conc..
0	1	0	1	0	1	0	1	0	1
0.4	0.9615	2	0.9488	1.8	0.8711	2	0.8013	0.4	0.978
4.4	0.6806	6	0.7889	3.8	0.7315	4	0.5929	2.4	0.6593
8.4	0.5795	10	0.6824	5.8	0.6187	6	0.4647	4.4	0.4725
12.4	0.5152	14	0.5922	7.8	0.5381	8	0.3734	6.4	0.3407
16.4	0.4671	18	0.5266	9.8	0.4683	10	0.3061	8.4	0.2637
20.4	0.4286	22	0.4672	11.8	0.42	12	0.2596	10.4	0.2143
24.4	0.3965	26	0.4119	13.8	0.3781	14	0.2244	12.4	0.1758
28.4	0.366	30	0.375	15.8	0.3437	16	0.1939	14.4	0.1516
32.4	0.3371	34	0.3422	17.8	0.3126	18	0.1731	16.4	0.1319
36.4	0.3178	38	0.3043	19.8	0.2868	20	0.1554	18.4	0.1176
40.4	0.2953	42	0.2807	21.8	0.2642	22	0.141	20.4	0.1077
44.4	0.2745	46	0.2561	23.8	0.2427	24	0.1282	22.4	0.0989
48.4	0.2584	50	0.2357	25.8	0.2256	26	0.1202		
52.4	0.2424	54	0.2172	27.8	0.2095	28	0.1122		
56.4	0.2327	58	0.2008	29.8	0.1966	30	0.1026		
60.4	0.2199	62	0.1885	31.8	0.1837	32	0.0962		
64.4	0.2087	66	0.1762	33.8	0.174				
68.4	0.2006	70	0.1619	35.8	0.1633				
72.4	0.1894	74	0.1516	37.8	0.1557				
76.4	0.1782	78	0.1434	39.8	0.1493				
80.4	0.1717	82	0.1373	41.8	0.1407				
84.4	0.1637	86	0.1291	43.8	0.1321				
88.4	0.1573	90	0.1209	45.8	0.1257				

50 ℃		75 ℃		100 ℃		125 ℃		150 ℃	
Time (sec)	Norm. Conc..	Time (sec)	Norm. Conc..	Time (sec)	Norm. Conc..	Time (sec)	Norm. Conc..	Time (sec)	Norm. Conc..
92.4	0.1509	94	0.1168	47.8	0.1203				
96.4	0.1445	98	0.1107	49.8	0.1149				
100.4	0.1396	102	0.1045	51.8	0.1101				
104.4	0.1348	106	0.1004	53.8	0.1063				
108.4	0.1292	110	0.0963	55.8	0.102				
112.4	0.1252	114	0.0943	57.8	0.0988				
116.4	0.122	118	0.0881						
120.4	0.1172	122	0.084						
124.4	0.114	126	0.082						
128.4	0.1091	130	0.0789						
132.4	0.1059	134	0.0775						
136.4	0.1027	138	0.0758						
140.4	0.0979	142	0.0738						
144.4	0.0947	146	0.0717						
148.4	0.0931	150	0.0676						
152.4	0.0907	154	0.0635						
156.4	0.0867								
160.4	0.0835								

Diffusion of cumene in NaY crystals

[Catalyst weight 8.5 mg, Flow rate 80 cc/min]

100 ℃		125 ℃		150 ℃		175 ℃	
Time (sec)	Norm. Conc..	Time (sec)	Norm. Conc..	Time (sec)	Norm. Conc..	Time (sec)	Norm. Conc..
0	1	0	1	0	1	0	1
3.2	0.8668	3.2	0.866	4	0.8023	6	0.6986
7.2	0.7115	7.2	0.7477	8	0.6852	10	0.5921
11.2	0.6662	23.2	0.5716	12	0.612	14	0.5312
15.2	0.6339	35.2	0.4954	16	0.5549	26	0.3942
31.2	0.5563	47.2	0.4376	20	0.5095	38	0.3181
39.2	0.5175	71.2	0.3574	24	0.4714	50	0.2572
59.2	0.4528	95.2	0.3009	36	0.3895	74	0.1857
67.2	0.4269	119.2	0.2602	48	0.3338	98	0.1416
79.2	0.401	143.2	0.226	60	0.2899	122	0.1126
91.2	0.3752	167.2	0.1997	72	0.2606	146	0.0913
115.2	0.3364	187.2	0.1827	84	0.2313	174	0.0746
135.2	0.3105	191.2	0.1787	96	0.2094	210	0.0594
158	0.2846	222.8	0.1564	120	0.1742	258	0.0441
184.4	0.2587	242.8	0.1432	133.6	0.1581		
236.4	0.2199	267.2	0.1301	150.4	0.1435		
258.4	0.207	291.2	0.117	168.4	0.1288		
281.2	0.194	329.2	0.1038	190	0.1142		
307.2	0.1811	379.2	0.0907	218	0.0996		
335.6	0.1682	447.2	0.0775	256	0.0849		
371.2	0.1552	527.2	0.0644	308	0.0703		
407.2	0.1423	647.2	0.0512	384	0.0556		
455.2	0.1294	827.2	0.0381				

100 ℃		125 ℃		150 ℃		175 ℃	
Time (sec)	Norm. Conc..	Time (sec)	Norm. Conc..	Time (sec)	Norm. Conc..	Time (sec)	Norm. Conc..
507.2	0.1164						
667.2	0.088						
847.2	0.0647						
1027.2	0.0517						
1267.2	0.0388						
1627.2	0.0259						

Diffusion of 1,3 DIPB in NaY crystals

[Catalyst weight 7.8 mg, Flow rate 90 cc/min]

150 ℃		170 ℃		190 ℃		210 ℃	
Time (sec)	Norm. Conc..	Time (sec)	Norm. Conc..	Time (sec)	Norm. Conc..	Time (sec)	Norm. Conc..
0	1	0	1	0	1	0	1
4	0.8863	4	0.8424	4	0.86537	4	0.762963
12	0.7959	12	0.7576	8	0.775617	16	0.607407
24	0.7442	24	0.697	12	0.73074	28	0.518519
40	0.6925	48	0.6182	16	0.693343	44	0.42963
56	0.6537	72	0.5636	20	0.663426	52	0.4
80	0.615	108	0.503	24	0.640987	60	0.365926
108	0.5762	164	0.4303	28	0.615557	72	0.325926
130	0.5504	198	0.3939	32	0.596111	88	0.281481
156	0.5245	228	0.3697	36	0.581152	102	0.251852
196	0.4858	272	0.3333	40	0.563201	118	0.222222
248	0.447	306	0.3091	44	0.546746	136	0.192593
290	0.4212	366	0.2727	48	0.531788	148	0.177778
336	0.3953	442	0.2364	52	0.51982	160	0.162963
384	0.3695	502	0.2121	56	0.506358	174.4	0.148148
464	0.3307	572	0.1879	60	0.491399	190	0.133333
544	0.3049	614	0.1758	64	0.482423	208	0.118519
624	0.2791	660	0.1636	68	0.46896	232	0.103704
784	0.2403	776	0.1394	72	0.458489	258	0.088889
904	0.2145	936	0.1103	76	0.446522	292	0.074074
1144	0.1757	1196	0.0788	80	0.439043	338	0.059259
1344	0.1499	1336	0.0667	84	0.430067	404	0.044444
1624	0.124	1496	0.0545	88	0.4181	524	0.026667
1984	0.0982	1756	0.0424	96	0.401645		
2504	0.0724	1950	0.0303	104	0.386687		
2824	0.0594			112	0.371728		
3304	0.0465			120	0.356769		
4024	0.0336			136	0.331339		
4624	0.0207			148	0.314884		
7864	0.0078			160	0.298429		
				172	0.281975		
				188	0.26552		
				216	0.237098		
				232	0.223635		
				252	0.20718		
				276	0.190726		
				300	0.175767		
				324	0.162304		

150 ℃		170 ℃		190 ℃		210 ℃	
Time (sec)	Norm. Conc..	Time (sec)	Norm. Conc..	Time (sec)	Norm. Conc..	Time (sec)	Norm. Conc..
				356	0.147345		
				392	0.132386		
				436	0.117427		
				484	0.102468		
				548	0.087509		
				628	0.07255		
				748	0.057592		
				888	0.042633		

Diffusion of 1,3,5 TIPB in NaY crystals

[Catalyst weight 11.6 mg, Flow rate 94 cc/min]

125 ℃		150 ℃		170 ℃		190 ℃	
Time (sec)	Norm. Conc..	Time (sec)	Norm. Conc..	Time (sec)	Norm. Conc..	Time (sec)	Norm. Conc..
0	1	0	1	0	1	0	1
8	0.90625	12	0.885714	12	0.853503	8	0.901408
16	0.765625	20	0.742857	16	0.802548	16	0.78169
28	0.585938	28	0.635714	24	0.700637	20	0.711268
40	0.453125	40	0.542857	32	0.624204	28	0.605634
52	0.390625	52	0.488571	44	0.547771	36	0.528169
68	0.34375	64	0.457143	60	0.496815	44	0.478873
84	0.3125	80	0.428571	72	0.471338	52	0.430986
108	0.28125	104	0.4	92	0.433121	64	0.380282
124	0.265625	120	0.385714	112	0.407643	76	0.338028
148	0.25	144	0.371429	134	0.382166	92	0.295775
180	0.234375	170	0.357143	156	0.356688	108	0.253521
228	0.21875	204	0.342857	184	0.33121	128	0.211268
300	0.203125	244	0.328571	212	0.305732	140	0.191549
452	0.1875	292	0.314286	228	0.292994	156	0.169014
652	0.171875	344	0.3	244	0.280255	176	0.140845
932	0.15625	404	0.285714	260	0.267516	190	0.126761
1292	0.140625	464	0.271429	280	0.254777	204	0.112676
1712	0.125	524	0.257143	300	0.242038	224	0.098592
2252	0.109375	596	0.242857	320	0.229299	246	0.084507
2972	0.09375	676	0.228571	344	0.216561	276	0.070423
3892	0.078125	752	0.214286	368	0.203822	320	0.056338
5452	0.0625	836	0.2	392	0.191083	384	0.042254
7372	0.046875	916	0.185714	420	0.178344		
10252	0.03125	1020	0.171429	448	0.165605		
		1136	0.157143	476	0.152866		
		1256	0.142857	520	0.140127		
		1416	0.128571	560	0.127389		
		1580	0.114286	612	0.11465		
		1756	0.1	652	0.101911		
		2016	0.085714	716	0.089172		
		2276	0.071429	792	0.076433		
		2716	0.057143	892	0.063694		
		3196	0.042857	1012	0.050955		
		3916	0.028571	1172	0.038217		
		5356	0.014286	1412	0.025478		
				1812	0.012739		

Diffusion of Para xylene in HZSM-5 Crystals
1st set of data (Catalyst weight 5.3, 66 cc/min)

75 °C		100 °C		125 °C		150 °C	
Time (sec)	Norm Conc.	Time (sec)	Norm Conc.	Time (sec)	Norm Conc.	Time (sec)	Norm Conc.
0	1	0	1	0	1	0	1
2	0.857323	0.4	0.948718	1	0.950062	2	0.870927
4	0.718434	2.4	0.846154	3	0.825218	4	0.705514
6	0.623737	4.4	0.75641	5	0.700375	6	0.601504
8	0.560606	6.4	0.679487	7	0.612984	8	0.506266
10	0.503788	8.4	0.589744	9	0.538077	10	0.426065
12	0.465909	10.4	0.519231	11	0.490637	12	0.390977
14	0.42803	12.4	0.480769	13	0.443196	14	0.350877
16	0.402778	14.4	0.446154	15	0.403246	16	0.319549
18	0.377525	16.4	0.416667	17	0.372035	18	0.288221
20	0.354798	18.4	0.391026	19	0.344569	20	0.266917
22	0.339646	20.4	0.365385	21	0.322097	22	0.246867
24	0.32197	22.4	0.346154	23	0.302122	24	0.22807
26	0.308081	24.4	0.330769	25	0.284644	26	0.213033
28	0.295455	26.4	0.311538	27	0.268414	28	0.200501
30	0.282828	28.4	0.297436	29	0.253433	30	0.18797
32	0.272727	30.4	0.284615	31	0.244694	32	0.175439
34	0.263889	32.4	0.271795	33	0.229713	34	0.16792
36	0.252525	34.4	0.261538	35	0.222222	36	0.157895
38	0.244949	36.4	0.251282	37	0.210986	38	0.150376
40	0.238636	38.4	0.241026	39	0.200999	40	0.14411
42	0.229798	40.4	0.232051	41	0.19226	42	0.137845
44	0.223485	42.4	0.226923	43	0.187266	44	0.130326
46	0.218434	44.4	0.217949	45	0.179775	46	0.125313
48	0.212121	46.4	0.210256	47	0.173533	48	0.120301
50	0.205808	48.4	0.205128	49	0.166042	50	0.115288
52	0.200758	50.4	0.197436	51	0.163546	52	0.111529
54	0.195707	52.4	0.192308	53	0.157303	54	0.106516
56	0.190657	54.4	0.185897	55	0.151061	56	0.102757
58	0.186869	56.4	0.180769	57	0.147316	58	0.099624
60	0.181818	58.4	0.175641	59	0.143571	60	0.096491
62	0.176768	60.4	0.170513	61	0.138577	62	0.092732
64	0.174242	62.4	0.166667	63	0.13608	64	0.090226
66	0.170455	64.4	0.162821	65	0.132335	66	0.087719
68	0.166667	66.4	0.158974	67	0.128589	68	0.085213
70	0.162879	68.4	0.154487	69	0.126092	70	0.08396
72	0.161616	70.4	0.151282	71	0.122347	72	0.080201
74	0.159091	72.4	0.148718	73	0.11985	74	0.078321
76	0.15404	74.4	0.144872	75	0.117353	76	0.076441
78	0.150253	76.4	0.139744	77	0.113608		

75 °C		100 °C		125 °C		150 °C	
Time (sec)	Norm Conc.	Time (sec)	Norm Conc.	Time (sec)	Norm Conc.	Time (sec)	Norm Conc.
80	0.14899	78.4	0.137179	79	0.11236		
82	0.146465	80.4	0.133333	81	0.109863		
84	0.143939	82.4	0.130769	83	0.107366		
86	0.141414	84.4	0.128205	85	0.104869		
88	0.138258	86.4	0.125641	87	0.102372		
90	0.136364	88.4	0.124359	89	0.101124		
92	0.135101	90.4	0.121795	91	0.099875		
94	0.133838	92.4	0.119231	93	0.097378		
96	0.131313	94.4	0.117308	95	0.094881		
98	0.128788	96.4	0.115385	97	0.093633		
100	0.126263	98.4	0.114103	99	0.091136		
102	0.125	100.4	0.111538	101	0.089888		
104	0.122475	102.4	0.110256	103	0.088639		
106	0.121212	104.4	0.107692	105	0.087391		
108	0.119949	106.4	0.105128	107	0.086142		
110	0.118687	108.4	0.103846	109	0.083645		
112	0.116162	110.4	0.102564	111	0.082397		
114	0.114268	112.4	0.101282	113	0.081149		
116	0.112374	114.4	0.1	115	0.079276		
118	0.111111	116.4	0.098718	117	0.078652		
120	0.109848	118.4	0.097436	119	0.077403		
122	0.108586	120.4	0.096154	121	0.076779		
124	0.107323	122.4	0.094872	123	0.076155		
126	0.106061	124.4	0.09359	125	0.074906		
128	0.104798	126.4	0.092308	127	0.073658		
130	0.103535	128.4	0.091026	129	0.072409		
132	0.102273	130.4	0.089744	131	0.071161		
134	0.10101	132.4	0.089103	133	0.069913		
136	0.099747	134.4	0.088462	135	0.068664		
138	0.098485	136.4	0.087179	137	0.067416		
140	0.097222	138.4	0.085897	139	0.066167		
142	0.09596	140.4	0.084615	150	0.06367		
144	0.094697	142.4	0.083333	168.4	0.057428		
146	0.093434	144.4	0.082051	188.4	0.051186		
148	0.092172	146.4	0.080769	262.4	0.038702		
150	0.090909	148.4	0.079487				
152	0.089646	150.4	0.078205				
154	0.089015	152.4	0.077564				
156	0.088384	154.4	0.076923				
158	0.087753						
160	0.08649						
162	0.085859						
164	0.085227						
166	0.084596						
168	0.083333						

Diffusion of Para xylene in HZSM-5 Crystals
2nd data set (66 cc/min)

75 °C		75 °C		100 °C		125 °C	
Time (sec)	Norm Conc.	Time (sec)	Norm Conc.	Time (sec)	Norm Conc.	Time (sec)	Norm Conc.
0	1	76	0.164122	0	1	0	1
2	0.851145	78	0.161578	2	0.906918	0.4	0.961165
4	0.736641	80	0.157761	4	0.818868	2.4	0.857605
6	0.647583	82	0.155216	6	0.743396	4.4	0.754045
8	0.577608	84	0.152672	8	0.667925	6.4	0.676375
10	0.526718	86	0.150127	10	0.61761	8.4	0.61165
12	0.484733	88	0.147583	12	0.567296	10.4	0.553398
14	0.450382	90	0.145038	14	0.52327	12.4	0.508091
16	0.42112	92	0.143766	16	0.480503	14.4	0.456311
18	0.395674	94	0.141221	18	0.454088	16.4	0.436893
20	0.374046	96	0.138677	20	0.422642	18.4	0.404531
22	0.354962	98	0.137405	24	0.378616	20.4	0.378641
24	0.339695	100	0.13486	28	0.340881	24.4	0.339806
26	0.3257	102	0.133588	32	0.310692	28.4	0.306149
28	0.312977	104	0.131043	36	0.285535	32.4	0.280259
30	0.298982	106	0.128499	40	0.265409	34.4	0.268608
32	0.287532	108	0.127226	42	0.25283	38.4	0.247896
34	0.278626	110	0.124682	44.4	0.240252	44.4	0.222006
36	0.268448	112	0.12341	48	0.227673	50.4	0.201294
38	0.259542	114	0.122137	52	0.215094	56.4	0.184466
40	0.253181	116	0.120865	56	0.202516	62.4	0.171521
42	0.243003	118	0.118321	60	0.189937	68.4	0.158576
44	0.236641	120	0.117048	66	0.174843	76.4	0.145631
46	0.23028	122	0.115776	72	0.16478	84.4	0.132686
48	0.223919	124	0.114504	79	0.152201	96.4	0.119741
50	0.217557	126	0.113232	88	0.139623	110.4	0.106796
52	0.212468	128	0.111959	98	0.127044	128.4	0.093851
54	0.207379	130	0.110687	111	0.114465	151	0.080906
56	0.20229	132	0.109415	126	0.101887	186.4	0.067961
58	0.198473	134	0.108142	148	0.089308	233.4	0.055016
60	0.193384	136	0.10687	174	0.07673	320.4	0.042071
62	0.189567	138	0.105598	214	0.064151	460.4	0.029126
64	0.185751	140	0.104326	282	0.051572		
66	0.180662	142	0.103053	386	0.038994		
68	0.176845	144	0.101781				
70	0.1743	146	0.100509				
72	0.170483	162	0.092875				
74	0.166667	170	0.087786				
		194	0.080153				
		204	0.075064				

Diffusion of Meta xylene in HSM-5 Crystal
1st data set (72 cc/min)

150 °C		175 °C		200 °C		220 °C	
Time (sec)	Norm Conc.	Time (sec)	Norm Conc.	Time (sec)	Norm Conc.	Time (sec)	Norm Conc.
Cata. Wt 8.3mg		Cata. Wt 8.8mg		Cata. Wt 6.7mg		Cata. Wt 7.9mg	
0	1	0	1	0	1	0	1
1	0.909751	0.8	0.922992	2	0.768177	0.6	0.780755
3	0.557054	2.8	0.482948	4	0.399368	2.6	0.451888
5	0.417012	4.8	0.339934	6	0.283456	4.6	0.293544
7	0.295643	6.8	0.279428	8	0.230769	6.6	0.242387
9	0.261411	8.8	0.240924	10	0.199157	8.6	0.210719
11	0.237552	10.8	0.213421	12	0.178082	10.6	0.190012
13	0.21888	12.8	0.19692	14	0.162276	12.6	0.171742
15	0.204357	14.8	0.180418	18	0.141201	14.6	0.159562
17	0.190871	16.8	0.169417	22	0.125395	16.6	0.149817
19	0.181535	18.8	0.159516	26	0.114858	18.6	0.142509
21	0.173237	20.8	0.151815	30	0.106428	20.6	0.135201
27	0.15249	22.8	0.146315	38	0.092729	22.6	0.129111
31	0.142116	24.8	0.139714	46	0.083246	24.6	0.123021
36	0.131743	26.8	0.134213	56	0.072708	26.6	0.119367
43	0.121369	28.8	0.130913	72	0.062171	28.6	0.114495
52	0.110996	30.8	0.126513	94	0.051633	30.6	0.109622
64	0.100622	32.8	0.122112	130	0.041096	32.6	0.107186
79	0.090249	34.8	0.118812	196	0.030558	34.6	0.103532
101	0.079876	36.8	0.116392	306	0.020021	36.6	0.099878
135	0.069502	38.8	0.112211	526	0.009484	38.6	0.097442
187	0.059129	46.8	0.10231			40.6	0.095006
269	0.048755	60.8	0.090576			42.6	0.09257
409	0.038382	76.8	0.080019			44.6	0.090134
619	0.028008	102.8	0.070407			46.6	0.08648
989	0.017635	140.8	0.060252			60	0.0743
		170.8	0.053905			81	0.062119
		271.2	0.042904			110	0.049939
		433.2	0.031903			164	0.037759
		743	0.021			264	0.025579

Diffusion of Meta xylene in HSM-5 Crystal
2nd set of data (44cc/min)

150 °C		175 °C		200 °C	
Time (sec)	Norm Conc.	Time (sec)	Norm Conc.	Time (sec)	Norm Conc.
Cata. Wt. 8.4 mg		Cata. Wt. 4.8 mg		Cata. Wt. 3.5 mg	
0	1	0	1	0	1
2.8	0.789474	2	0.798122	2	0.836915
4.8	0.555556	4	0.539906	4	0.533502
6.8	0.426901	6	0.377934	6	0.369153
8.8	0.345029	8	0.305164	8	0.2933
10.8	0.298246	10	0.258216	10	0.255373
12.8	0.263158	12	0.230047	12	0.226296
14.8	0.233918	14	0.211268	16	0.192162
16.8	0.216374	16	0.191315	20	0.169406
18.8	0.19883	18	0.178404	24	0.154235
20.8	0.185965	20	0.169014	28	0.141593
22.8	0.173099	22	0.159624	34	0.127686
24.8	0.167251	24	0.150235	40	0.116308
26.8	0.157895	26	0.144366	50	0.103666
28.8	0.150877	28	0.137324	64	0.091024
30.8	0.146199	30	0.132629	82	0.078382
32.8	0.140351	32	0.126761	112	0.06574
34.8	0.134503	34	0.124413	156	0.053097
36.8	0.130994	36	0.119718	254	0.040455
38.8	0.126316	38	0.116197	424	0.027813
40.8	0.122807	40	0.112676		
49	0.111111	42	0.110329		
60	0.099415	44	0.107981		
77	0.087719	46	0.10446		
102	0.076023	48	0.102113		
144	0.064327	50	0.098592		
217	0.052632	52	0.096244		
357	0.040936	54	0.09507		
577	0.02924	56	0.093897		
		72	0.08216		
		94	0.070423		
		134	0.058685		
		204	0.046948		
		334	0.035211		
		584	0.023474		
		884	0.015737		

Diffusion of Ortho Xylene in HZSM-5 Crystal
1st set of data (Catalyst weight 5.3 mg,72 cc/min)

180 °C		180 °C		200 °C		220 °C		240 °C	
Time (sec)	Norm Conc..	Time (sec)	Norm Conc..	Time (sec)	Norm Conc..	Time (sec)	Norm Conc..	Time (sec)	Norm Conc..
0	1	45	0.090404	0	1	0	1	0	1
1	0.688889	46	0.089444	1	0.827288	1	0.682081	0.6	0.944383
2	0.555556	47	0.088715	2	0.504893	2	0.485549	1.6	0.555061
3	0.344444	48	0.087986	3	0.314911	3	0.312139	2.6	0.288098
4	0.272222	49	0.087257	4	0.256189	4	0.265896	3.6	0.216908
5	0.237778	50	0.086528	5	0.228555	5	0.23815	4.6	0.192436
6	0.215556	51	0.085799	6	0.20783	6	0.219653	5.6	0.171301
7	0.198889	52	0.085069	7	0.194013	7	0.208092	6.6	0.160178
8	0.186667	53	0.08434	8	0.18365	8	0.196532	7.6	0.149055
9	0.177778	54	0.083611	9	0.174439	9	0.187283	8.6	0.140156
10	0.17	55	0.082882	10	0.16753	10	0.180347	9.6	0.132369
11	0.161111	56	0.082153	11	0.15947	11	0.17341	10.6	0.12792
12	0.156667	57	0.081424	13	0.15141	12	0.16763	11.6	0.121246
13	0.152222	58	0.080694	16	0.137594	13	0.16185	12.6	0.116796
14	0.146667	59	0.079965	17	0.135291	15	0.150289	13.6	0.110122
15	0.142222	60	0.079236	19	0.128382	16	0.146435	14.6	0.106785
16	0.138889	61	0.078507	22	0.121474	18	0.138728	15.6	0.102336
17	0.134444	62	0.077778	27	0.111111	20	0.131792	16.6	0.098999
18	0.132222	63	0.07735	33	0.100748	24	0.121387	17.6	0.095662
19	0.13	64	0.076923	42	0.090386	27	0.112717	18.6	0.092325
20	0.127222	65	0.076496	52	0.080791	33	0.100193	22.6	0.081201
21	0.123889	66	0.076068	67	0.070067	38	0.09104	27.6	0.070078
22	0.122222	67	0.075641	85	0.06003	45	0.080925	34.6	0.060685
23	0.12	68	0.075214	111	0.050086	55	0.070415	40.6	0.053763

180 °C		180 °C		200 °C		220 °C		240 °C	
Time (sec)	Norm Conc..	Time (sec)	Norm Conc..	Time (sec)	Norm Conc..	Time (sec)	Norm Conc..	Time (sec)	Norm Conc..
24	0.117778	69	0.074786	129	0.044329	67	0.060281	50.6	0.046348
25	0.115556	70	0.074359	200	0.032815	86	0.050096	54.6	0.043382
26	0.113333	71	0.073932	320	0.022	94	0.046243	82.6	0.031
27	0.111111	72	0.073504			135	0.034682	170.6	0.015
28	0.11	73	0.073077						
29	0.108889	74	0.07265						
30	0.107778	75	0.072222						
31	0.105556	76	0.071795						
32	0.103333	77	0.071368						
33	0.102222	78	0.07094						
34	0.101111	79	0.070513						
35	0.1	80	0.070085						
36	0.09904	81	0.069658						
37	0.098081	82	0.069231						
38	0.097121	83	0.068803						
39	0.096162	84	0.068376						
40	0.095202	85	0.067949						
41	0.094242	86	0.067521						
42	0.093283	87	0.067094						
43	0.092323	88	0.066667						
44	0.091364	127	0.055556						
		188	0.044444						
		278	0.033333						

Diffusion of Ortho Xylene in HZSM-5 crystal
2nd set of data (80 cc/min)

125 °C		150 °C		180 °C		200 °C	
Time (sec)	Norm Conc	Time (sec)	Norm Conc	Time (sec)	Norm Conc	Time (sec)	Norm Conc
0	1	0	1	0	1	0	1
3	0.595186	2	0.608746	2.5	0.339839	0.5	0.691489
4	0.502188	3	0.505178	3.5	0.270953	1	0.446809
5	0.447484	5.5	0.378596	6	0.207807	1.5	0.37234
6	0.40372	8	0.321059	9	0.173364	2	0.335106
9	0.327133	11	0.275029	12.25	0.150402	3	0.287234
12.75	0.272429	13.5	0.240506	14.5	0.138921	5	0.244681
15	0.250547	16	0.228999	18.25	0.12744	8.5	0.202128
18	0.228665	20.75	0.205984	22.75	0.115959	11.75	0.180851
22.5	0.206783	26.75	0.182969	29	0.104478	14	0.170213
25	0.195842	30.5	0.171461	37.5	0.092997	16	0.159574
28.5	0.184902	35.5	0.159954	50	0.081515	19	0.148936
32.5	0.173961	41.5	0.148446	69.5	0.070034	22.5	0.138298
37	0.16302	49	0.136939	93	0.058553	26.5	0.12766
43.5	0.152079	57.5	0.125432	136	0.047072	31.5	0.117021
51	0.141138	70	0.113924	198.5	0.035591	37	0.106383
60.5	0.130197	85	0.102417	293.5	0.02411	44	0.095745
74	0.119256	107	0.090909	483.5	0.012629	52.5	0.085106
91.5	0.108315	137	0.079402			63.5	0.074468
114	0.097374	177	0.067894			78	0.06383
149	0.086433	232	0.056387			96.5	0.053191
194	0.075492	322	0.044879			122.5	0.042553
254	0.064551	456	0.033372			157.5	0.031915
334	0.053611	687	0.021864			215	0.021277
444	0.04267	1152	0.010357			335	0.010638
609	0.031729						
894	0.020788						
1300	0.014						
1644	0.009847						

Diffusion of 1,3 Di isopropyl benzene in Alumina crystal

[Catalyst weight 2.7 mg., flow rate 98 cc/min]

125 °C		150 °C		170 °C		190 °C	
Time (sec)	Norm Conc	Time (sec)	Norm Conc	Time (sec)	Norm Conc	Time (sec)	Norm Conc
0	1	0	1	0	1	0	1
5	0.903077	5	0.911854	2.5	0.920635	2.5	0.889643
8	0.846154	8	0.820669	5	0.849206	4.5	0.770798
12	0.769231	12	0.714286	7	0.777778	6.5	0.617997
16	0.692308	16	0.6231	10	0.674603	8.5	0.490662
20	0.630769	19	0.56231	13	0.587302	10	0.405772
25	0.553846	27	0.440729	16	0.507937	11.5	0.34635
29	0.507692	32	0.379939	20	0.428571	14.5	0.252971
35	0.446154	37	0.334347	22	0.396825	17	0.203735
43	0.384615	43	0.288754	25.5	0.349206	19.5	0.168081
50	0.338462	48	0.258359	28.5	0.31746	22.75	0.134126
56	0.307692	58	0.212766	30	0.301587	25	0.117148
63	0.276923	68	0.182371	33.5	0.269841	28	0.10017
71	0.246154	74	0.167173	38	0.238095	32.25	0.083192
75.5	0.230769	80	0.151976	43.25	0.206349	38.5	0.066214
88	0.2	87	0.136778	46.25	0.190476	52.5	0.049236
94	0.184615	97	0.121581	50	0.174603	90	0.032258
99	0.169231	107	0.106383	54	0.15873	377.5	0.01528
109	0.153846	119	0.091185	58.5	0.142857		
119	0.138462	137	0.075988	64.5	0.126984		
129	0.123077	167	0.06079	71.5	0.111111		
144	0.107692	207	0.045593	81.5	0.095238		
165	0.092308	367	0.015198	89	0.079365		
189	0.076923			109	0.063492		
229	0.061538			139	0.047619		
289	0.046154			199	0.031746		
409	0.030769						

Diffusion of 1,3,5 Tri isopropyl benzene in alumina crystal

[Catalyst weight 2.9 mg., flow rate 104 cc/min]

75 °C		100 °C		125 °C		150 °C	
Time (sec)	Norm Conc	Time (sec)	Norm Conc	Time (sec)	Norm Conc	Time (sec)	Norm Conc
0	1	0	1	0	1	0	1
20	0.982759	4	0.991957	4	0.992337	6	0.984975
44	0.948276	10	0.978552	14	0.92848	16	0.911519
74	0.896552	18	0.951743	24	0.832695	26	0.81803
94	0.862069	28	0.911528	36	0.730524	38	0.701169
124	0.810345	40	0.857909	48	0.641124	50	0.601002
144	0.775862	46	0.831099	60	0.565773	66	0.500835
166	0.741379	56	0.790885	72	0.500639	82	0.417362
188	0.706897	62	0.764075	84	0.445722	98	0.350584
210	0.672414	84	0.676944	96	0.398467	114	0.300501
236	0.637931	104	0.612601	108	0.360153	134	0.250417
262	0.603448	124	0.5563	120	0.32567	153	0.217028
276	0.586207	144	0.509383	132	0.296296	166	0.200334
328	0.52069	164	0.469169	144	0.269476	192	0.166945
368	0.482759	184	0.428954	156	0.246488	214	0.15025
408	0.446552	204	0.396783	168	0.227331	236	0.133556
448	0.413793	224	0.36193	178	0.213282	266	0.116861
488	0.37931	244	0.339142	188	0.200511	306	0.100167
528	0.351724	264	0.315013	200	0.187739	356	0.083472
608	0.310345	284	0.294906	212	0.174968	426	0.066778
688	0.275862	304	0.274799	226	0.162197	546	0.050083
768	0.241379	364	0.227882	242	0.149425	716	0.033389
888	0.206897	444	0.187668	261	0.136654	960	0.016694
1008	0.172414	504	0.160858	286	0.123883		
1208	0.137931	584	0.134048	316	0.111111		
1328	0.12069	634	0.120643	350	0.09834		
1488	0.103448	704	0.107239	396	0.085568		
1688	0.086207	774.8	0.093834	450	0.072797		
1928	0.068966	864	0.080429	536	0.060026		
2328	0.051724	984	0.067024	646	0.047254		
2928	0.034483	1164	0.053619	876	0.034483		
4128	0.017241	1404	0.040214				
		1764	0.02681				
		2484	0.013405				

Diffusion of 1,3 Di isopropyl benzene in FCC catalyst pellet

Catalyst weight 9 mg, flow rate 90 cc/min]

150 °C		170 °C		190 °C		210 °C	
Time (sec)	Norm Conc	Time (sec)	Norm Conc	Time (sec)	Norm Conc	Time (sec)	Norm Conc
0	1	0	1	0	1	0	1
2	0.852547	2	0.852725	2	0.900273	3	0.881735
3	0.731903	3	0.720177	3	0.790984	4	0.809461
4	0.597855	4	0.572901	4	0.654372	5	0.710907
5	0.483914	5	0.455081	5	0.51776	6	0.618922
6	0.396783	6	0.366716	6	0.415301	7	0.546649
7	0.336461	7	0.315169	8	0.301913	8	0.487516
8	0.296247	9	0.263623	11	0.258197	10	0.408673
10	0.24933	14	0.21944	14.5	0.230874	12	0.35611
13	0.22252	17.5	0.204713	17	0.217213	16	0.277267
19	0.19571	23	0.189985	20.5	0.203552	22	0.211564
24.5	0.182306	30.5	0.175258	25	0.189891	27	0.172142
33	0.168901	41	0.16053	29.5	0.17623	34	0.13272
46	0.155496	60	0.145803	35	0.162568	41	0.106439
77	0.142091	96	0.131075	42	0.148907	45.5	0.093298
132	0.128686	126	0.116348	52	0.135246	51	0.080158
222	0.115282	196	0.10162	65	0.121585	59	0.067017
342	0.101877	266	0.086892	81	0.107923	71	0.056505
494	0.088472	347	0.072165	101	0.094262	101	0.040736
710	0.075067	473	0.057437	131	0.080601	168	0.021025
962	0.061662	671	0.04271	164	0.06694	208	0.014455
1322	0.048257	971	0.02651	209	0.053279		
1772	0.034853	1451	0.011782	279	0.039617		
2582	0.018767			374	0.025956		
				644	0.012295		

Diffusion of 1,3,5 Tri isopropyl benzene in FCC catalyst pellet

[Catalyst weight 8 mg, flow rate 104 cc/min]

125 °C		150 °C		190 °C		210 °C	
Time (sec)	Norm Conc	Time (sec)	Norm Conc	Time (sec)	Norm Conc	Time (sec)	Norm Conc
0	1	0	1	0	1	0	1
7	0.851064	10	0.81775	10	0.821429	5	0.896104
14	0.702128	13	0.762282	16	0.761905	8	0.844156
19	0.574468	16	0.690967	24	0.630952	11	0.753247
23	0.489362	18	0.635499	30	0.553571	14	0.649351
28	0.404255	22	0.549921	36	0.479167	17	0.551948
35	0.319149	25	0.492868	43	0.404762	19	0.493506
40	0.276596	29	0.429477	48	0.360119	23	0.402597
46	0.234043	33	0.381933	54	0.315476	27	0.337662
50.5	0.212766	41	0.318542	62	0.270833	31	0.285714
56.5	0.191489	47	0.286846	72	0.22619	36	0.246753
65	0.170213	51	0.270998	85	0.181548	40	0.220779
78	0.148936	55.5	0.255151	91	0.166667	49	0.181818
105	0.12766	61	0.239303	98	0.151786	59	0.155844
170	0.106383	71	0.223455	105.5	0.136905	66	0.142857
575	0.085106	84	0.207607	114	0.122024	74	0.12987
875	0.076596	107	0.191759	125	0.107143	85	0.116883
1175	0.070213	140	0.175911	141	0.092262	99	0.103896
1475	0.06383	191	0.160063	162	0.077381	121	0.090909
2000	0.058511	261	0.144216	187	0.0625	154	0.077922
2525	0.053191	361	0.128368	228	0.047619	194	0.064935
3050	0.047872	476	0.11252	312	0.032738	264	0.051948
3575	0.042553	601	0.096672			379	0.038961
		751	0.080824			619	0.025974
		958	0.064976			1129	0.012987
		1216	0.049128				
		1576	0.033281				
		2356	0.017433				

Diffusion of Cumene in FCC catalyst pellet

Catalyst weight 12mg, flow rate 33cc/min]

150 °C		175 °C		200 °C		225 °C	
Time (sec)	Norm Conc	Time (sec)	Norm Conc	Time (sec)	Norm Conc	Time (sec)	Norm Conc
0	1	0	1	0	1	0	1
2	0.816339	2	0.866844	1	0.960474	1	0.9375
4	0.499683	4	0.520639	3	0.69697	3	0.75
6	0.373021	6	0.36751	5	0.459816	5	0.5375
8	0.336289	8	0.327563	7	0.393939	7	0.45
10	0.31349	10	0.299601	9	0.361001	9	0.4
12	0.297023	12	0.283622	11	0.334651	11	0.36375
14	0.284357	14	0.268975	13	0.316206	13	0.3325
16	0.274224	16	0.259654	15	0.301713	15	0.3075
18	0.265358	18	0.251664	17	0.289855	17	0.28625
20	0.259025	20	0.243675	19	0.277997	19	0.2675
22	0.246358	22	0.235686	21	0.270092	21	0.25
24	0.241292	24	0.23036	23	0.262187	23	0.235
26	0.236225	26	0.223702	25	0.254282	25	0.22125
28	0.231159	28	0.219707	27	0.247694	27	0.2075
30	0.227359	30	0.215712	29	0.239789	29	0.195
32	0.222293	32	0.210386	31	0.235837	31	0.18625
34	0.219759	34	0.206391	33	0.229249	33	0.17625
36	0.215959	36	0.203728	35	0.223979	35	0.1675
38	0.21216	38	0.201065	37	0.221344	37	0.16
40	0.20836	40	0.197071	39	0.216074	39	0.15125
42	0.205826	42	0.194407	41	0.209486	41	0.14375
44	0.203293	44	0.191744	43	0.205534	43	0.1375
46	0.199493	46	0.18775	45	0.205534	45	0.13125
48	0.19696	48	0.186418	47	0.197628	47	0.125
50	0.19506	50	0.183755	49	0.194993	49	0.12
52	0.19316	52	0.181092	51	0.191041	51	0.11625
54	0.190627	54	0.178429	53	0.188406	53	0.1125
56	0.188094	56	0.177097	55	0.188406	55	0.10875
58	0.18556	58	0.174434	57	0.184453	57	0.10375
60	0.184294	60	0.173103	59	0.181818	59	0.1
62	0.183027	62	0.170439	61	0.179183	61	0.0975
64	0.181127	64	0.169108	63	0.176548	63	0.095
66	0.179227	66	0.165113	65	0.172596	65	0.09
68	0.177961	68	0.163782	67	0.16996	67	0.0875
70	0.175427	70	0.16245	69	0.168643	69	0.08625
72	0.172894	72	0.161119	71	0.166008	71	0.08375
74	0.171628	74	0.159787	73	0.163373	73	0.08125
76	0.169728	76	0.158455	75	0.160738	75	0.07875
78	0.169094	78	0.157124	77	0.158103	77	0.07625
80	0.167828	80	0.155792	79	0.154809	79	0.075

150 °C		175 °C		200 °C		225 °C	
Time (sec)	Norm Conc	Time (sec)	Norm Conc	Time (sec)	Norm Conc	Time (sec)	Norm Conc
82	0.166561	82	0.154461	81	0.152833	81	0.07375
84	0.165294	84	0.153129	83	0.150198	83	0.0725
86	0.164028	86	0.151798	85	0.14888	85	0.07125
88	0.162761	88	0.150466	87	0.146245		
90	0.161495	90	0.149134	89	0.144928		
92	0.160228	92	0.147803	91	0.142292		
94	0.158961	94	0.147137	93	0.140975		
96	0.157695	96	0.146471	95	0.139657		
98	0.156428	98	0.14514	97	0.13834		
110	0.151362	100	0.143808	99	0.137022		
122	0.145028	102	0.142477	101	0.134387		
134	0.140595	104	0.141145	103	0.131752		
146	0.136162	106	0.139814	105	0.131094		
154	0.132362	108	0.138482	107	0.129117		
158	0.131096	110	0.137816	109	0.1278		
170	0.127296	112	0.13715	111	0.126482		
182	0.123496	114	0.135819	113	0.125165		
194	0.119696	116	0.135153	115	0.123847		
206	0.115896	118	0.134487	117	0.12253		
240	0.10703	132	0.129827	119	0.121212		
298	0.094364	152	0.121172	121	0.121212		
370	0.081697	196	0.107856	123	0.119895		
466	0.069031	250	0.094541	125	0.118577		
690	0.053832	310	0.081225	155	0.104084		
		392	0.063915	185	0.090909		
				225	0.077734		
				261	0.064559		

Diffusion of Benzene in FCC catalyst pellet

[Catalyst weight 10mg, flow rate 33cc/min]

100 °C		125 °C		150 °C		175 °C		200 °C	
Time (sec)	Norm Conc	Time (sec)	Norm Conc	Time (sec)	Norm Conc	Time (sec)	Norm Conc	Time (sec)	Norm Conc
0	1	0	1	0	1	0	1	0	1
2	0.843387	2	0.797921	2	0.76431	2	0.757336	1	0.871528
4	0.646172	4	0.624711	4	0.607183	4	0.554176	3	0.616898
6	0.506961	6	0.463048	6	0.438833	6	0.396163	5	0.443287
8	0.416473	8	0.37067	8	0.354658	8	0.317156	7	0.315972
10	0.37703	10	0.321016	10	0.315376	10	0.277652	9	0.243056
12	0.349188	12	0.295612	12	0.281706	12	0.249436	11	0.206019
14	0.323666	14	0.275982	14	0.260382	14	0.226862	13	0.184028
16	0.306265	16	0.257506	16	0.242424	16	0.208804	15	0.167824
18	0.288863	18	0.243649	18	0.225589	18	0.193002	17	0.153935
20	0.274942	20	0.230947	20	0.214366	20	0.181716	19	0.142361
22	0.263341	22	0.220554	22	0.20202	22	0.1693	21	0.130787
24	0.25174	24	0.209007	24	0.190797	24	0.159142	23	0.122685
26	0.242459	26	0.202079	26	0.180696	26	0.150113	25	0.116898
28	0.234339	28	0.19515	28	0.171717	28	0.14447	27	0.112269
30	0.226218	30	0.188222	30	0.166105	30	0.136569	29	0.107639
32	0.219258	32	0.180139	32	0.158249	32	0.130926	31	0.103009
34	0.211137	34	0.174365	34	0.152637	34	0.125282	33	0.099537
36	0.205336	36	0.169746	36	0.147026	36	0.121896	35	0.096065
38	0.199536	38	0.163972	38	0.141414	38	0.117381	37	0.09375
40	0.192575	40	0.160508	40	0.135802	40	0.112867	39	0.091435
42	0.189095	42	0.155889	42	0.132435	42	0.109481	41	0.08912

100 °C		125 °C		150 °C		175 °C		200 °C	
Time (sec)	Norm Conc	Time (sec)	Norm Conc	Time (sec)	Norm Conc	Time (sec)	Norm Conc	Time (sec)	Norm Conc
44	0.183295	44	0.15127	44	0.127946	44	0.106095	43	0.086806
46	0.179814	46	0.147806	46	0.124579	46	0.102709	45	0.084491
48	0.175174	48	0.144342	48	0.122334	48	0.100451	47	0.083333
50	0.170534	50	0.139723	50	0.12009	50	0.098194	49	0.081019
52	0.167053	52	0.137413	52	0.117845	52	0.095937	51	0.078704
54	0.163573	54	0.133949	54	0.1156	54	0.093679	53	0.077546
56	0.160093	56	0.13164	56	0.113356	56	0.091422	55	0.076389
58	0.156613	58	0.12933	58	0.109989	58	0.089165	57	0.075231
60	0.154292	60	0.127021	60	0.107744	60	0.088036	59	0.074074
62	0.150812	62	0.124711	62	0.105499	62	0.085779	61	0.072917
64	0.148492	64	0.122402	64	0.103255	64	0.083521	63	0.071759
66	0.146172	66	0.120092	66	0.10101	66	0.082393	65	0.071181
68	0.143852	68	0.117783	68	0.098765	68	0.081264	67	0.070602
70	0.141531	70	0.116628	70	0.096521	70	0.080135	69	0.070023
72	0.139211	72	0.115473	72	0.094276	72	0.079007	71	0.069444
74	0.135731	74	0.113164	74	0.092031	74	0.077878	73	0.068287
76	0.134571	76	0.110855	76	0.090348	76	0.076749	75	0.067708
78	0.132251	78	0.108545	78	0.088664	78	0.075621	77	0.06713
80	0.13109	80	0.10739	80	0.087542	80	0.074492	79	0.066551
82	0.12877	82	0.106236	82	0.08642	82	0.073363	81	0.065972
84	0.12761	84	0.105081	84	0.085859	84	0.072235	83	0.065394
86	0.12413	86	0.103926	86	0.084736	86	0.071106	85	0.064815
88	0.12297	88	0.102771	88	0.084175	88	0.069977	87	0.064236
90	0.12065	90	0.101617	90	0.083614	90	0.068849	89	0.063657
92	0.11949	92	0.099307	92	0.083053	126	0.057562	91	0.063079

100 °C		125 °C		150 °C		175 °C		200 °C	
Time (sec)	Norm Conc	Time (sec)	Norm Conc	Time (sec)	Norm Conc	Time (sec)	Norm Conc	Time (sec)	Norm Conc
94	0.118329	94	0.096998	94	0.082492	180	0.046275	93	0.061458
96	0.116009	96	0.095843	118	0.068462			95	0.061921
98	0.114849	98	0.094688	154	0.057239			97	0.061343
100	0.113109	100	0.093533	202	0.046016				
102	0.111949								
104	0.110789								
106	0.109049								
108	0.107889								
110	0.106729								
114	0.105568								
118	0.102088								
120	0.100928								
122	0.099768								
124	0.098608								
126	0.097448								
128	0.096288								
130	0.095128								
132	0.093968								
134	0.092807								
136	0.091647								
138	0.090487								
140	0.089907								
142	0.089327								

Appendix C

Computer program

[Sample program]

Main MATLAB program to calculate the diffusivity and the L values

```
%%%%%%%%%%%%%%%%%%%%%%%%%%%%%%%%%%%%%%%%%%%%%%%%%

clear all
close all
clc
global A B N L DR2
%% CALLING JACOBIAN MATRIX TO SOLVE DIFFERENCIAL EQUATION
jacobi10;
%%%%%%%%%%%%%%%%%%%%%%%%%%%%%%%%%%%%%%%%
%% LOADING EXPERIMENTAL DATA FILE AND ASSIGNING X AND Y VALUES
data150;
x_ex=data150(:,1);
y_ex=data150(:,2);

%%%%%%%%%%%%%%%%%%%%%%%%%%%%%%%%%%%%%%%%%%%%%%%%%
%%%%%%%%%%%%%%%%%%%%%%
%% Give value from chart to calculate slope
Y1=0.34;
X1=0;
Y2=0.1;
X2=2000;
%%%%%%%%%%%%%%%%%%%%%%%%%%%%%%%%%%%%%%%%%%%%%%%%%
%%

%########## GIVE THE VALUE OF INTERCEPT ##########%
%%%%%%%%%%%%%%%%%%%%%%%%%%%%%%%%%%%%%%%%%%%%%%%%%
%%
Intercept=Y1;
%##############################################%

%%%%%%%%%%%%%%%%%%%%%%%%%%%%%%
slope=log(Y1/Y2)/(X1-X2);
%%%%%%%%%%%%%%%%%%%%%%%%%%%%%%%%%%%%%%%%%%%%%%%%%

% SOLVING THE DR2 AND L VALUES FROM
```

```
% THE SLOPE AND INTERCEPT OF THE LONG TIME STRAIGHTLINE
syms b L DR2

eq1=b*cot(b)+L-1;
eq2=-b^2*(DR2)-slope;
eq3=2*L/(b^2+L*(L-1))-Intercept;

[DR2 L b]=solve(eq1,eq2,eq3);
%%%%%%%%%%%%%%%%%%%%%%%%%%%%%%%%%%%%%%%%%%%%%%%%%
DR2=double(DR2);
L=double(L);
%%%%%%%%%%%%%%%%%%%%%%%%%%%%%%%%%%%%%%%%%%%%%%%%%
%%%%%%%%%%%%%%%%%%%%%%%%%%%%%%%%%%%%%%%%%%%%%%%%%
%% USING THE ODE15S TO SOLVE THE DIFFERENCIAL EQUATION
[t,q]=ode15s('zlc_function',[0:5:8000],ones(1,N));

q_end150=(-A(N+1,1:N)*q'/(A(N+1,N+1)+L))';

q150=[q q_end150];

%% PLOTING THE RESULTS --->> ONLY THE BOUNDARY NODE SIMULATED
RESULT
semilogy(t,q_end150,'linewidth',1.5)
hold on
semilogy(x_ex,y_ex,'o')
hold off
title('ZLC Desoprtion Curve for 1,3 DIPB in NaY at 150 ^oC at 90 cc/min')
ylabel('Normalized Concentration')
xlabel('Time in sec')
axis([0 7000 0.01 1])
grid on
%########## Display the values ############
DR2
D_150DIP=DR2*(.45e-6)^2
L_150DIP=L

%%%%%%%%%%%%%%%%%%%%%%%%%%%%%%%%%%%%%%%%%%%%%%%%
```

Function file to calculate the ZLC diffusion model equation

```
%%%%%%%%%%%%%%%%%%%%%%%%%%%%%%%%%%%%%%%%%%%%%%%%
function dqdt=zlc_function(t,q)
global A B N L DR2

q_end=-A(N+1,1:N)*q/(A(N+1,N+1)+L);

dqdt=DR2*B(1:N,:)*[q;q_end];
```

VITA

Name	Sharif Fakhruz Zaman
Religion	Muslim
Nationality	Bangladeshi
Education	Bachelor of Science in Chemical Engineering Bangladesh University of Engineering and Technology (BUET) September, 1999.
	MS in Chemical Engineering King Fand University of Petroleum & Minerals, Dhahran, Saudi Arabia April, 2004.